'The economic potential of deep, direct use geothermal systems in the Netherlands'

By

B.R. van Dongen
4260074

in partial fulfilment of the requirements for the degree of

Master of Science
in Applied Earth Sciences

at the Delft University of Technology.

First Supervisor:	Prof. dr. D. F. Bruhn,	TU Delft
Daily Supervisor:	Dr. A. Daniilidis MSc,	TU Delft

January 2019

TUDelft

Abstract

For this thesis, a probabilistic techno-economic model is developed for deep, direct use geothermal projects in the Netherlands. As a case study, data from the future DAP doublet (TU Delft) is inserted wherein multiple scenarios are researched that model variations in well capacity, energy prices, project design, government policies, brine gas content and heat demand available. For the case study, the model considers technical and economic uncertainties over a period of 50 years. These uncertainties are incorporated in the form of probability distributions and 15000 Monte Carlo iterations. By modeling these scenarios, an overview is developed of the economic performance of a deep district heating project based on the Net Present Value (NPV), Levelized Cost of Heat (LCOH), Internal Rate of Return (IRR), Profitability Index (PI) and payback time. Additionally, an evaluation of the effectiveness of the Dutch subsidy scheme is researched combined with the main financial obstacles associated with geothermal exploitation. The reference scenario of the case study resulted in a 90% probability of a positive NPV with a median PI of 1.5. Higher returns are delivered from scenarios where the subsidy policies were altered in a way that they are more suitable for district heating purposes. A scenario where high constant demand was simulated combined with an extra initial investment for the purpose of heat storage, resulted in the best performing scenario overall. Considering the demand available for this case study, the fixed operational cost, SDE base sum and gas/water ratio are the most important parameters in terms of NPV sensitivity. In order to achieve the desired growth of the Dutch geothermal sector, focus should be aimed at the realisation of sufficient heat network deployment, heat storage options and more project specific subsidies.

Contents

1   Introduction

Geothermal energy is the thermal energy stored in the earth's interior. This energy is distributed between the host rock and the natural fluid that is contained in its fractures and/or pores above ambient temperatures. This energy is formed by two different mechanisms: one is residual heat created at the moment of the formation of the earth and is resulting from gravitational and collisional energy [1]. This energy flows to the crust by upward convection and conduction processes from the earth's mantle and core [2]. The other mechanism is the decay of the radioactive isotopes uranium, thorium, and potassium mainly located in the upper crust [3]. The earth's crust is on average 40 km thick and bears an estimated $5.4 *10^{21}$ MJ of geothermal energy [1]. The thermal energy stored in the earth could be considered immense if it is compared to the total global energy consumption of $6*10^{14}$ MJ in 2015 [4]. However, due to several technical and thermodynamical limitations, only a fraction of this heat can be utilized.

At the base of the continental crust, temperatures range from 200 to 1000 °C [3]. This heat is transferred towards the surface mainly by conduction processes caused by the temperature difference between deep hot zones and shallow colder zones. This process creates an average geothermal gradient of 25 to 30 °C/km above the surface ambient temperature [3] [5]. In areas where the basement rock has undergone rapid sinking, basin sediments are relatively young and the geothermal gradient may be lower than 10 °C/km [1]. At tectonically active locations or along fault lines however, the gradient can be up to 5 to 10 times the average value. At these locations, a few kilometres from the surface there are magma bodies undergoing cooling that are still in a liquid state or in the process of solidification and are releasing high amounts of heat, such that the geothermal gradient can reach values well above 100 °C/km [5].

The basic principle of geothermal exploitation is as follows: hot fluid from the geothermal system is produced through a production well where its heat is extracted at the surface. The cooled fluid from the surface is then re-injected through an injection well. This fluid can be produced in the form of hot water, steam or both. Further utilization of this fluid divides geothermal energy exploitation into two sectors: electricity generation and heating, with the latter also referred to as direct use geothermal energy.

It was in the 20th century that geothermal energy was first harnessed on a large scale for space heating, industry and electricity generation. Prince Piero Ginori Conti initiated electric power generation with geothermal steam at Larderello, Tuscany, in 1904 [6]. The first large scale district heating service started in Iceland in 1930. Geothermal energy has been produced commercially for over 90 years, and for five decades on the scale of thousands of MW, with 14 GW total capacity installed for electricity generation on a global scale at this time [7].

1.1   Electricity generation

Electricity is generated with the use of high pressured, 130°C+ steam or hot water produced mainly from naturally fractured tectonically active systems and Enhanced Geothermal Systems (EGS) [5]. The steam that is produced from these reservoirs powers a turbine that in turn generates electricity in the attached generator. To reach similar subsurface temperatures in the Netherlands, depths of over 4 km need to be drilled to produce steam hot enough for electricity production. As of 2018, no such wells have been successfully drilled in the Netherlands.

With increasing depth, natural fractures get narrower until they completely close due to immense overburden pressures. In this case there is no to very little permeability left from the reservoir. Often these kinds of reservoirs and other deeper situated, non-porous crystalline basement rocks are artificially stimulated to increase permeability. Reservoirs that require stimulation or enhancement are also known as Enhanced Geothermal Systems [2]. The three main methods are thermal, chemical (in carbonate reservoirs) and hydraulic stimulation [2]. With hydraulic stimulation, fluid pathways are artificially opened or extended by injecting water or fracking fluid under high pressures inside the reservoir.
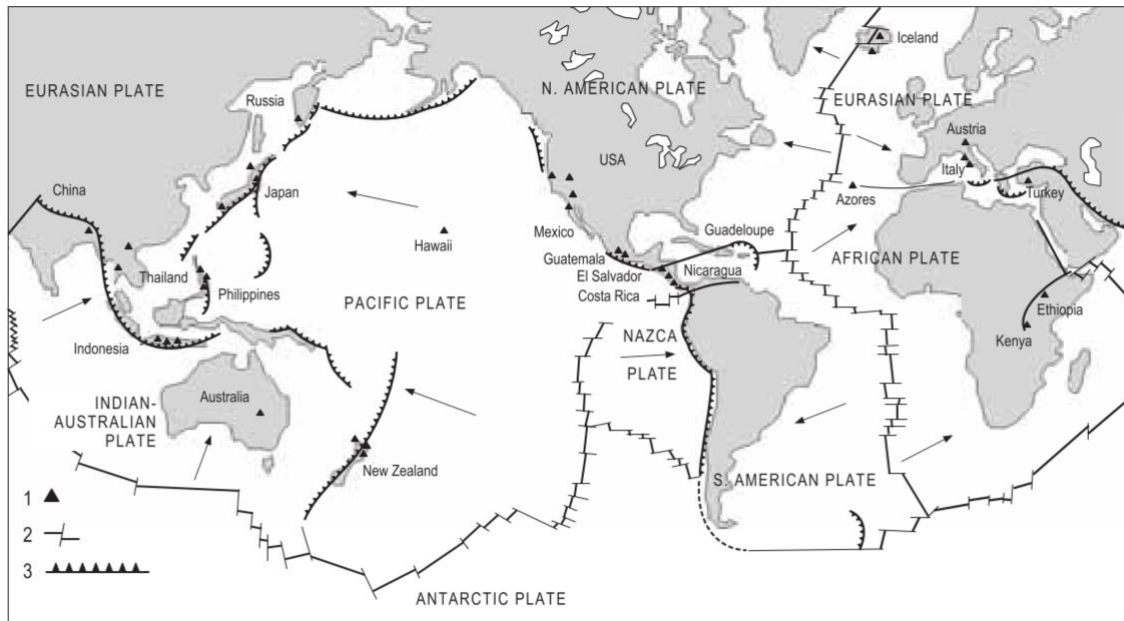
Figure 1: Tectonic plates, oceanic ridges, oceanic trenches, subduction zones and geothermal fields Arrows indicate plate subduction direction. (1) Geothermal fields producing electricity; (2) mid-oceanic ridges crossed by transform faults (3) subduction zones [1]

In general, geothermal power plants are located in areas where the geothermal gradient is well above average (Figure 1). In terms of installed capacity in Europe, Turkey is leading with 1200 MW of total capacity in 2018, followed by Italy and Iceland with an installed capacity of 944 and 755 MW respectively [7].

1.2   Direct use of geothermal energy

In the geothermal heating sector, shallow geothermal energy production is with 67% of the total installed capacity, by far the largest sector of direct geothermal energy use in Europe in 2016 [8]. In this subsector, shallow geothermal energy is utilized from depths ranging from 10 to 500m. Below the depth of around 10 to 20m, seasonal temperature changes have no influence on the subsurface temperature [9]. These constant temperatures can be utilized with ground source heat pumps for heating or cooling purposes and underground thermal energy systems for hot and cold storage [10].

The second geothermal heating sector goes far beyond these depths. Deep direct use geothermal energy is characterized as geothermal energy exploited from hydrothermal aquifers exceeding a depth of 500m for the purpose of district heating, agricultural heating, balneology and individual space heating [8]. A hydrothermal system is a geothermal resource that naturally contains the three key components for a working geothermal system. These are the presence of a heat source, a fluid and fluid pathways. Fluid pathways can exist in the form of pores, fractures or karst.

In the Netherlands, geothermal energy is currently limited to direct use only. For this thesis, the focus is set on deep direct use geothermal energy in the form of a hydrothermal system as indicated by the red circle in Figure 2.
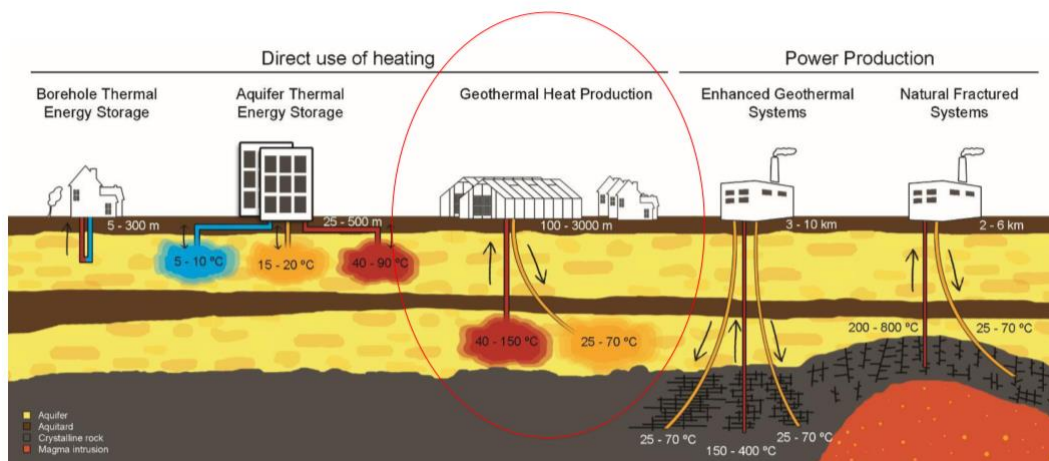
Figure 2: Geothermal systems overview. The focus of this thesis is set on geothermal heat production for greenhouse and district heating purposes [11]

1.3 Geothermal and Climate

From a climate point of view, our present energy system, which is primarily based on fossil fuels, is unsustainable in the long term. Depleting fossil fuel reserves combined with the large environmental impact of greenhouse-gas emissions indicate the need for change. Because of this, the European Council endorsed an energy and climate framework for 2030 that includes EU- wide targets of at least a reduction of 40% greenhouse gas emissions relative to 1990 emissions, with a minimum of 27% of the produced energy derived from renewable energy sources [12]. Greenhouse gas emissions in the Netherlands amounted to 196 megaton CO_2 equivalents in 2015. 80% of these emissions are associated with the use of energy, with at least half originating from heating purposes in the form of industrial process heat, space heating and tap water [13].

Direct use geothermal heat has ideal characteristics for local district and greenhouse heating applications [14]. It can be operated as either base-load or estimated-load capacity and is unlike solar and wind energy, independent of seasonal changes in terms of energy output [15][16]. Today, electricity sources supply less than half of the Dutch energy demand directly. The rest is needed in the form of heat which is mainly delivered by burning natural gas. [17]. The 17 realised geothermal projects in the Netherlands have an average CO_2 emission of 7 kg/GJ compared to 57 kg/GJ of CO_2 released by burning natural gas [18]. In a case where the geothermal pumps would be powered by renewable electricity however, the CO_2 emissions are zero.

Geothermal heat is therefore an ideal renewable energy source that can function as a large contributor in achieving these climate targets and can provide a large part of the energy demand in the form of heat in an environmentally friendly manner.

1.4 Dutch Geothermal projects

Direct use geothermal energy in the Netherlands has been subjected to great development through the last ten years [19]. Between 2009 and 2014, the amount of energy produced from geothermal projects grew with a rate of 30% per year from 0.3 PJ in 2009 to 1.5 PJ in 2014 [20]. Growth in production numbers was still visible between 2014 and 2015 but a decline in in the number of realized projects is noticeable from 2014 forward [20] (Figure 3).
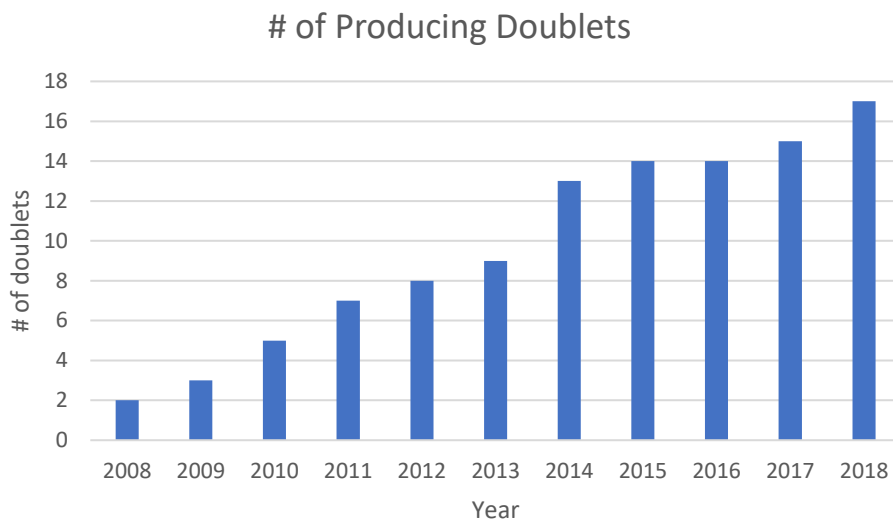
Figure 3: Number of producing doublets in the Netherlands from 2008 – 2018 [21][18]

At present, 17 deep (> 500m) geothermal energy projects are installed and producing, with 3 projects realised but not in production yet and 23 projects are waiting their approval [18],[22]. To increase the interest in geothermal energy, multiple policies and knowledge enhancing developments were initiated by government and private sectors [10]. In 2018 a masterplan was set up by a collaboration of geothermal organizations Platform Geothermie, DAGO, WN and EBN. Their goal is to increase the annual geothermal production from 3 PJ in 2018 to 50 PJ in 2030 and more than 200 PJ in 2050. As a reference, 1 PJ/year can provide heat to approximately 20.000 homes in the Netherlands [18].

2   Problem definition

To achieve the amount of growth as stated by the masterplan, a cost reduction of 30 – 50% over the life cycle of a geothermal system needs to be realised. This cost reduction is necessary to keep attracting sufficient investors and minimize the cost of the renewable energy transition for society. The cost reduction can be achieved by upscaling and improving the coordination of exploration and exploitation processes [18]. By upscaling the geothermal sector, geological uncertainties, technical risks and overall cost will be decreased significantly [18]. Therefore, more insight is needed in the cost and uncertainties of geothermal projects on an individual level. The importance and impact of technical and economic parameters and their uncertainties remains crucial for each project. A scenario analysis is essential for a better understanding of the economic performance and viability of geothermal projects today, and in the future. Every individual project has its own revenue stream and expenses based on the capacity of the wells, project design, government policies and the heat demand of the surrounding area. By modelling variations of these parameters, an overview is developed of the economic feasibility of a project including an evaluation of the effectiveness of the Dutch subsidy scheme and the main financial obstacles associated with geothermal exploitation.

The aim of this research is summarized in the following research questions:

What is the current status regarding the economic feasibility of deep, direct use geothermal projects in the Netherlands and how can this be improved for future projects?

To answer this main question, the following sub questions need to be answered first:

1. How does the current Dutch subsidy scheme perform on an individual project level of today? How could it be made more efficient?
2. What is the effect of decoupling the geothermal heat price from fossil fuel prices?
3. What is the sensitivity of the financial performance to the various technical and economic uncertainties of geothermal projects/systems?

2.1 SDE+

To encourage the production of renewable energy a subsidy scheme was set up in 2012 by the ministry of economic affairs called Stimulering Duurzame Energie (SDE) [23]. The current subsidy scheme can be insufficient when applied to the more challenging projects as stated in [24]. For this thesis, one of the goals is the identification and discussion of alternative SDE+ grant structures for future projects. The advantages of a grant structure that is designed for individual geothermal projects are investigated, so that a suggestion could be made for the revision of the SDE+ grant for future geothermal projects.

2.2 Geothermal investments and financing

Additionally, updated cost calculations for geothermal well drilling, site equipment and project financing are discussed to show their effect on the financial outcome of a project. The cost of geothermal well drilling is very specific for each project due to the different number of wells drilled per contract. Cost per well will decrease significantly with increasing numbers of wells drilled due to a potential learning effect. This learning effect is created by an increase in experience and knowledge of the local geology and drilling conditions associated with every additional well drilled. [25].

On the long term, district heating could meet the largest demand (65%) in geothermal heating relative to greenhouse heating [18]. In 2050, geothermal district heating could potentially grow to 135 PJ if the required heat networks are installed [18]. District heating requires an alternative method of project planning and design due to the differences in heat demand compared to greenhouse heating. Another point to consider is the way projects are financed. This is changing rapidly due to the increasing experience gained from existing projects, which results in lower costs of debt and better financing options overall.

2.3 Heat prices

The importance of the geothermal heat price is analysed. In the Netherlands, the heat price of any energy source is limited by the price of heat generated from natural gas. Geothermal heat prices for 2018 are computed as 90% of the market price for natural gas. This method of energy price determination, results in the separation of revenue streams from their operating costs and are subject to price fluctuations in natural gas prices [14]. In this case, to get more accurate predictions about the future feasibility of geothermal projects, more insight is needed in the behaviour of future gas prices. Additionally, an alternative geothermal heat price, such as a fixed rate, will be considered in the economic study.

2.4 Case study

For this thesis, a techno-economic model is developed based on the model by Daniilidis et al. [24] for deep, direct use geothermal systems in the Netherlands. The model will be used on one case study.

For this case study, simulated data were gathered from the future DAP well at Technical University Delft. Foundation DAP was initiated in 2008 by students and alumni at the department of Geosciences and Engineering and aims to provide the TU Delft with a sustainable heat source combined with a geothermal research facility through the realization of a geothermal doublet on campus [26]. The targeted reservoir for this doublet is the Delft Sandstone Member (DSSM) of the Lower Cretaceous formation in the West Netherlands Basin (Figure 4) [27].
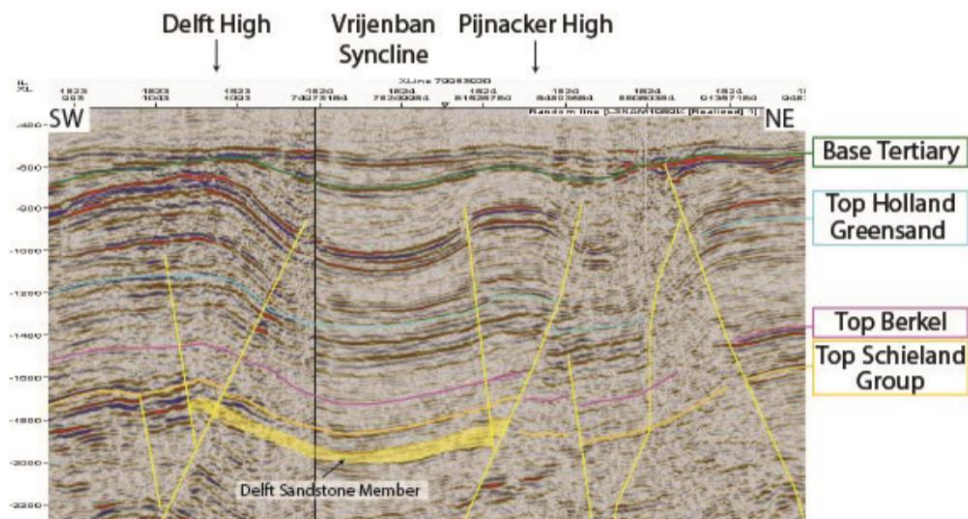
Figure 4: Depth-converted seismic cross section through the geothermal license area. The Delft Sandstone Member, indicated with yellow, is located in a gentle broad syncline bounded by the Delft and Pijnacker High [27]*.*

The DSSM is part of the Nieuwerkerk Formation and consists of a fluvial succession formed in the early Cretaceous, during and after a major rifting phase in the West Netherlands Basin (WNB). Generous amounts of reservoir data are available for this sandstone reservoir from oil and gas well drillings. However, these gas and oil wells were drilled on the structural highs of this structure whereas the geothermal wells are targeted in the syncline of the formation [27]. Another dataset of the Nieuwerkerk Formation, which is targeted by approximately 40 exploration licenses, show large variations in thickness and Net-to-Gross ratio (N/G). N/G is the net reservoir volume over the sum of the volume of all reservoir bodies. The thickness varies from 50 to almost 200m and the N/G ranges from 15 to 70% in different sections of the reservoir [28]. For fluvial reservoir systems, a N/G below 50% has a significant effect on the connectivity of the reservoir, as a result of sand bodies being isolated by shale bodies [29]. Lower reservoir connectivity results in a shorter lifetime and lower performance of the doublet [29]. At the location of TU Delft, cores and cutting analyses combined with seismic well-tie studies showed that the best potential in terms of high lateral and vertical connectivity were found in the uppermost 40 m of the DSSM, which is therefore considered the most promising target for the placement of the geothermal doublet [27].

In September 2017, an estimated 45-million-euro SDE+ subsidy was approved by the ministry of economic affairs. The main challenges for this project to actually receive the funding are finding sufficient demand (especially in summer), as well as reaching a low enough return temperature of the brine and the handling of the co generated gas [30].

By modelling this case study, a conclusion in terms of economic feasibility and general performance based on different design decisions and government policies for direct use geothermal development of single doublet systems in the Netherlands has been established.

3   Method and model description

The model is developed with the Monte Carlo simulation software Goldsim [31]. Goldsim is a tool for decision-making and risk analysis by simulating future performance while quantitatively representing the uncertainty and risks inherent in complex systems. The model for this thesis will be a revised and expanded version of the model mentioned in [24]. Uncertainties in any aspect regarding technical and financial aspects are implemented in the form of probability distributions.

3.1 Model data and stochastic sampling

For every scenario modelled, 15000 iterations are run to properly model the possible range of uncertainty of the results. Each stochastic element is sampled based on its sample frequency. This is either once per iteration or multiple times within an iteration. There are two different types of distributions used in the model depending on the data available. If the mean value and standard deviation are known, a normal distribution is used as a stochastic element. In general, a normal distribution is symmetric when inserted in the model but can also be bounded at one or both sides. This is called a truncated normal distribution. An example is shown in Figure 5.
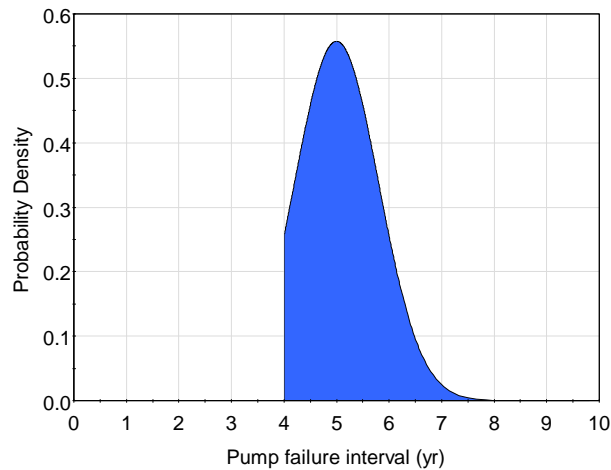
Figure 5: Example of a truncated normal distribution, bounded at 4 years.

When only a few data percentiles are available such as 10th, 50th (median) and 90th percentile, which is a very common method for risk evaluation in the oil and gas industry, a triangular distribution is inserted. This data could be in the form of P10 – mode – P90 or min (P0) – mode – max (P100). Mode represents the most frequent value of the dataset. It is important to mention that normally in risk evaluation, the P10 value indicates a best-case scenario and P90 the worst case. In the model, P10 is a value where 10% of the data are equal to, or lower than this value. P90 stands for 90% of the data being equal to or lower this value. Depending on the range of the provided data, a triangular distribution can be symmetric or asymmetrical. An example of an asymmetric triangular distribution is given in Figure 6.
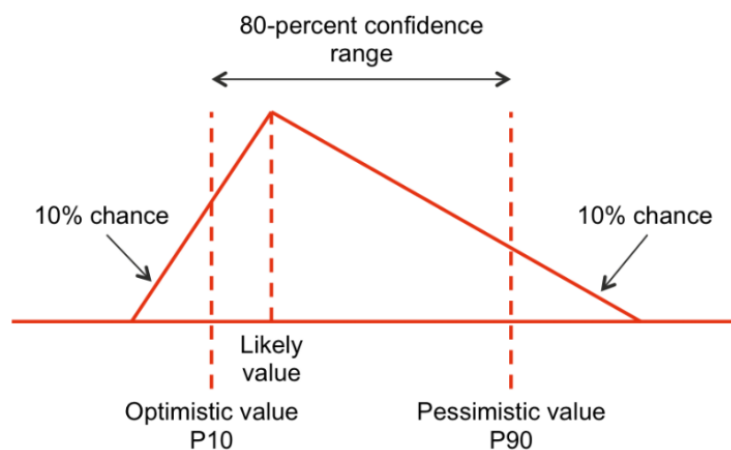
Figure 6: Example of an asymmetric triangular distribution including percentiles.

For the different scenarios, multiple financial evaluation methods are inserted, to evaluate the project's economic performance. These include the Net Present Value (NPV), Internal Rate of Return (IRR), Profitability Index (PI) and the Levelized Cost of Heat (LCOH). Additionally, a sensitivity analysis is performed on the model's variables. With this method a complete overview is developed of the economic feasibility of each scenario including a visualization of the effectiveness of the Dutch subsidy scheme and the main financial and technical obstacles. The model is designed to accommodate all envisioned geothermal projects in the Dutch context. Different failure criteria will then indicate if certain inputs are possible in terms of economic or technical limits. These criteria will be further discussed in section 3.4.6. Table 1 shows the input parameters that are already implemented from literature sources. Each element has a certain type, sample frequency and value.

Table 1: Model inputs for the modules of construction, production, financial parameters and economics gathered from literature sources.

Module	Element	Source	type	Sample frequency per iteration	Value	units
Construction	Well cost scaling factor	(section 3.2.1)	Triangular dist. min-mode-max	Once	1.4-1.5-1.8	-
	Network cost urban	[32]	Triangular dist. min-mode-max	Once	800-1000-1100	Eur/m
	Network cost rural	[23]	Triangular dist. min-mode-max	Once	200-300-400	Eur/m
	First well contingency	[est.]	Triangular dist. min-mode-max	Once	100-110-120	%
	Control facility cost	[23]	Data	-	1	MEur
	Injection pump cost	[22] + est.	Data	-	0.5 * ESP cost	MEur
	ESP cost	[33] + est.	Selector	Once	Section 2.3.3.1	MEur
	Heat exchanger cost	[22]	Data	-	35	KEur/MW
	Gas separator cost	[34]	Data	-	1	MEur
	Co-generator cost	[35]	Selector	Once	Section 2.3.3.3	
	Abandonment cost	[36]	Data	-	125	KEur/well
	Unforeseen cost	[37]	Triangular dist. min-mode-max	Once	5-8-12	% of constr. cost
Production	Energy gas HHV	[38]	Data	-	35.17	MJ/m^3
	Energy gas LHV	[38]	Data	-	31.65	MJ/m^3
	Co-generator input & output	[39]	Selector	Once	Section 2.3.3.3	-
	Temperature loss tubing	[40]	Triangular dist. min-mode-max	Once	1-2-3	°C
	Control facility efficiency	[est.]	Triangular dist. min-mode-max	Once	94-96-98	%
	Pumps efficiency (prod + inj.)	[33], [41], [37]	Triangular dist. Min-mode-max	Once	55-65-70	%
	ESP failure interval	[33]	Truncated Normal dist.	Once	Mean: 5 Min: 4 S.d.: 0.8	Years
	Downtime ESP replacement + well overhaul	[33] + est.	Triangular dist. Min- mode-max	Every year	10-15-20	days
	Workover cost	[36]	Triangular dist. Min-mode-max	Every 5 years	30-250-1200	KEur
Financial parameters	Inflation rate	[est.]	Data	-	1.5	%
	Cost of debt	[42]	Data	-	2 (nominal)	%
	Cost of equity	[42]	Data	-	14.5 (nominal)	%
	Gas price	(Section 2.5.2)	Prediction data	Every year	Section 2.5.2	Eur/kWh
	Electricity price	(Section 2.5.3)	Prediction data	Every year	Section 2.5.3	Eur/kWh
	Electricity Tax	[43]	Data	-	0.01404	Eur/kWh
	SDE+ 2018 prices	[44]	Data	-	Section 2.5.1	Eur/kWh
	Depreciation rate	[45]	Data	-	6.67	%/yr
	Corporate tax	[46]	Data	-	25	%
	Drilling insurance	[47]	Data	-	7	% of constr. cost
Economics	Fixed OpEx	[41]	Data	-	5% of initial investment	Eur/year
	Heat price	[48]	Data	-	90% of Gas price	Eur/kWh

The project specific data that is required to run the model are shown in Table 2. If parts of this data are not provided by the operator, default values are inserted in the model.

Table 2: Project specific data requested from the geothermal operator. The default values are formed from a combination of estimations and data from existing geothermal projects. Default values are shown instead of the values of the case study due to their confidentiality. Data can be delivered as probability or fixed values. Drilling cost are not included here but are calculated by the model as a function of depth, market value and learning curve (3.3.1).

Stage	Input	unit	Default value
Exploration	Cost	KEuro	150
	Duration	yrs	1
Wells	# of wells	#	2
	Temperature:		
	production (per well)	°C	85
	Injection (per well)	°C	35
	Depth wells		
	MD production well(s)	m	2600
	MD injection well(s)	m	2350
	TVD Production well(s)	m	2300
	TVD Injection well(s)	m	2200
Pumps	production pressure difference at ESP per well at maximum capacity	bar	30
	Flow rate per doublet	m^3/h	300
	injection pressure difference per well at maximum capacity	bar	40
Heat network	Length	m	1000
	installation time	days	20
Drilling location	Cost of drilling area (preparation and installation)	MEur	1
Gas production	Gas/Water ratio	m^3/m^3	1
Demand	Average demand of heat on yearly basis	% of max capacity	95% Winter 80% Spring 50% Summer 75% Autumn
Project lifetime	Years until estimated abandonment after first production	years	40
Brine calculations	Salinity	ppm	120000
	Pressure heat exchanger	bar	30
Financing	Loan duration	Years	15
	Debt percentage	%	70

3.2 Exploration

The first phase of a geothermal project consists of the exploration phase. Before any exploration can be initiated, a permit needs to be granted from the ministry of economic affairs and climate. To receive this permit, the project operator needs to collect and hand in data of the potential geothermal area the operator wants to explore. These data include a general geological research study also known as a ''quick scan''[23]. If this quick scan shows any potential in terms of the presence of aquifers at the right depth and location, an exploration plan can be made. This plan describes in general terms how the project operator is planning to perform the exploration, exploitation and the location of the potential reservoir and drill site is discussed. Additionally, the operator needs to show that the right preparations are made in terms of safety and health for the people working on site. The final demand for the permit is a declaration of sufficient technical and financial capacities to realize the project. If all these steps are fulfilled and accepted, an exploration permit will be granted for the duration of 3 to 5 years [23]. The owner of this permit is the only one allowed to do any geothermal related drillings in the licensed area, but must do so before three years have passed, or the license will be withdrawn. The estimated time to get a permit is around seven to ten months [23].

When the permit is granted, the project operator initiates a larger, more detailed geological study where historical data from previous drillings and seismic surveys are investigated. In some cases, new seismic data are acquired, which increases the exploration cost substantially. This large study is an important step to realize a project. The gathered data are used for the feasibility study where the economic potential of a project is evaluated. With information from the geological study, an estimation is made about the expected capacity of the doublet. For the finances, subsidies and insurances a 90% estimation certainty of the capacity is referred to for the potential of a project. This ''worst case'' scenario is taken to avoid over optimistically estimations and to account for any production decrease during later production stages. In general, the actual production capacity of most projects is usually between the P70 and P90 estimated capacities [49].

If all previous steps are successful and satisfactory, a drill design can be made. With this design, multiple drill options and locations are considered, and their cost is determined together with the potential production capacities and risks. After completing this step an area permit (in Dutch: Wabo) can be requested which usually takes up to 8 weeks to complete. When this permit is granted the drilling and installation of the required equipment can be started.

For the exploration phase the model has two main inputs: the exploration time and cost. This exploration time is taken after the exploration permit is granted. The default values are given in Table 2.

3.3 Development

The development module includes the drilling of the wells, the installation of the heat network and purchasing and instalment of the equipment necessary for operating a geothermal project. The projects total investment is made out of the construction, exploration, unforeseen and insurance costs. These individual cost items are introduced and explained in the following sections.

3.3.1 Well Drilling

Geothermal drilling expenditures can account for more than 60 to 75% of the total project investments [50]. An example of the main individual variables influencing the costs of drilling and completion of a 2400 m geothermal well are shown in Figure 7:

INDIVIDUAL WELL COST DRILLING AND COMPLETION
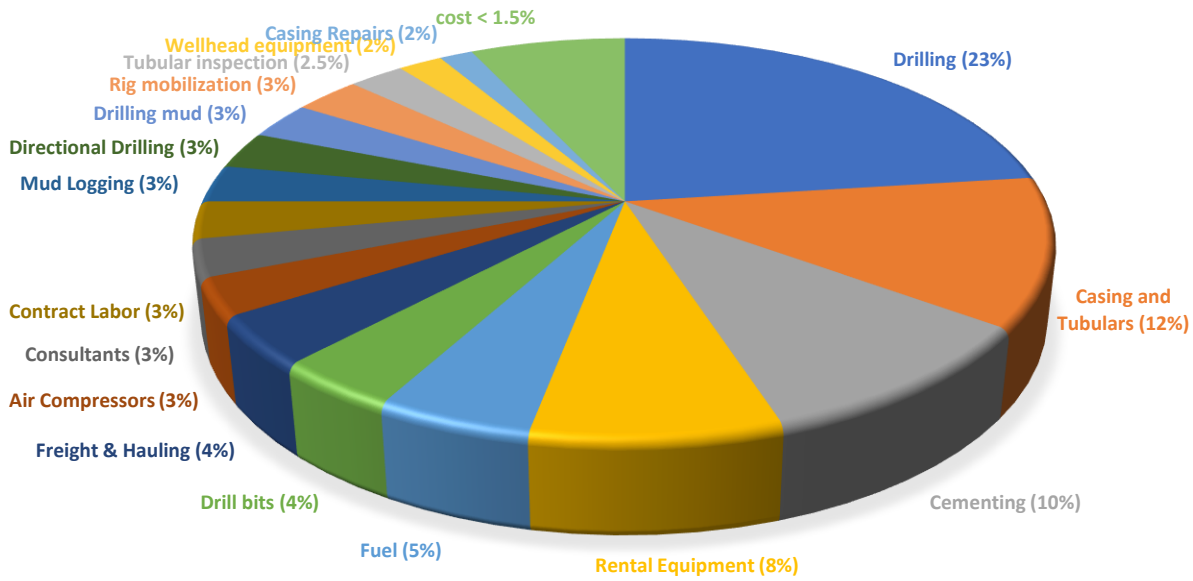
Figure 7: Individual cost categories for a 2400m EGS well. A hydrothermal well is often drilled in softer rock that could increase the rate of penetration (ROP) and therefore, lower the drilling costs compared to the denser rock found in EGS. On the other hand, lower ROP due to the loss of mud circulation is a common problem when drilling more porous rock as found in hydrothermal wells. In general, the differences in formation lithology and various location specific costs, reduces the overall cost variability by only 11%. [50]

For the drilling cost per well as function of depth, the equation from [51] is used for the model:

$$C_{well} = s * (0.2 * Z^2 + 700 * Z + 25000)`$$

Eq. (1)

Where,

C_{well}: Cost per well (Euro)
s: Well cost scaling factor
Z: Well depth measured along hole

The cost for drilling a well can change depending on many factors in the market. If the market conditions were to fluctuate significantly, the well scaling factor can be adjusted according to the latest market conditions. Van Wees et. al. [41] uses a default value of 1.5. Due to the high uncertainty of this approach, the value for the well cost scaling factor for the model is sampled between 1.4 and 1.8 instead of a fixed value. These boundaries are selected from plotting a combination of Equation 1 and two other well drilling cost approaches, as explained below. The three methods are plotted in Figure 8.

The first approach from [25] consists of a cost study of an extensive US and non-US database of 104 hydrothermal and EGS wells drilled between 1972 and 2002 and 42 wells drilled between 2008 and 2013. The equation used for this approach is:

$$C_{well} = (1.72 * 10^{-7} * Z^2 + 2.3 * 10^{-3} * Z - 0.62) * E_c$$

Eq. (2)

Where,
Z: Well depth measured along hole
E_c: Conversion factor Dollar to Euro of 0.87

The second study, performed by [50] includes probability distributions that are determined based on detailed cost records of U.S. geothermal wells drilled or designed from 2009 to 2013, as well as cost data from drilling equipment manufacturers and vendors. The depth range from this study is limited from 2400 to 4600m. The equation used for this approach is:

$$C_{well_{P50}} = 3.56 * \exp(2.72 * Z) * E_c$$ Eq.(3)

The P50 value from this distribution is plotted in Figure 8:

Figure 8:Well cost as function of Depth. Equation 1 is taken from van Wees(x), where x represents the well cost scaling factor. Equation 2 and 3 are referred to as Lukawski1 and Lukawski2.

The distribution boundaries for the model are shown in Figure 9 where Equation 1 is plotted with a scaling factor of 1.4 and 1.8. Cost uncertainty increases with depth as shown by Figure 9. This increase of risk is the result of the increased likelihood of difficulties during drilling and the less predictable drilling conditions with increasing depth [50].
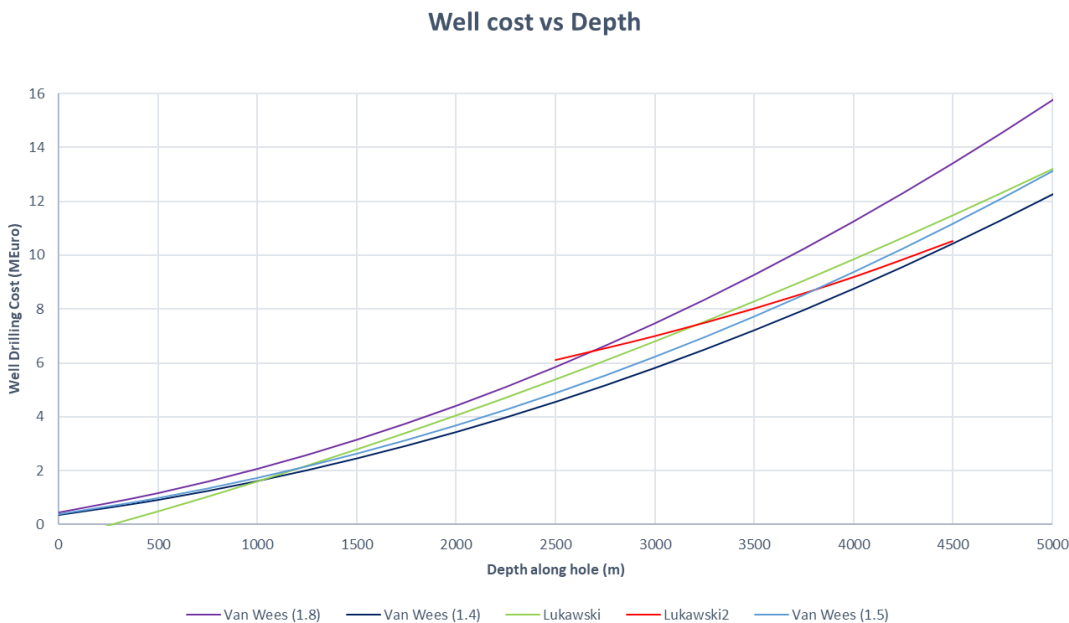
Figure 9: Well scaling factor boundaries inserted. Equation 1 is indicated by van Wees(x), where x represents the well cost scaling factor. Equation 2 and 3 are referred to as Lukawski1 and Lukawski2.

The first well in a geothermal, oil or gas field is drilled with limited prior knowledge about the formation characteristics. Because of this reason, these wells are riskier and take more time to drill which in turn increases the cost. A contingency element is added to the first well that samples a possible increase in cost due to unexpected difficulties during drilling operations (Table 1).

The experience gained from the first well combined with an increased knowledge of the subsurface, results in a learning curve. Estimations about this learning curve for geothermal drilling were done by [25] and are inserted in the model in the form of best, average and worst learning curve (Figure 10). The learning curve element is sampled once per iteration with an equal probability for each curve. The learning fraction is then added to each additional well drilled. In a case where more than two wells are drilled, this learning curve can have significant positive results in terms of the feasibility of a project. An industry average for the 6th well for example is likely to cost no more than 78 percent of the first well [25]. This so called upscaling of geothermal projects is seen as one of the key elements in lowering geothermal production costs for future projects [17].
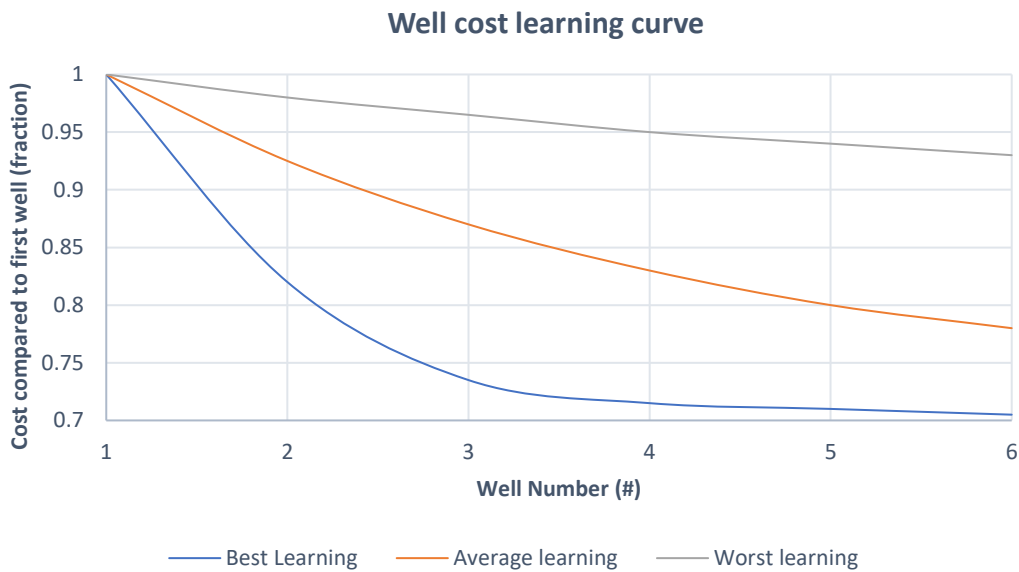
Figure 10 Well cost learning curve as function of the number of wells drilled [25]

In Figure 11, the well drilling cost method from the model is compared to the average historical well drilling costs of 14 Dutch geothermal doublets as described in [22]. The cost differences are small, with the model cost results being 200 kEuro less compared to the SDE+ calculations. If a learning curve from past projects is considered, this difference is easily justified.
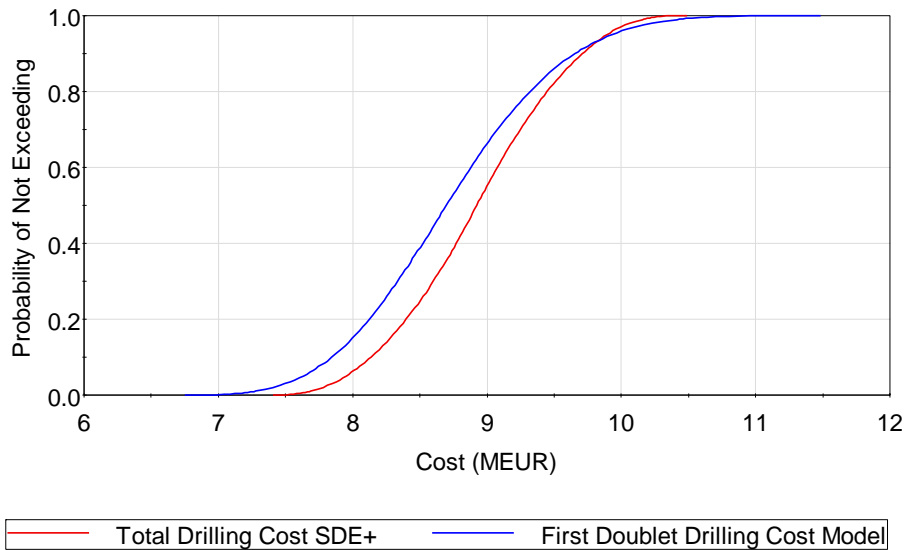
Figure 11: Comparison of the estimated drilling cost of a Dutch geothermal doublet between average historical data of 14 existing projects and the model results of the reference scenario after 15000 iterations. The SDE+ drilling cost is only dependent on the capacity of the wells whereas the drilling cost of the model is calculated as a function of the depth, scaling factor and learning curve.

The drilling cost for SDE+ calculation is calculated as 777 euro per realized kW_{th} capacity of the doublet (Figure 12) [22]. For an unrealized project in the model, the well cost is calculated as 80% of the expected P50 capacity. This 80% factor is referred to as the power realisation factor and will be further elaborated in scenario 5: SDE+ realisation factor correction.
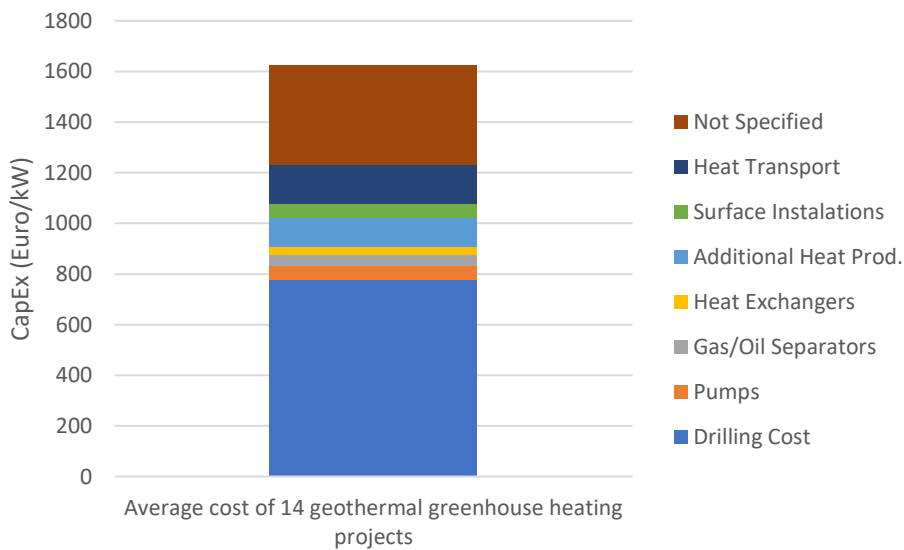
Figure 12: Average Capital expense per category of 14 realized greenhouse heating projects.

3.3.2   Heat Network

To transport the heat to greenhouses, buildings and homes, a heat network needs to be installed. The cost of this network is dependent on multiple factors such as pipe diameter, insulation, length and location. The model samples a distribution for the network cost dependent on the length and location for the different design possibilities as mentioned above. Installation in rural areas is cheaper compared to urban areas due to shorter installation times, lower costs considering less traffic control needed, more working space available and less strict policies. The cost per length for each area are given in Table 1.

In terms of timing an assumption is made that the network is installed and paid for after a successful production test of the first well. The second well is drilled simultaneously with the network installation. This is done to decrease the risk of the investment. When a first well is successful in terms of sufficient production capacity,

the risk of project failure decreases significantly. If the distribution network is installed after the completion of the second well, precious production time could be lost due to potentially large installation times.

For district heating purposes in the Netherlands, the heating network installation and client connections are considered the responsibility of an energy operator [37]. In other words, a geothermal operator is only responsible for supplying the heat from reservoir to heat exchanger. Because of this, an option is available in the model to exclude the cost of network instalment if desired so that the geothermal revenues received are exclusively from the amount of heat delivered to the energy operator.

3.3.3 Equipment

A geothermal project can be designed in multiple ways. In Dutch geothermal projects, a few standard parts of equipment are considered necessary. For the circulation of the water, three pumps are installed. One circulation pump at the surface, an injection pump and an Electrical Submersible Pump (ESP) which is inserted inside the production well. The energy from the produced water is extracted with a heat exchanger. The chances of producing some form of hydrocarbons combined with the water is considered high when producing from the Dutch subsurface [34]. This high probability of hydrocarbon production makes it a necessity to buy and install a separator to separate the gas from the fluid. This gas can then be sold to a nearby grid or burned in a generator and/or boiler. Other, smaller parts of equipment include screens and filters to separate the sand, corrosion and other fine particles from the production water. Lastly, equipment for controlling and measuring the production process is installed. This controlling equipment and other smaller equipment necessities are considered in the model as the cost for the control facility. Some costs for the equipment are largely dependent on the capacity of the project. This is implemented in the model for the co-generator, heat exchanger and ESP which will be further elaborated in the upcoming chapters.

3.3.3.1 ESP

The ESP string, consisting of a motor, seals and pump, is an important part in the geothermal system. It lifts the water to the surface for heat harvesting purposes. For the design of the ESP an inflow curve needs to be derived [33]. This can be done by performing a well inflow/delivery test or by inserting estimated values for aquifer transmissivity, skin factor and friction losses in the casing and tubing. From this curve, the ESP power rating can be determined for the desired production flow rate and pressure difference at the well head. The components of the ESP string together with the power cable, transformer and speed drive each have their own efficiency. All these parts combined have an overall efficiency of at least 55% [33]. In Dutch geothermal wells, most ESP pumps are made by Baker Hughes. Only the well of Duijvestijn tomaten has an ESP installed from the company Canadian advanced ESP [33]. Baker Hughes estimates an average lifetime of 5 years can be achieved in Dutch geothermal applications with increasing lifetime in the near future [33].

Logically a higher-powered ESP is more expensive compared to lower powered pumps. Therefore, different ESP's are considered in the model in terms of price and power as shown in Table 3. The prices are partly taken from [33] and pumps exceeding 0.8 MW are estimated prices due to the limited availability of cost data. The power calculation is done in section 3.4.4 from which an ESP can be selected in this module. The ESP replacement interval is given in Table 1. The downtime of replacing the pump is, with proper planning, estimated to be around 2-3 days if a reserve pump is stored prior the replacement date. In the model, the downtime of the replacement of the ESP is combined with the overall well maintenance time (Table 1).

Table 3: ESP cost in relation to pump capacity.

Capacity ESP (MW)	Estimated Cost (kEUR)
< 0.5	300
0.5 − 0.8	600
0.8 − 1.0	800
1.0 − 1.2	1000
> 1.2	1200

3.3.3.2 Gas separation unit

To this day, almost every geothermal well drilled in the Netherlands contains some dissolved gas in the produced water. In one particular case even some additional oil is produced [34]. Because of this, a gas separation unit or degasser is considered for purchase before initial production commences if production testing indicates gas present in the production brine. This so called ''bycatch'' cannot exceed a yearly average of 3.6 m^3 of gas phased hydrocarbons per m^3 of water or 5m^3 of oil per day [34]. In a case where the production does exceed this limit, but the hydrocarbon production alone isn't financially feasible, the geothermal licensee and the hydrocarbon licensee at that location need to discuss how the potential earnings should be divided. In a case where the amount of hydrocarbons is economically feasible on its own, the geothermal license is no longer valid, and a new hydrocarbon license needs to be requested if there is no license already active. The new hydrocarbon licensee is then allowed to produce the hydrocarbons and geothermal heat combined if desired. No additional geothermal license is required [34].

For most scenarios in the model it is assumed that the gas/water ratio is greater than zero at initial production stages. Therefore, a gas separation unit will be bought when the first well is successfully drilled.

3.3.3.3 Co-generator

For the model, different sizes of generators are considered depending on the gas produced at full capacity. As a reference, the brand Jenbacher [39] is chosen which is the same brand used at the geothermal site of Duivesteijn tomaten. Four different generators can be selected in the model, each with a different input, efficiency, output and price, as shown in Table 4.

Table 4: Generator specifications [39]*.*

Type (Jenbacher)	J312	J320	J420	J616
Energy input (kW)	1015	2697	3443	5860
Electrical efficiency (%)	39.9	39.6	41.4	45.7
Thermal efficiency (%)	49.1	49.4	47.2	42.4
Estimated price (KEur)	350	600	800	1200

3.3.4 Abandonment plan

When one or more wells do not deliver the required amount of heat to keep a project feasible, the well will be abandoned when further exploitation is not possible or desired. This moment is in most cases at the end of a project lifetime but can also happen close after realizing a well if it keeps performing under a feasible threshold [36]. The operator must close the well and has to return the wellsite to the original setting. The ministry of economic affairs expects that an operator has enough financial reserves to safely abandon the wells at all times [36].

In the model, abandonment is initiated at the end of a project expected lifetime. All wells will be plugged and abandoned and paid for simultaneously.

3.4 Production

This module computes the generated heat production, gas production, pump power requirements, the associated costs and the specifics of the co-generator in terms of gas input and heat and electricity output.

3.4.1 Heat production

The geothermal energy from a production well can be calculated using Equation 4:

$$P_{well} = q * \Delta T * C_{brine}$$

<div align="right">Eq.(4)</div>

Where,

P_{well}: Thermal power well (W)
q: Flow rate (m³/s)
ΔT: Temperature difference producer-injector (C°)
C_{brine}: Volumetric heat capacity of the brine (J/m³*K)

The thermal power of the well is calculated from aquifer to wellhead where a temperature loss from aquifer to the surface is considered. At the time of first production, this temperature loss is significantly higher compared to tubing heat losses in later production stages, due to the cooling effect of the surrounding rocks. With time, these rocks get heated themselves and the cooling of the ascending fluid changes to a constant rate (Table 1) [52]. For the model this warming up period is estimated to take 2 years [52], with an initial temperature loss of 5% of the aquifer temperature on top of the constant heat loss temperature.

The volumetric heat capacity is calculated as a function of the specific heat and the density of the brine. The density of the brine is determined using the polynomial equation from [53] as a function of the temperature, pressure and salinity at the heat exchanger location as shown by Equation 5 and 6:

$$\rho_w = 1 + 1 * 10^{-6} \left(\begin{array}{c} -80T - 3.3T^2 + 0.00175T^3 + \\ 489P - 2TP + 0.016T^2P - 1.3 * 10^{-5}T^3P \\ -0.333P^2 - 0.002TP^2 \end{array} \right)$$

<div align="right">Eq.(5)</div>

And

$$\rho_b = \rho_w + S \left\{ \frac{0.668 + 0.44S + 1 * 10^{-6}}{[300P - 2400PS + T(80 + 3T - 3300S - 13P + 47PS)]} \right\}$$

<div align="right">Eq.(6)</div>

Where,

ρ_w: Density water (g/m³)
ρ_b: Density brine (g/m³)
T: Temperature at heat exchanger (°C)
P: Pressure at heat exchanger (MPa)
S: Salinity as weight fraction (ppm/1e⁶)

The specific heat capacity at a constant pressure (C_p (J/kg°C)) is then calculated using the equation from [54]:

$$C_p = 4180 - 4.396 * \left(\frac{S}{100} \right) * \rho_b + 0.0048 \left(\frac{S}{100} \right)^2 * \rho_b^2$$

<div align="right">Eq.(7)</div>

The volumetric heat capacity in (J/m³°C) is then obtained with a simple multiplication:

$$C_{brine} = C_p * \rho_b$$

<div align="right">Eq.(8)</div>

To get this heat from well to customer, the energy needs to be passed through well head, surface pipes, heat exchanger and network. These steps result in further heat loss. For the model, the doublet can be designed at customer level where the desired well capacity from Equation 4 is used as an input and heat losses from the network are considered. The installed effective capacity therefore needs to be higher to make up for the heat network losses as shown by Equation 9. If the project is designed for district heating purposes, where the heat is delivered to the network operator, only the heat loss of the wellhead, surface piping and heat exchanger is considered.

$$P_{system} = P_{well} \left(\eta_{facility} * \eta_{transm} \right)$$

<div align="right">Eq.(9)</div>

Where,

P_{system}: Thermal power capacity system (W)
P_{well}: Thermal power capacity well (W)
$\eta_{facility}$: Efficiency surface facilities (%)
η_{transm}: Efficiency heat network (%)

A geothermal system in the Netherlands often does not produce at full capacity all year round. Especially with district heating, heat demand in the summer is significantly lower compared to the winter months [20]. To implement this fluctuation, a daily demand element is inserted in the model. The required effective flow rate at a certain installed capacity can be determined using Equation 10:

$$q_{eff} = \frac{P_{well}}{\Delta T * C_{brine}} * f_{m\,seasonal}$$

Eq.(10)

Here $f_{m\,seasonal}$ is inserted as a daily percentage of the maximum capacity of the system. q_{eff} therefore, can change on a daily basis.

3.4.2 Gas production

An initial gas/water ratio is given as an input for the model in m³/m³. With this ratio, the amount of gas produced is calculated using the effective flow rate from Equation 10. Considering the expected lifespan of a geothermal system, the probability is high for this ratio not to be stable throughout the project's lifetime. Therefore, an option is added to the model where the expected moment of first decline in years after initial production can be inserted together with the rate of decline in percentage per year. This is an input requested from the project operator if available. If this number is not available, a stable ratio will be considered for the reference case due to the large uncertainty for this input.

3.4.3 Co-Generation

If an operator is not willing or able to sell the produced gas, a co-generator could be purchased to utilize the gas, to generate electricity and heat. To determine the capacity of the co-generator, the total calorific value of the gas is determined at maximum production using the net calorific value (LHV) of 31.65 MJ/m³ [38].
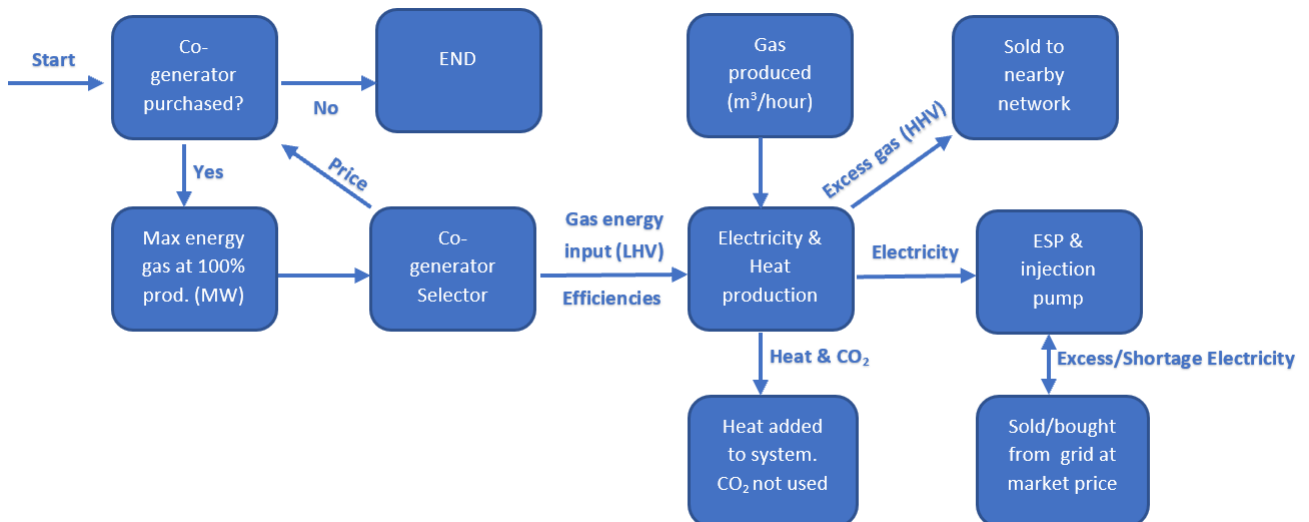
Figure 13: Co-generator flowchart. The CO₂ generated by burning the gas is not further used in the model.

Any excess gas would be minor but can be sold, assuming no extra costs for transportation. The electricity will be used in situ for the equipment on site. Any excess or shortage of electricity for this setup can be taken or inserted from the grid at the electricity market price at that time. This market price will be further elaborated in the chapter financial parameters. An overview of the model's co-generator process is given in Figure 13.

Nearly half of the generator output is in the form of heat. This heat can be used to further increase the production temperature if required. The general efficiency of this process is between 95 − 98 % [21]. In a scenario where a co-generator is bought, this heat is combined with the geothermal heat produced. CO_2 gasses from the burning of the gas can be usefully inserted inside the greenhouses for greenhouse growing processes or could be potentially sold to a CO_2 grid nearby. The further use of CO_2 is not implemented in the model. Figure 14 shows an example result of the output of a co generator.
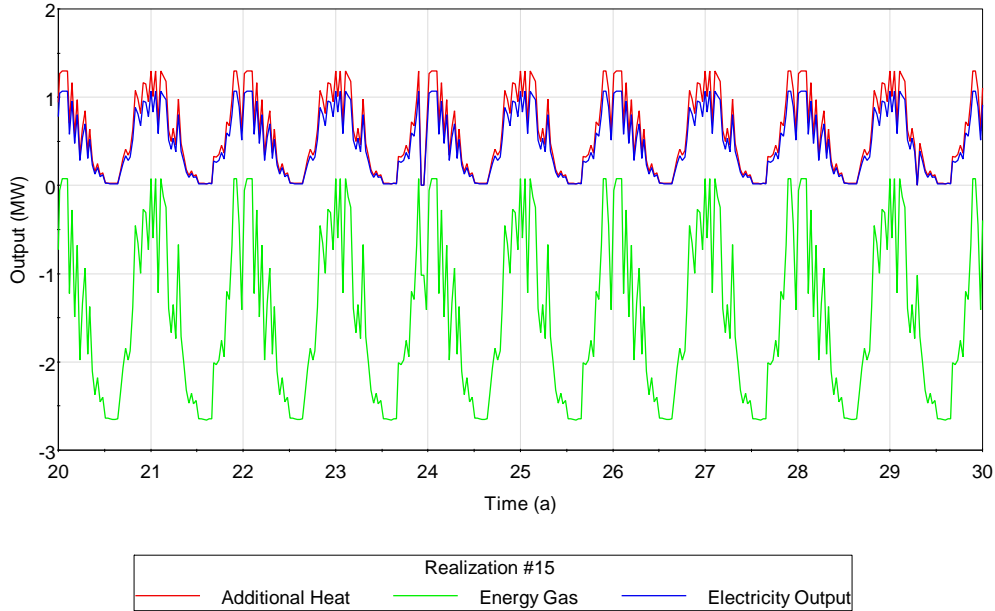
Figure 14: Heat, electricity and gas output example of a single iteration of the co-generator scenario. The energy of the gas is calculated by converting the volume of gas to the LHV of the gas. A negative gas output indicates the part of energy that is consumed by the generator. Very little excess gas is left over at maximum gas input when the generator's capacity fits the amount of gas available.

3.4.4 Pumps

A good way to indicate the performance of a geothermal system is using the Coefficient of Performance (*CoP*). The *CoP* indicates the ratio of the produced thermal power (P_{well}) over the energy needed by the pumps (P_{pumps}) as shown by Equation 11:

$$CoP = \frac{P_{well}}{P_{pumps}}$$

Eq.(11)

The power needed for the ESP and injection pump is calculated using a slightly revised Equation from [20]:

$$P_{pumps} = \frac{\Delta P * q}{\eta}$$

Eq.(12)

Where,

P_{pumps}: Power Pumps (W)
ΔP: Pressure difference (Pa)
q: Flow rate (m³/s)
η: Efficiency pump (-)

The pressure difference ΔP supplied by the pumps is made up of three components [55]:

1. Reservoir pressure drawdown

$$\Delta P_r = \left(\frac{q*\mu}{2\pi kh}\right) * \ln\left(\frac{d_p}{r_w}\right)$$

Eq.(13)

Where,

μ: Viscosity (Pa.s)
k: Permeability (m^2)
h: Thickness net reservoir (m)
d_p: Length between wells (m)
r_w: Well radius (m)

2. Skin pressure effect

$$S = \frac{k-k_v}{k_v} * \ln\frac{r_v}{r_w}$$

Eq.(14)

$$\Delta P_S = S * \frac{q*\mu}{2\pi kh}$$

Eq.(15)

Where,

S: Skin (-)
k_v: Permeability damaged zone (m^2)
r_v: Radius damaged zone (m)

3. Casing and tubing friction losses

$$\Delta P_f = 4f * \frac{1}{2}\rho * v^2 * \frac{L}{D}$$

Eq.(16)

Where,

f: fanning friction factor (-)
ρ: Solution Density (Kg/m^3)
v: Stream velocity (m/s)
L: Length well (m)
D: Diameter well (m)

The pressure difference from Equation 12 is then calculated by combining equation 13, 15 and 16:

$$\Delta P = \Delta P_r + \Delta P_s + \Delta P_f$$

Eq. (17)

Subsurface uncertainties in aquifer properties, like reservoir depth and temperature, typically range between 5 and 10%. The uncertainty of the net transmissivity however, which is the product of the net aquifer thickness and permeability commonly ranges in the order of 300 – 3000% [51]. These high uncertainties are caused by the large possible heterogeneity of the aquifer in Net-to-Gross ratio, thickness, aquifer permeability and fault permeability.
To produce at a sufficient flow rate (150 – 250 m3/hr) within reasonable pump efficiencies, the transmissivity of the net aquifer need to be at least 10 to 15 Dm [55]. The minimal net thickness of an aquifer in the Netherlands is set to be 20m [18], [55]. With a net aquifer thickness of 20m, the aquifer's permeability should be at least 500 mD to reach the lower limit transmissivity of 10 Dm.

In general, a well as injector is substantially poorer in performance and thus requires higher pump pressures than using the same well as producer [56]. There are two ways in which a geothermal injection well differs from a producer well: The low temperature from the injection brine results in higher density and viscosity of the fluid, compared to the warmer brine from the production well. A higher density increases the well injection rate, whereas a higher viscosity decreases this rate. TNO has studied the impacts of these two factors and concludes that the viscosity has, in most cases, the dominant effect [56]. In Dutch geothermal wells, the viscosity of cold injected brine is approximately 1.5 to twice as high as that of production brine depending on the temperature difference. The difference in viscosity explains very well why the observed injectivity is occasionally 2/3 to half the equivalent of the production well [56].

Skin is a dimensionless factor calculated to determine the production efficiency of a well by comparing actual conditions with theoretical or ideal conditions. A positive skin value indicates some damage or influences that are decreasing the permeability around the well bore. A negative skin indicates enhanced permeability. A positive skin can be partly the result of insufficient cleanout of the wells after drilling, leading to a mix of drilling fluid solids, drilling grease and formation solids forming a filter cake potentially in both wells [56]. Additionally, added skin can be caused by the wrong use of filters, alternated brine composition, and scaling in the form of calcium carbonate precipitation as a direct result from cooling the brine and degassing the brine from CO_2. Degassing the brine from CO_2 results in a more alkaline environment where soluble bicarbonate in the brine changes to insoluble carbonate [56].

The pressure difference from casing and tubing friction losses is dependent on the flow velocity, composition of the brine, tubing roughness, length and diameter of the well. Geothermal wells are often drilled in a standard doublet layout with two deviated wells from the same surface location. The large distance between the wells at aquifer level, increases the overall length of the wells and increases the pumping energy required. Additionally, a large distance increases the drilling cost and the chance on poor reservoir connectivity as a result of geological flow barriers such as sealed faults and poor sandstone body connectivity [28].

Overall the components from Equations 13 - 16 are highly dependent on a collection of reservoir and fluid characteristics, well design decisions and operational practices [56]. Therefore, the pressure difference for the wells is requested from the project operator. These estimates are collected from simulation data prior to production testing. Hence that the quality of the reservoir studies and simulation data have major influence on the risk of an underperforming geothermal system. Especially when the desired well capacity is nearing technical and policy limits.

The pressure difference from Equation 13 and 15 are linearly dependent on the flow rate. Equation 16 however, is not. Friction in the borehole increases exponentially with increased flow rates, which in turn limits the performance of the pumps [51].

The pressure difference provided from the operator would preferably be the pressure at full capacity of the well. When the pressure at full capacity is provided, an assumption can be made that the flow rate and pressure difference behave linearly with decreasing flow rates at lower demands. This assumption is a simplified (over) estimation of the pressure difference in the well but would be far more ideal than recalculating the Fanning friction factor as a function of the Reynold number and pipe roughness with every change in the flow rate.

3.4.5   Workovers

The maintenance of a geothermal system is done regularly throughout its production life. When a so-called work-over operation is performed, the production is temporally seized to perform inspections and maintenance on the wells. This is preferably done when the ESP is scheduled for revision or replacement [57]. Main operations consist of removing possible build-up of sands and corrosion particles. In the model, a triangular distribution is inserted based on Table 5 where the minimum cost for a workover would be a lab test (30k Euro). The most likely value is set on 250k Euro and the worst-case scenario (P100) would be 1.2 million Euro. This amount seems a bit excessive, because high cost stimulation workovers should not be necessary every 5 years or so, but a scenario similar to the doublet of Ammerlaan for example, where the production tubing got fractured after a few years of production due to a design flaw should be considered in the model as well in terms of repairing cost. The specific amount for this repair is not openly specified but could easily exceed the cost for a general stimulation workover as shown in Table 5. With the distribution as described above, the mean overhaul cost (ESP replacement + workover) in the model is around 230 kEuro/year. In a general geothermal business case a reserve of 250k euro per year for ESP and general workovers is common [37].

Stimulation method	Description	Estimated costs (kEur)
Lab tests	Control and sample analysis	30 (max 50)
Well inspection	Visual inspection casing and filters	30
Clean out	Coiled tubing cleaning	150
Reversed circulation	Cleaning due to reversing injector - producer	300
Twin-pumps	Extra production pump in injection well	400
Hydraulic stimulation	High pressure skin removal and creation of fractures	400/well
Propped Frac	Hydraulic stimulation combined with sand injection to keep fractures open	600/well

3.4.6 Failure Criteria

The model is developed in a way that every conceivable project can be inserted. Failure criteria are inserted that indicate if certain inputs are feasible in terms of economic or technical limits. The first criterion involves the injection pressure. The maximum injection pressure mainly depends on the permeability of the reservoir, the density of the brine and the depth of the well. A general maximum tubing head pressure is set in the Wabo exploitation plan as a lower safety limit to avoid unintentional fracking or subsidence when injecting the cooled brine back into the reservoir [58]. The maximum tubing head pressure is given by Equation 18:

$$Max\ THP = TVD_{inj} * (0.135 - grad.\,inj\ brine)$$
<div align="right">Eq.(18)</div>

Where,

$Max\ THP$: Maximum tubing head pressure injection well (bar)

TVD_inj: True vertical depth top reservoir injection well (m)

$Grad_{inj.brine}$: Hydraulic gradient injection brine

The density of the injection brine is higher compared to the produced brine due to its temperature and pressure. This is calculated using the equations used in section 3.3.1. If the pressure criterion is triggered, a warning is given in the model when the simulation has completed. If the injection pressure is exceeding the limit with a minor margin, extra research on the horizontal stresses of the area in question could be requested to approve these injection pressures. When this limit is exceeded with a larger margin however, production flow rates should be adjusted accordingly.

The next criterion is based on the Coefficient of Performance. The lower limit for the model for the case study is set at 10. This limit is 5 units lower than the targeted CoP of 15 that is used in [41] and [51]. A CoP of 15 is much harder to achieve at peak demand for district heating projects compared to the greenhouse heating projects where the lower limit of 15 is based on. This is due to the volatile heat demand associated with district heating. Demand spikes for short periods of time, characterized by a low, but positive CoP are less costly compared to limiting the overall capacity of the geothermal system to stay above a CoP of 15. Additionally, the concept of CoP can be considered limited. The CoP is based on the energy ratio of heat and electricity but should also include the price ratios of these energies to make better estimates of the lower limit of this number. Nevertheless, when the limit of 10 is reached, a warning is given by the model. Simultaneously, the maximum heat demand is corrected with a -10% adjustment by the CoP adjuster element. This should be enough when the model was just exceeding the CoP limiter. In a case where the limiter is exceeded by a larger margin, this correction should be adjusted to higher correction percentages accordingly.

3.5   Financial parameters

For this module, subsidy, taxes, depreciation and the financing option are discussed. Also, prediction scenarios are given for the future gas and electricity prices. The future gas price in particular is essential for a geothermal project in the Netherlands. Potentially high future gas prices could function as a good incentive to boost the geothermal sector. Another important aspect concerning future gas prices are government policies making the price of geothermal heat dependant on the price of gas. If this gas price dependency stays in the future, an overview of future gas price predictions is essential for economic performance measurements of a geothermal project. Gas and electricity prices are also important for a project's operational expenses. Potential produced gas can be sold or inserted in a co-generator or boiler. If an operator chooses to directly sell the produced gas, Income is dependent on the price of gas and the cost of electricity required for the pumps.

3.5.1   SDE+

The SDE+ subsidy provides financial compensation for producers of renewable energy. In the case of geothermal energy production, the maximum subsidy period is set to 15 years, with a total of 6000 to 7000 full capacity subsidized production hours per year (approx. 68.6% to 79.9% respective load factor), depending on the reservoir depth of the project. In 2016, additional heat production scenarios were added to apply for the grant. These include producing geothermal heat from one or two abandoned gas or oil wells and expanding existing projects with one extra well in the form of a triplet well setting [59].

Table 6: SDE+ 2018 prices

SDE+ 2018 Geothermal *Prices in Euro/kWh*	Base Sum	Correction sum (2018)	Base price	Full Cap. hours	Subsidy years
> 500m	0.053	0.017	0.016	6000	15
Oil/Gas well >500m	0.053	0.017	0.016	6000	15
Extra well (triplet) >500m	0.034	0.017	0.016	6000	15
> 3500m	0.060	0.017	0.016	7000	15

The cost price of the thermal energy production is set as the base sum and does not change during the subsidy period. The market price of the renewable energy is established in the correction sum and is revised at the end of each year. The minimum market price of the geothermal heat is set in the base price and does not change during the subsidy period. The SDE+ contribution consists of the difference between the base sum and the correction sum [59] (Equation 19).

$$SDE\ subsidy = Base\ Sum - Correction\ sum \qquad \text{Eq. (19)}$$

Where,

$SDE\ subsidy$: Subsidy per kWh produced (Euro/kWh)
$Base\ sum$: Cost of heat (Euro/kWh)
$Correction\ sum$: market price of geothermal heat (Euro/kWh)

The prices for SDE+ 2018 are given in Table 6. Dutch research institution ECN revises its recommendation each year for the way the correction sum is calculated. For SDE+ 2018 the correction sum is calculated as 90% of the Dutch gas market price (TTF) (Equation 20) [48]. The TTF price is based on the High Heating Value (HHV) of gas. The amount of heat released during the combustion of gas is set in the Low Heating Value (LHV). The conversion from HHV to LHV is equal to 90%. This conversion makes the geothermal heat price equal to the LHV price of gas and makes the level of the SDE+ contribution dependent on future gas price developments.

$$Correction\ sum = TTF * \frac{HHV}{LHV} \qquad \text{Eq. (20)}$$

Where,

TTF: Dutch natural gas market price (Euro/kWh)
HHV: High Heating Value Dutch natural gas (35.17 MJ/m^3)

LHV: Low Heating Value Dutch natural gas (31.65 MJ/m^3)

At the start of a production year, an estimation is made of the gas price and the total heat production for the production year to come. With these estimates, the amount of subsidy is calculated and payed to the producer at the beginning of the production year. At the end of the year, potential differences in terms of amount of heat produced and the actual gas prices are accounted for. For the model, subsidy pay-outs based on yearly estimations are not possible. Therefore, the pay-outs are calculated and added to the overall revenues in real time. In other words, for every kWh produced by the model, a subsidy is received and added to the cash flow.

3.5.2   Future Gas prices

The Nationale Energieverkenning (NEV) is an initiative of the Dutch ministry of economic affairs that provides an overview of the advancements of the Dutch energy management in an international context [60]. Advancements in mostly the exogenous factors like economics, demography, fuel and CO_2 prices, technology and human behaviour have a large influence on the energy management of a country. Therefore, it is inevitable that the NEV price projections are created with high uncertainty [60]. The main goal of the NEV is to create the most plausible future predictions using the most recent insights in the previously mentioned exogenous factors. By doing this, one reference scenario is created: NEV 2017. By implementing a so-called uncertainty bandwidth combining this scenario, a possible range in prices is added to implement the high uncertainties in the exogenous factors.
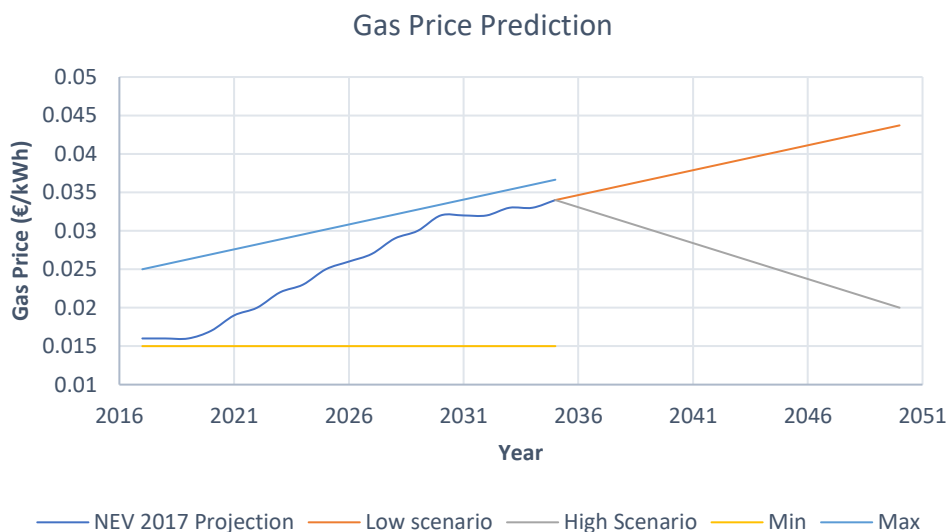
Figure 15: Gas price prediction (uninflated) 2018-2050 [60], [61]

For the model, the reference scenario from NEV 2017 is inserted as the most likely gas price prediction for the years 2018 – 2035 with the uncertainty bandwidth as the minimum and maximum gas price ranges [62] (Figure 15). The NEV scenario is predicted until the year 2035 and has a general increase in gas price for the next 17 years. For the years following this date, a prediction scenario is inserted from the Dutch Centraal Planbureau and the Planbureau voor de Leefomgeving (CPB/PBL) [61]. This agency made two prediction cases for a period starting in 2030 until 2050 categorized as a high or low scenario. These scenarios include the most important uncertainties including global climate policy, fossil fuel reserves, air quality control, technical and economical advancements, political tensions controlling energy supply and technical acceptance of society. Global climate policy is considered as the most dominant uncertainty [61]. Without a global climate policy, greenhouse gas emissions will keep rising and the advancements in technologies low in CO_2 emissions will stay at a minimum [61]. To avoid confusion, the scenario names are switched around and are based on the behaviour of the future gas price instead of economic growth when they are further mentioned in the text. A high scenario indicates increasing gas prices and a low scenario indicate declining gas prices. A ''high'' scenario is a case where low global economic growth is realized combined with limited willingness for international collaboration between countries, with an unsuccessful global climate agreement as a result. This in turn leads to a relatively low

reduction in greenhouse gas emissions, slow decline in the cost of renewable energy technologies and relatively high (fossil fuel) energy prices. The low scenario describes the opposite case where national policies make room for global climate policies where renewable energy technologies flourish and therefore decrease in cost. The general cost for fossil fuels will also decrease, but with stricter climate policies, the demand will fall. The result of the two scenarios on the future gas price predictions are shown in Table 7.

Table 7: High and Low gas price scenario [61]

Year	2030	2050	2030	2050
Scenario	High	High	Low	Low
Euro/kWh	0.035	0.044	0.017	0.020

After 17 years, the low or high scenario will be inserted in the model, each with a discrete probability of 50%. The price slope of the years 2035 to 2050 (time at 17 – 32 years) is calculated using the difference between the scenario's 2050 price and of the last sample of the NEV distribution divided by a period of 15 years. To simulate realistic price fluctuations during these years a standard deviation of 0.001 Eur/kWh is added for each year sampled. For the years 2050 and beyond any prediction of gas price behaviour is realistically impossible due to
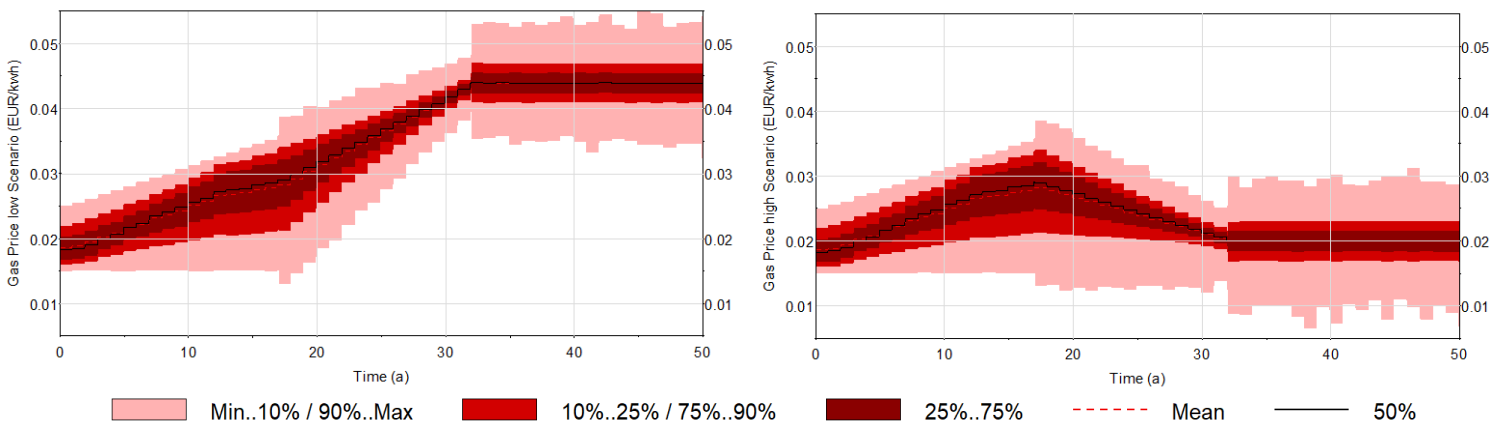
Figure 16: High and low gas price scenario on the left and right respectively. Simulation is run with 15000 iterations.

the high uncertainties of the market behaviour in this time span. Therefore, for these remaining years, the last sampled gas price is taken from the year 2050 (year 32) with an added standard deviation of 0.002 Eur/kWh until the project comes to an end. The distribution of both scenarios when simulated in the model are given in Figure 16:

3.5.3   Future Electricity prices

For the future electricity prices a similar price prediction is done by the NEV 2017 as shown in Figure 17. The most likely scenario predicted by the NEV shows a moderate increase in price due to a pressing effect of the expected growth and overcapacity of renewable energies from the Netherlands and Germany in the coming years [60]. The NEV electricity price projection is directly connected to the future price predictions of gas, coal and CO_2. An increase in fuel and CO_2 prices will result in a similar rise in electricity prices [60]. Again, the NEV price predictions are given until the year 2035. Unfortunately, there is no recent (free) literature available for the expected electricity market behaviour for the years after this date. Therefore, for the first 17 years the electricity price for the model is sampled from the NEV price projection as a median value with the bandwidths as a minimum and maximum price. For the years beyond, the last sampled price is taken from the year 2035 with a standard deviation for each coming year of 0.005 Eur/kWh. This standard deviation is taken from the price range of the NEV projection. On top of the electricity price, a tax is added in the model when electricity is bought from the grid [43]. This energy tax is found in Table 1.
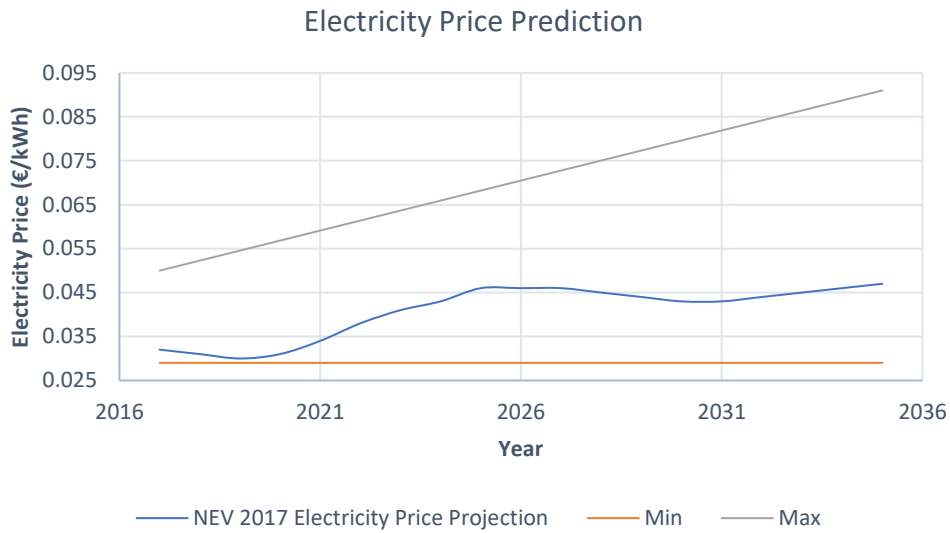
Figure 17: Electricity prices bandwidth and projection 2018-2035

3.5.4   Financing

The way geothermal projects are financed is constantly changing. Not only do the technologies improve with time by learning and innovation, but the risks involved with these kinds of projects are predicted more accurately as more practical experience is gained with time. In general, the riskier the project, the more financing expenses the project bears. In 2018, most Dutch geothermal projects are financed in a 70/30 debt-over-equity ratio. Looking back at earlier SDE+ projects, this ratio could get as low as 40/60 [42]. The cost of debt of geothermal projects in 2018 is set at 2% and is applicable for a so called Groen financiering (Green financing). This saves 0.5% off the cost of debt over some other SDE+ categories [42]. The cost of equity is set to 14.5% due to the generally high-risk profile accompanied with geothermal projects. The total nominal average cost of capital is 5.4%. This is calculated using the Weighted Average Cost of Capital (WACC) method using Equation 21. After the financing term of 15 years, the WACC is lowered to 4.35% due to the absence of cost of debt after this period.

$$WACC = \frac{E}{V} * Re + \frac{D}{V} * Rd * (1 - Tc) \qquad \text{Eq.(21)}$$

Where,

E: Market value of equity (0.3)
V: Total market value of the project's financing (E+D)
Re: Cost of equity (14.5%)
D: Market value of debt (0.7)
Rd: Cost of debt (2%)
Tc: Corporate tax (25%)

The total market value of the project's financing consists of the construction costs, unforeseen costs and the reserves. The reserves are made out of the costs of abandonment and costs for first ESP replacement. There are tax deductions available on interest paid, which are often to the benefit of a project. Because of this, the net cost of an operator's debt is the amount of interest the operator is paying, minus the amount it has saved in taxes as a result of its tax-deductible interest payments. This is why the after-tax cost of debt is Rd * (1 − corporate tax rate) [63].
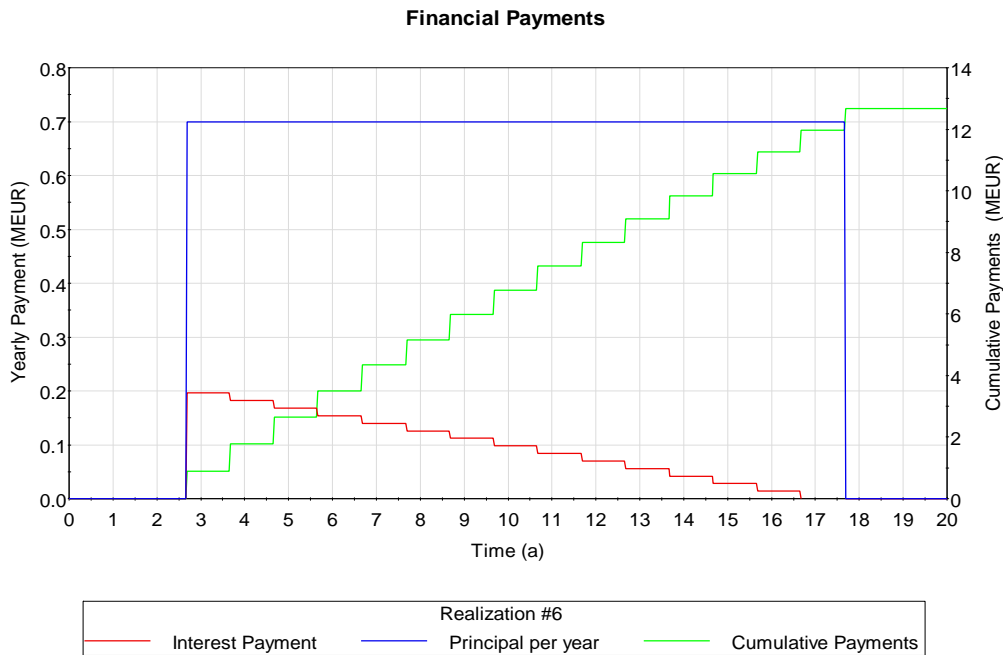
Figure 18: Financing example with a loan of 15 million Euro of which 70% is debt financed. The left and right axis apply to the yearly payments and cumulative payments respectively.

In the model, constant annual principal payments are done during the 15-year subsidy term. Interest is payed annually on a linear basis. An example for a finance amount of 15 million euros is given in Figure 18.

3.5.5   Corporate tax

In the Netherlands, the corporate tax for projects exceeding an annual profit of € 200.000 is set on 25% [46]. Prior to 2014, these taxes could be discounted for geothermal operations in the form of the so called Energie Investerings Aftrek (EIA), but since then, SDE+ and EIA are no longer combined [46]. For the tax calculations in the model, the yearly cashflow is calculated at the end of each production year derived from the operational income, interest and depreciation payments. The operational income is derived from the heat, gas, subsidy and electricity income minus the operational costs. The annual profit is calculated with Equation 22:

$$Profit = Operational\ income - interest - depreciation$$ Eq.(22)

The depreciation is evenly spread over the subsidy period of 15 years and consists of 100% of the construction cost. This results in a depreciation rate of 6.7% per year if no salvage value is considered after 15 years of production. This 15 years term is used due to the fact that the SDE+ base sum is calculated with an assumption of zero salvage value at the end of the subsidy period [45].

Taxes are paid at the end of each production year, over the positive annual fiscal profit.

If last year's fiscal profit is positive, the present year fiscal profit is equal to the profit of that year. If last year's profit is negative (loss), the present year fiscal profit is equal to the sum of last year's loss + present year profit [37].

3.5.6   Insurance

The final element to the total investments is the insurance cost. The ministry of economic affairs created an insurance policy to decrease the financial losses if a doublet does not perform as initially expected. The insurance pays out 85% of the doublets construction cost when it performs below the expected P90 capacity, as a fraction of the realised capacity as shown by Equation 23:

$$Payout = 0.85 * \frac{Capacity\ realized}{P90\ capacity} * associated\ costs$$ Eq. (23)

The premium for this insurance is 7% of the associated cost. For the model the premium is calculated as 7% of the construction cost. Pay-out scenarios are not implemented in the model.

3.6 Economic indices

Revenues and expenses come together in the economics module. Here, different financial evaluation methods are inserted to evaluate the project's economic performance. The time value of money is considered in the Net Present Value, Profitability Index and Levelized Cost Of Heat. The financing costs are implemented in the Weighted Average Cost of Capital that is used as the discount rate for these evaluation methods. Additionally, the Internal Rate of Return is determined that calculates the maximum discount rate at which a project's NPV is equal to zero. The levelized cost of heat is calculated to determine the heat production cost per energy amount produced at any time during production. These evaluation methods are calculated for every time step in the model. This means that the economic performance of a project can be illustrated at any given time between the start and end of production.

3.6.1 Expenses

The capital expenses consist of the exploration costs and construction costs for the wells and equipment. The operational cost is formed by maintenance cost, ESP replacement, well workovers, electricity costs of the pumps and a fixed rate as function of the construction cost + unforeseen cost. Other expenses that are considered are financing and tax payments which are paid annually. The cost for running the pumps are paid in real time. The maintenance on the pump and wells is paid for at the moment that this maintenance is executed.

In general, geothermal projects have multiple unforeseen expenses before or after the moment of first production. A doublet for example, can be struggling to produce continuously at the desired capacity in the first production stages [23]. This could be the result of a generally poor initial project design, early well scaling or corrosion, filter clogging due to high sand production, high skin removal costs due to inefficient well cleaning etc. [36]. Because of this, an element is added to the model which incorporates a percentage of the construction costs as unforeseen cost added to the total investment [37].

3.6.2 Revenues

The revenues in the model are made out of the operational income of the heat and gas production, combined with electricity revenues if a co-generator is selected for purchase. Additionally, subsidy income is also considered as revenues in the model. All revenues are calculated in real time. In other words, income generated per produced kWh is added to the revenues at the moment it is produced.

3.6.3 Net Present Value

As a result of scarcity of means, where scarcity refers to the basic economic problem: the gap between limited (scarce) resources and theoretically limitless wants, postponing or advancing a payment has a certain value. This is indicated by the time value of money. The value of the amount paid or received in the future, calculated on the day of today, is indicated by the present value of that amount as shown by Equation 24:

$$PV = \frac{C_t}{(1+r)^t}$$

Eq.(24)

Where,

PV: Present value (Euro)
C_t: Cashflow at time t (Euro)
r: Interest/inflation/discount rate (%)
t: Time (Basic timestep model = 1 day)

With geothermal operations, there is a flow of income and expenses with changing amounts over time. The model calculates the future value of the sum of these cash flows as the Cumulative Cash Flow (CCF). The present value of this flow of payments can be calculated by discounting the sum of all payments separately. This discounted cumulative cash flow is also known as the Net Present Value and is given by Equation 25:

$$NPV = \sum_{t=0}^{n} \frac{C_t}{(1+r)^t} \qquad \text{Eq.(25)}$$

The general rule is that an investment with a positive NPV will be profitable, and an investment with a negative NPV will result in a net loss. This concept is the basis for the Net Present Value rule, which dictates that only investments with positive NPV values should be considered as an investment opportunity.

The NPV is treated as if it were all equity financed. In other words, no financing cash flows are included in the NPV analysis [64]. The future cash flows should be discounted using the WACC method from section 3.5.4. This is the average cost of finance of the business. If WACC is used as the discount rate, the cost of finance is effectively incorporated into the NPV analysis. This is why finance cash flows are ignored, as the impact of finance is included by using the WACC as the discount rate. The cash flows inserted in the model to calculate the NPV are nominal. Which means that inflation is considered in every future cash flow. If the cashflows are nominal, the Weighted Cost of Capital should be nominal as well [64].

With this method of value determination, the time value of money is of great influence. Therefore, it is important to insert a specific order of payment and revenue stream in the model. Some parts of expensive equipment for example will only be bought after solid production testing to make sure adequate size and performance is delivered. An overview of the timing of the cash flows are shown in Table 8:

Table 8: Timing overview of the different cash flows of the model

Investment/payment/revenue	Timing of cashflow
Exploration cost	At simulation start
First well cost, insurance, drilling installation cost	After exploration completed
Second well cost, Gas separation unit, Network cost, Heat exchanger	After completion 1st well
Power facility and pumps	After completion doublet
Co-generator, unforeseen cost	At first production
Abandonment cost	At projects end
Gas, heat, electricity and subsidy revenues	Real time
Operational cost (fixed + elec. Pumps)	Real time
Pump and well maintenance/overhaul	At moment of maintenance
Tax payments	Yearly

3.6.4 Internal Rate of Return

The Internal Rate of Return (IRR) is the discount rate at which a project's NPV is equal to zero (Equation 26). The IRR is calculated in real time by the model, so that a minimal discount rate can be shown at every moment of the project's lifetime. The general business rule for the IRR is to accept an investment if the IRR exceeds the cost of capital in the project's lifetime.

$$Internal\ Rate\ of\ Return = \sum_{t=0}^{n} \frac{C_t}{(1+r)^t} = 0 \qquad \text{Eq.(26)}$$

3.6.5 Profitability Index

The profitability index is calculated as the ratio between the present value of future cashflows (NPV) over the discounted market value of the investments prior to first production as shown by Equation 27:

$$Profitability\ Index = 1 + \left(\frac{\sum_{t=0}^{n} \frac{C_t}{(1+r)^t}}{\sum_{t=0}^{n} \frac{I_t}{(1+r)^t}} \right)$$

Eq.(27)

With,

C_t: Cashflow at time t (Euro)
I_t: Investment at time t (Euro)
n: project's lifetime (years)

The profitability index rule is a variation of the net present value rule. In general, if NPV is positive, the profitability index would be greater than 1. If NPV is negative, the profitability index would be below 1. Thus, calculations of PI and NPV would both lead to the same decision regarding whether to proceed with or abandon a project. However, the profitability index differs from NPV in one important respect: being a ratio, it ignores the scale of investment and provides no indication of the size of the actual cash flows.

3.6.6 Levelized cost of heat

The levelized cost of heat is an economic performance method to measure the present market value per kWh of geothermal energy produced at a certain time in the projects life as shown by Equation 28:

$$LCOH = \frac{\sum_{t=1}^{n} \frac{CapEx_t + OpEx_t}{(1+r)^t}}{\sum_{t=1}^{n} \frac{Heat_t}{(1+r)^t}}$$

Eq.(28)

Where,

$CapEx_t$: Capital expense at year t (Euro)
$OpEx_t$: Operational cost at year t (Euro)
$Heat_t$: Heat production at year t (MWh)

A LCOH analysis is a good tool to compare the cost of energy of geothermal systems to conventional fossil fuel systems such as coal-fired or natural gas power plants or to renewable systems, such as solar, wind and nuclear power.

3.6.7 Payback time

The model counts the time it takes for the Net Present Value to reach zero after the initial negative NPV at the start of production. This time is taken from the first moment of production until NPV = 0. A project is considered acceptable when the payback time is before or close to the end term of the subsidy [37].

3.7 Scenario analysis

To answer the research questions, multiple scenarios are simulated in the model. Every scenario has alternative variables compared to the reference scenario. A description is given for each scenario below combined with a general overview provided in Table 11.

3.7.1 Reference Scenario (RF)

For the reference scenario, the basic design of the DAP well is modelled, without heat pumps or co-generator. The project specific data described in Table 2 are provided by Perpetuum Energy Partners [65] and are confidential. The numbers for the heat demand are provided from the TU Delft and consist of real time heat demand data of 2017 (Figure 19). Prior to 2021, the demand consists only of heat consumption of the university. After 2021, an estimated 7000 MWh will be added from new connections to the Hogeschool Inholland and nearby student housing. For the calculations of the future demand, 30% of the 7000 MWh are spread evenly across the year for the purpose of household usage such as cooking, showering and cleaning. The remaining 70% is spread in equal ratios compared to the data from 2017. For the model, this demand pattern is assumed constant for every consecutive year after 2021 and is used in every scenario except for scenario 6 where a constant yearly demand is modelled.
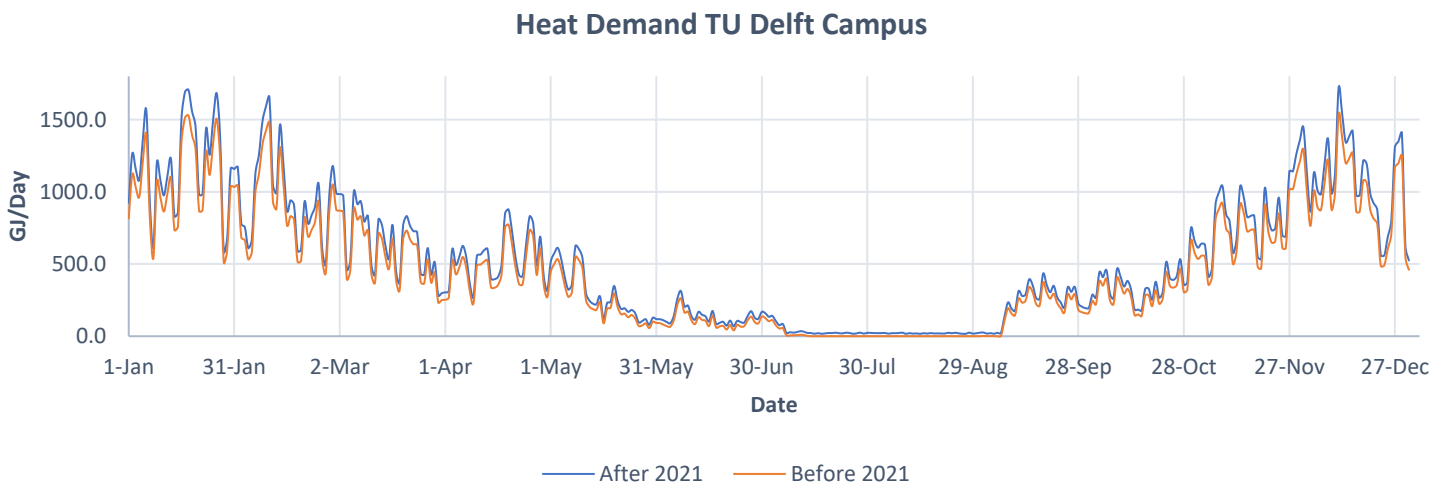
Figure 19: Real time heat demand per day of the TU Delft Campus in 2017

3.7.2 Fixed heat price (FHP)

It is difficult to predict how the geothermal heat price will develop over the years. The price could for example stay dependant on fossil fuel prices or it can be independently settled between producer and energy operator based on the cost of production. Due to this uncertainty, a fixed heat price of 7 Euro/GJ is modelled as a scenario. 7 Euro/GJ is taken as a fixed heat price because the same value is used as a heat price for an geothermal business case by [37] and also ranges between the heat prices used in a geothermal performance assessment model done by [41]. With this scenario we can measure how this method of heat pricing affects the economic performance compared to a heat price as a fraction of the gas market price.

3.7.3 District heating concept subsidy SDE+ 2018 (DHC)

As of the year 2018, all producing geothermal projects in the Netherlands have been installed for greenhouse heating purposes, with only one doublet under development for district heating. On the long term however, district heating could present the largest demand in geothermal heating [18]. The categories from the SDE+ 2018 do not include a district heating scenario yet. However, an advised base sum and cost predictions are already made by ECN in case such a project starts producing in the near future. The reference case of the DAP well is a project that is designed for district heating. Therefore, it would be interesting to show how the concept base sum for district heating reflects on the economic performance of this project. In general, a district heating project is characterized with a lower number of full capacity hours compared to greenhouse heating projects. Due to the high temperature heating requirements of a district heating network, it can be very challenging to efficiently use the thermal energy available. Because of these differences, the expected cost per kWh will be higher compared to greenhouse heating projects. The base price and full capacity hours are shown in Table 9.

Table 9: SDE+ 2018 District heating concept prices [22]

SDE+ 2018 Geothermal concept prices *(Euro/kWh)*	Base Sum	Correction sum (2018)	Base price	Full Cap hours	Subsidy years
District heating >500 m	0.106	0.017	0.016	3500	15

3.7.4 Increased injection temperature (ITT)

The heat from a greenhouse heating project is often cooled down to 35°C [20]. In district heating however, this low return temperature is harder to achieve due to high temperature required for the heating systems in the district heating networks of today. For this scenario, the injection temperature is increased with 10°C on top of reference reinjection temperature of 35°C. By modelling this scenario, an economic outcome is calculated when the expected return temperatures are not as low as expected.

3.7.5 SDE+ realisation factor correction (RFC)

The DAP well project is a project in its early existence. No wells are yet drilled, and production estimates required for subsidy and insurance applications have large uncertainties. Looking back at applications from 14 producing geothermal projects, a clear overestimation trend is recognized [22]. When the projects were actually producing with a stable capacity, on average, 80% of the previously predicted P50 maximum capacity could be achieved [22]. The lower than expected capacity is mainly caused by limited well performance. Injectivity rates/indices are often substantially lower than those expected before drilling, or those expected based on observed reservoir properties [56]. A reduction in well flow performance increases the pump pressures necessary to achieve the desired capacity of the wells. High flowrates and pump pressures can lower the Coefficient of Performance (CoP) under a preferred/acceptable lower limit. Additionally, the pressures required to inject the brine back into the reservoir can exceed a safety limit set up by SodM and therefore limit the flow rates overall [58]. The final cause of the capacity overestimation was created by the limitation in finding enough demand to cool down the brine to the expected return temperature [22].

For this scenario, the capacity of the wells is a fixed value in the model instead of a distribution. The capacity is taken as the predicted P50 case for all elements of Equation 4. The capacity is then multiplied with the so-called Power realisation factor of 0.8. The added CoP adjuster element in the model (section 3.4.4) is set to 0% due to the already existing limitation created by the power realisation factor.

3.7.6 Constant demand throughout the year (CDY)

For this scenario, a constant 80% well capacity is produced year-round. This creates an 80% load factor on a yearly basis. There are no fluctuations in flow rate except for the moments of maintenance. To realistically produce at this constant rate and fully cool down the brine to 35 degrees all year round for district heating purposes, additional investments are needed such as (subsurface) heat storage options, network adjustments, technologies that can utilize the heat in the summer such as organic Rankine cycles and heat pumps combined with shallow wells. Therefore, an estimated 5 million is added to the initial investments to create a more realistic scenario. 5 million is a very rough estimate relative to the additional investments needed to realize a scenario like the one described here. Most of the technologies are relatively new and estimated cost of these technologies are not freely available.

3.7.7 Gas utilized in gas generator (GGG)

To this day, almost every geothermal well drilled in the Netherlands contained some dissolved or free gas with the produced water [34]. This gas can be used in-situ for the gas boiler, co-generator or can be sold to a nearby grid. With greenhouse heating geothermal projects, the produced gas is often used in a co-generator to supply additional heat to the system and generate electricity that is used for the pumps. Additionally, the CO_2 from the gas burning process can be utilized in the greenhouse growing processes. For this scenario, a co-generator is bought as initial investment where the produced gas is inserted in the generator instead of being sold to the grid. Gas revenues can have a high, positive influence on the economic performance of a doublet. On the other hand, electricity bought from the grid can increase the operational costs of the pumps significantly if electricity prices are high and CoP numbers are low.

3.7.8 Declining gas concentration during production period (DGC)

For the reference scenario, a constant gas/water ratio is assumed during the project's lifetime. For the DGC scenario, this ratio declines after a certain production time. When gas revenues are high, a decline in gas production could result in overall losses of a project.

Two producing geothermal projects located in Pijnacker, the Netherlands, are targeting the same sandstone formation as targeted by the reference scenario. Both where finished in 2010 and show no decline in gas production since first production. Because of this reason, a P10 probability of 7 years is chosen for this scenario. The other probabilities and decline rates are based on rough estimates. The P90 probability of 25 years seems excessive, but an increase in gas production is not considered in this scenario, but can happen as seen in the last 7 months of production data available from Ammerlaan [66].

Table 10: Gas Decline Scenario

	P10	Mode	P90
First decline after initial production (years)	7	15	25
Production decline rate (%/yr)	5	10	15

3.7.9 No gas revenues (NGR)

A reference geothermal business case provided by Rösingh [Pers. Comm] and the business case illustrated in [20] do not include any gas revenues for the yearly cash flows. Therefore, to analyse the economic performance based on geothermal heat production on its own, a scenario is modelled where no gas revenues are considered. This scenario provides an economic performance overview of a project that is only dependent on revenues originating from heat production and subsidy income. This scenario could be useful in a situation where there is no gas co-production, or the gas is reinjected. For this scenario, the gas separator is not included in the initial investment.

3.7.10 High initial subsidy (HIS)

For this scenario, the subsidy base amount is not constant but starts high and decreases over time. At production start, the base amount equals to 0.10 Eur/kWh with an annual decrease of 0.91^t, wherein t denotes the time in years. These numbers are chosen in such a way that the starting base sum is realistic (close to the concept subsidy) and that an equal amount of subsidy is received after 15 years of production compared to the reference scenario. This scenario shows how a project performs economically when subsidy pay-out timing is changed without changing the total sum at the end of the subsidy period.

Table 11: Scenario variables overview. Every scenario has the same variables as the reference scenario in red, unless stated otherwise in the scenario's column.

	(1) RF	(2) FHP	(3) DHC	(4) ITT	(5) RFC	(6) CDY	(7) GGG	(8) DGC	(9) NGR	(10) HIS
Heat price	90% of gas price	Fixed as 7 Euro/GJ								
Subsidy base sum	0.053 Euro/kWh		0.106 Euro/kWh							0.10 Eur/kwh -0.91^t
Full capacity hours	6000 hours/year		3500 hours/year							
injection temperature	35°C			45°C						
CoP Correction	-10%			-13%	0%					
Capacity wells	Probability distribution parameters				80% of P50 capacity					
Demand per day	History data TU Delft campus					80% of max capacity				
Altered investment	(-)					5 million Euro	Co-generator		No gas separator	
Additional Revenues	Gas + subsidy						Subsidy, Heat, gas & elect.		Subsidy only	
Gas/water ratio	Constant							Declining during production		

4 Results and Discussion

An accuracy test is performed between different number of iterations to find a compromise between accuracy of the results and stability of the model. From this test, the number of iterations for each scenario is settled at 15000 (Appendix A). With 15000 iterations, there are still some significant differences in the minimum and maximum values between simulation runs. These changes should be taken in consideration when comparing the maximum and minimum values of the different scenarios. Between the 10th and 90th percentile however, changes are less than 1% between simulation runs and are therefore better suited for economic performance analysis.

Firstly, all financial evaluation methods are shown for every scenario at 30 and 50 years of the project's life. Well layouts of most geothermal systems are designed to produce energy efficiently for a period of at least 30 years [67]. A lifetime of 50 years could be achievable with the DAP case study but involves higher chances on minor temperature decrease of the reservoir and therefore lower well capacity [37]. For the model, thermal breakthrough is not taken into account at any point of the project's life.

These results are followed by a sensitivity analysis of the model's variables. The final results are the scenario specific results where the main differences in economic performance are explained on a technical level.

The economic evaluation results are illustrated using a box and whisker plot. The meaning of this plot is given in Figure 20.
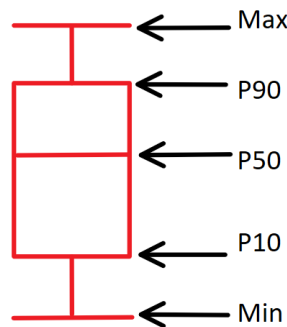
Figure 20: Box and Whisker plot. Max and Min are equal to P100 and P10 respectively

The order and colours of the scenario results are identical for the economic evaluation and the individual results. This is shown in the following list:

1. *Reference Scenario* — 🟥 *(RF)*
2. *Fixed Heat Price* — 🟧 *(FHP)*
3. *District Heating Concept Subsidy SDE+ 2018* — ⬜ *(DHC)*
4. *Increased Injection Temperature* — 🟨 *(IIT)*
5. *SDE+ Realisation Factor Correction* — 🟦 *(RFC)*
6. *Constant Demand Throughout the Year* — 🟩 *(CDY)*
7. *Gas Utilized in Gas Generator* — 🟦 *(GGG)*
8. *Declining gas concentration during production period* — 🟫 *(DGC)*
9. *No Gas Revenues* — 🟪 *(NGR)*
10. *High Initial Subsidy* — 🟦 *(HIS)*

4.1 Financial evaluation methods

On a general level, mainly due to the large uncertainties of the future energy prices, uncertainty increases with time for every scenario, which makes it difficult to recognize the uncertainty from other variables involved besides the future energy prices. To clarify this issue, a sensitivity analysis is performed on the other variables at the end of this subchapter.
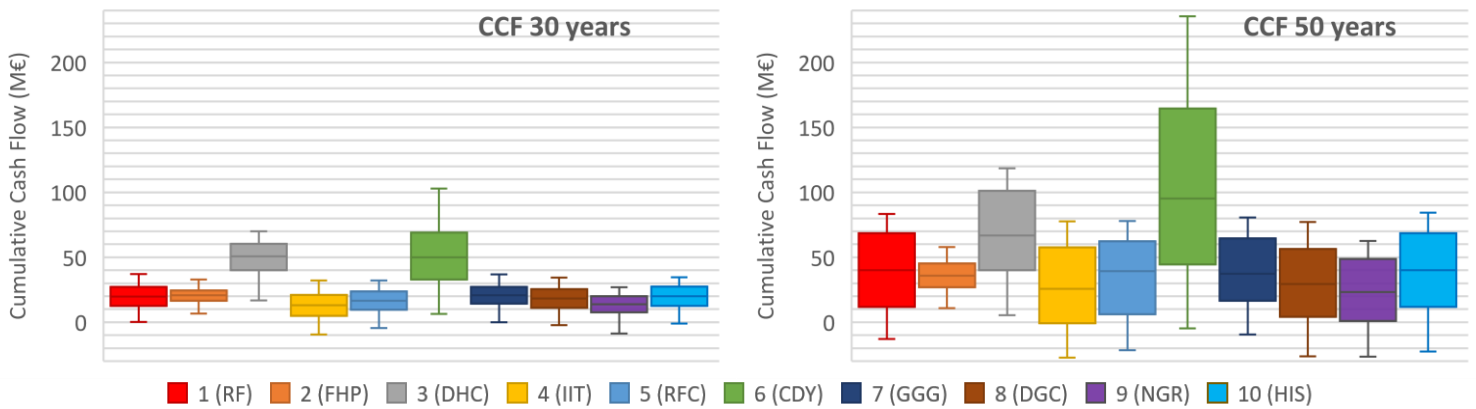
Figure 21: Cumulative Cash flow in M€ at 30 and 50 years.

The Cumulative Cash Flow is shown in Figure 21. The DHC and the CDY scenarios generate the highest cash flow, showing similar P50 estimates at 30 years. At 50 years, the P10 to P100 cashflow of the CDY scenario outperforms all scenarios but bearing the highest variance in its results. The FHP scenario shows the smallest variance with a positive cashflow even at P0 at both time periods. All remaining scenarios show very similar variance, with increased risk on negative cashflows after 50 years compared to the results at 30 years. The HIS scenario, where high early subsidies are paid, show equal cash flows for both time periods compared with the RF scenario. The lowest amount of cash flow is generated by the ITT scenario with a negative, minimum and P10 cash flow of -27.2 and -0.75M€ at 50 years respectively.
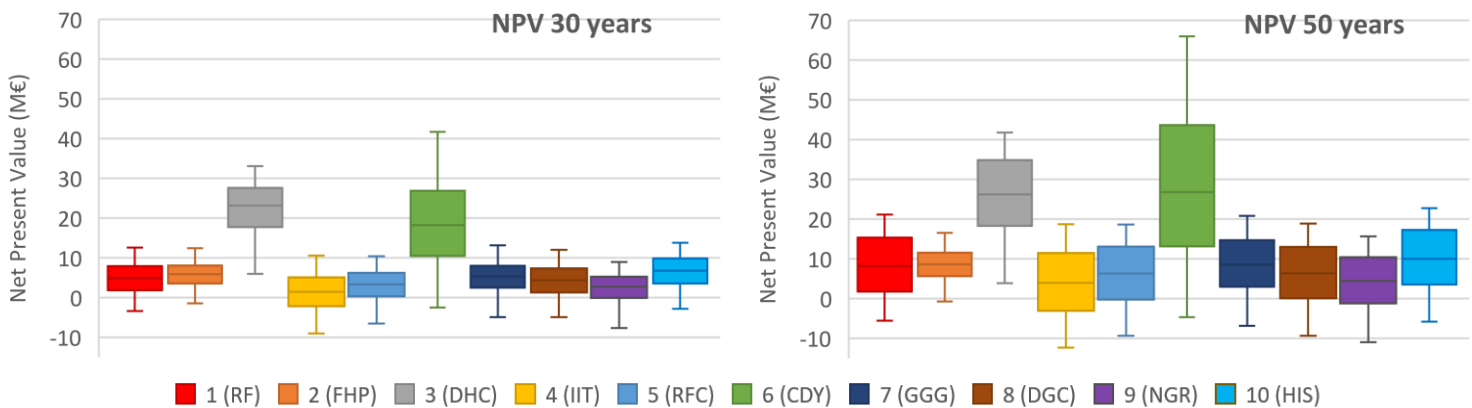
Figure 22: Net Present Value in M€ at 30 and 50 years

The discounted cumulative cash flow is shown in Figure 22 as the Net Present Value. For the NPV, the timing effect of the cash flows result in different performance ratings between the scenarios compared to Figure 21. The HIS scenario shows a higher NPV for both 30 and 50 years compared to the RF scenario and the DHC scenario outperforms the CDY scenario at 30 years. This can be explained by the high early cash flows of the HIS and DHC scenarios compared to the stable, but lower cash flows of the RF and CDY scenario. At 50 years, the P90 and max NPV of the CDY exceed the DHC scenario, but the possibility of a negative NPV remains zero for the DHC scenario, which makes it the most preferable in terms of investing. A project with a projected NPV that exceeds 0 is considered as an investment opportunity. With this rule in mind, a scenario like ITT and NGR show increased risk (>10%) over the other scenarios in not exceeding the 0-euro mark at 30 and 50 years and therefore will be the least favourable to investors.
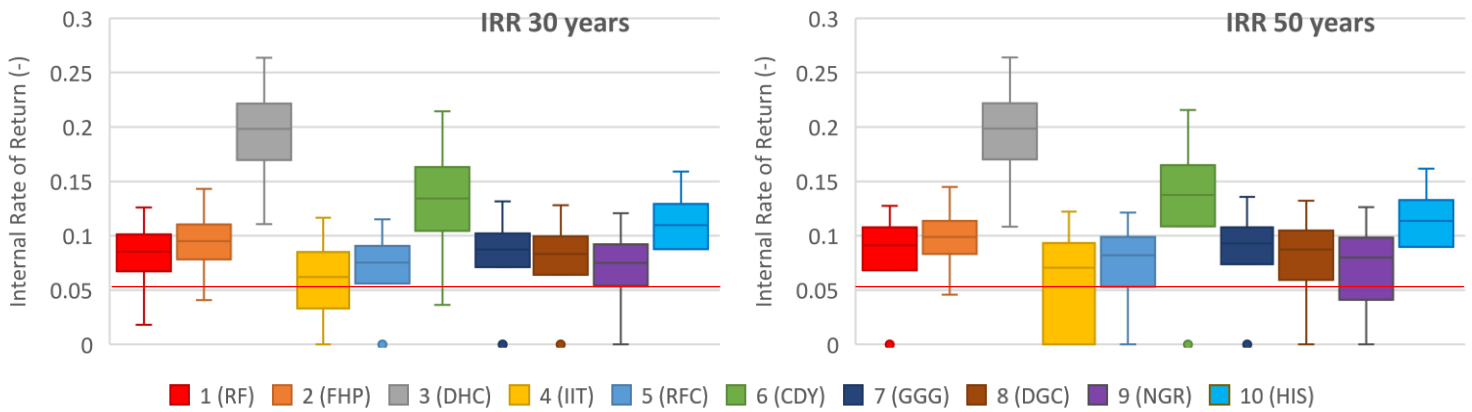
Figure 23: Internal Rate of Return at 30 and 50 years. For the scenarios where the cashflow dropped below zero, a return of 0 is calculated by the model. The dots are outlier points that indicate a datum point exceeding the range between the other data points. The red line indicate the discount rate (WACC) of 5.4% that is used for all scenarios.

The Internal rate of return is shown in Figure 23. The general business rule for the IRR is to accept an investment if the IRR exceeds the cost of capital in the project's lifetime. The average cost of capital of the model is indicated with a thin red line. For all scenarios, at least 50% of the iterations exceeds this limit, with the ITT and NGR scenario showing the highest risk of reaching below the average cost of capital, especially at the 50 years mark. The DHC scenario is the only scenario where no probability exists that the data is lower than the WACC of the model. Additionally the DHC scenario outperforms all other scenarios between P10 and P100. Looking back at the NPV, CDY outperforms the DHC scenario at 50 years for the high percentiles. This is not visible when looking at the IRR at 50 years. This is caused by a combination of higher initial investments (+ 5 million) and more moderate cash flows during the subsidy period for the CDY scenario compared to the DHC scenario.
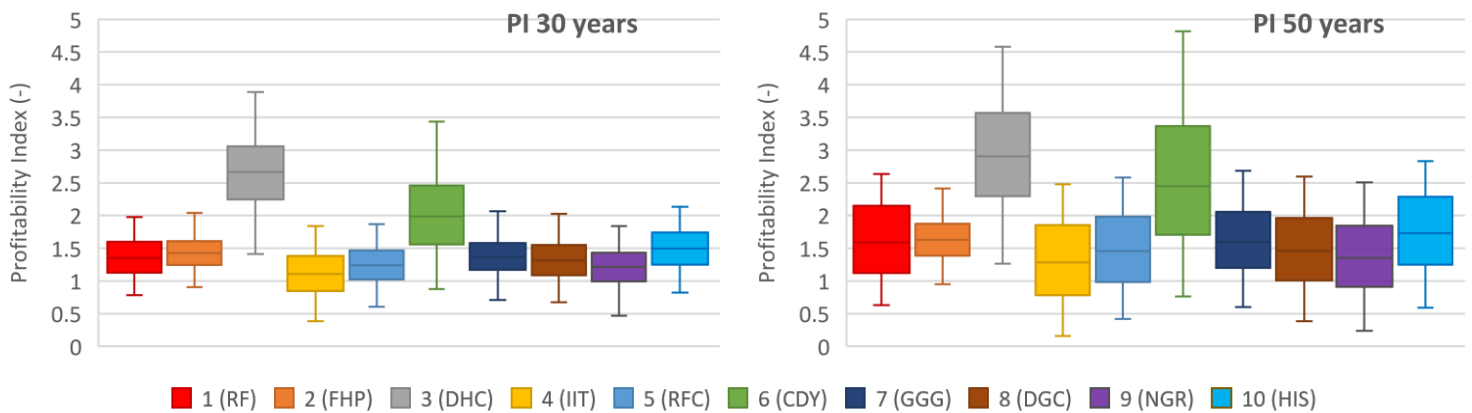
Figure 24: Profitability index at 30 and 50 years.

The profitability index is shown in Figure 24. A profitability index of 1.0 is the lowest acceptable measure on the index, as any value lower than 1.0 would indicate that the project's present value (PV) is less than the initial investment. The scenarios ITT, RFC (only at 50 years) and NGR do not exceed the value of 1 for their 10th percentiles, indicating higher investment risks compared to the other scenarios. Again, the DHC scenario is the only scenario which does not get below a value of 1 for any of the iterations simulated.
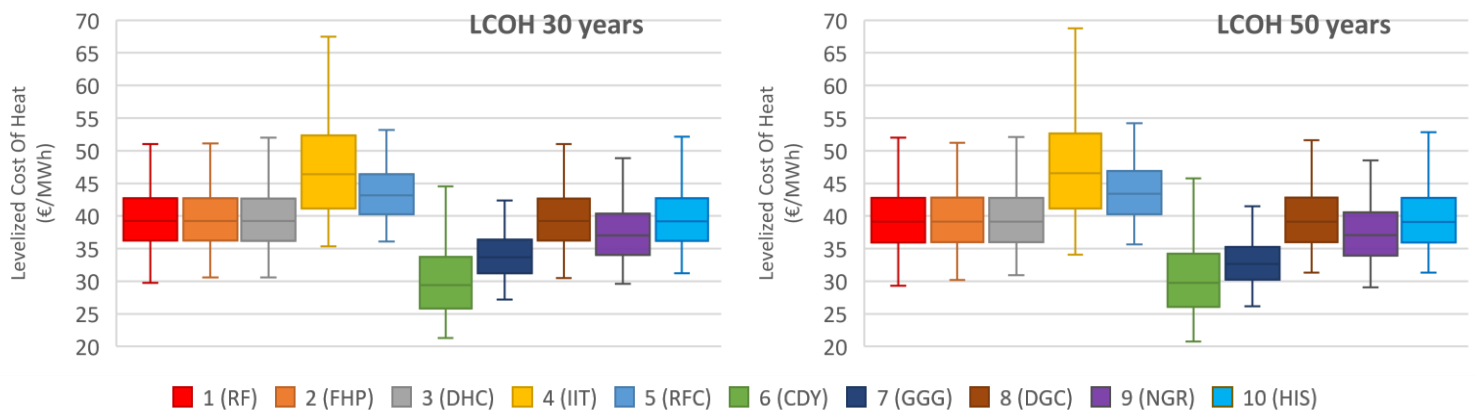
Figure 25: Levelized Cost of Heat at 30 and 50 years.

The Levelized Cost of Heat is shown in Figure 25. Scenario RF, FHP, DHC, DGC, and HIS have similar cost of heat because no changes are applied to the amount of heat produced and costs being made. The NGR scenario has a lower LCOH compared to the scenarios previously mentioned, due to a smaller initial investment caused by the absence of a gas separator purchase. For the ITT and RFC scenario however, the capacity of the doublet is lowered which directly results in more cost per kWh produced. For the CDY scenario, a larger initial investment is made but more heat is produced compared to the reference scenario. The increased operational cost and higher initial investment from this scenario weigh less than the added heat production revenues. Therefore, the CDY has a significantly lower LCOH compared to the other scenarios, which indicate that if the 5 million in additional investments is estimated too low, additional room for extra investments is available. For the GGG scenario, the initial investment is increased with the purchase of a co-generator. But due to the absence of (most of) the pumping cost, the LCOH decreases beyond the reference scenario level.

A LCOH analysis is a good tool to compare the cost of energy of geothermal systems to other renewable technologies. In Figure 26 an overview is given of the Levelized Cost of Energy of different renewable energy technologies [68]. Both LCOH and LCOE measure the lifetime costs divided by the energy produced. The only difference between LCOH and LCOE is the form of energy used to keep the process going. In LCOE this is considered as fuel and in LCOH as electricity.
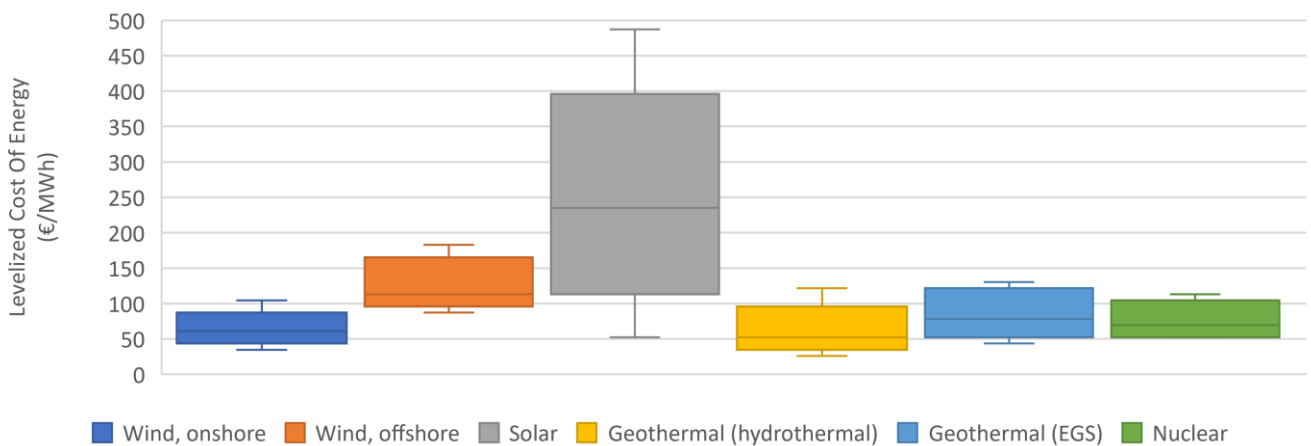
Figure 26: Levelized Cost of Energy comparison in €/MWh between alternative energy technologies [63], with a dollar to Euro conversion of 0.87. The P50 LCOE of hydrothermal systems results in 52 €/MWh whereas the models RF P50 LCOH results in 40 €/MWh. The differences could be explained by different discount rates being used, average production temperature, timing of the investments, the dollar to euro conversion or operational cost differences in terms of energy cost of the pumps.

The results from the model are a little lower compared to the P50 values of Hydrothermal projects in Figure 26 but fit this distribution nicely overall.
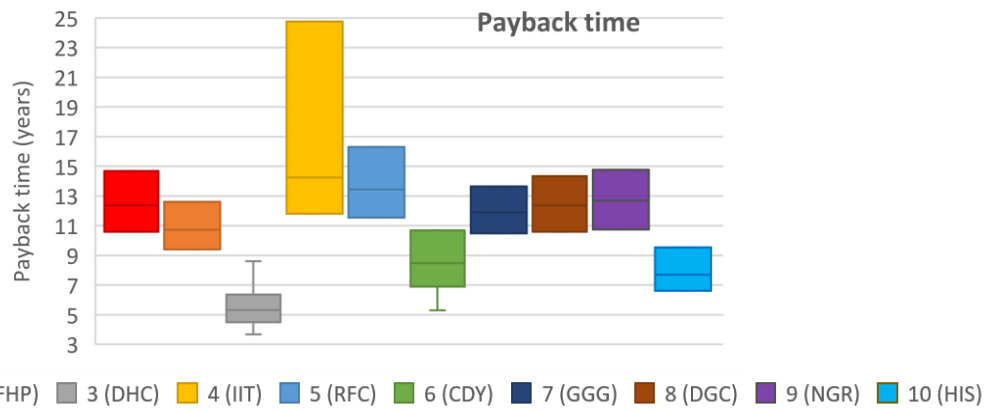
Figure 27: Payback time in years after first production. The scenarios where the whiskers are missing indicate on one or more results of no payback. In a case of no payback (min = 0) the maximum value holds no extra meaning.

The payback time is given in Figure 27. Due to the higher overall subsidies of the DHC scenario, payback times are reached very early after first production. The HIS scenario has due to its high early subsidies a significant advantage over the rest of the scenarios where the subsidy is paid out using current policies as a constant base amount. Nevertheless, a probability does exist for this scenario and all other scenarios that are missing a P0 whisker, that payback is not reached at the end of the project's lifetime. The CDY scenario could see its first payback around 5 years due to the high constant heat revenues characteristic for this scenario. For the remaining scenarios, the P10 to P90 payback values are ranging between 10 and 16 years except for the ITT scenario, that has a high probability (+- 30%) in a payback time far beyond the end term of the subsidy. A project is considered acceptable when the payback time is before or close to the end term of the subsidy. For the model this term is 15 years after first production (+- year 18).

Overall the DHC and CDY scenarios are economically the best performing scenarios. For both scenarios, gas is considered as a revenue. To illustrate how depended the high NPV's of these scenarios are to the gas revenues, an additional simulation is run where both scenarios are compared to a scenario where no gas revenues are considered. The NPV results are shown in Figure 28:
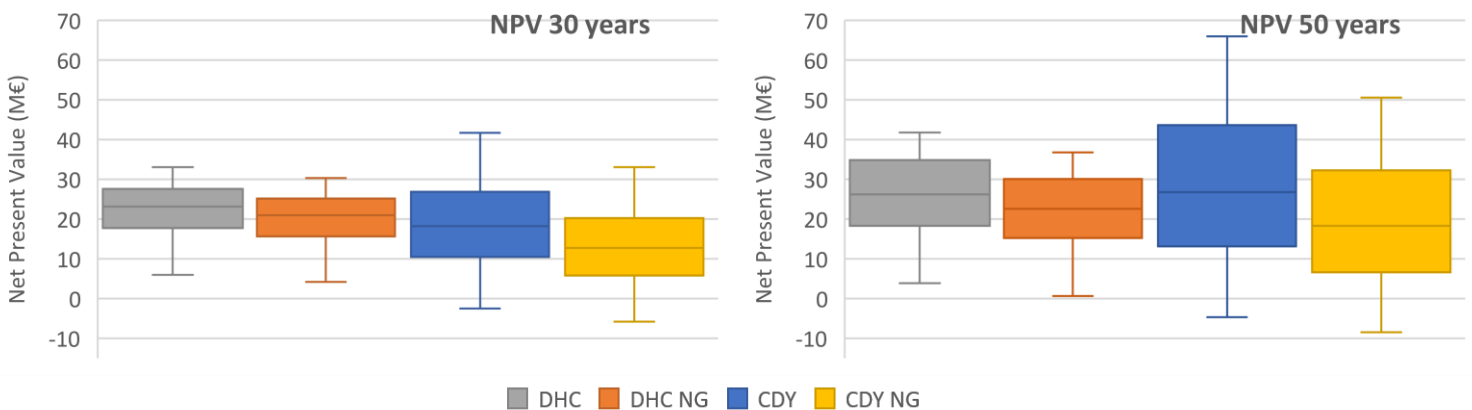
Figure 28: Comparison between the two best performing scenarios where each scenario is illustrated with and without gas revenues considered. NG stands for the no gas revenue scenario. The variance decreases for both scenarios when no gas revenues are considered due to the large uncertainty of the future gas prices. In terms of gas dependence, the P50 NPV of the DHC scenario decreases with 10 to 16% for 30 and 50 years respectively. The NPV for the CDY decreases 44% for both time periods.

From Figure 28 it is shown that the dependence on the gas price is significantly higher for the CDY scenario compared to the DHC scenario. This can be explained by the different dominant sources of revenues for these scenarios. The dominant revenues for the DHC scenario are the high subsidies. The CDY got its dominant revenue stream from a high constant flow rate of heat and gas. Because of this, The CDY scenario decreases the most in NPV when gas revenues are not considered. The initial investment for both scenarios where no gas revenue is considered is 1 million less than the original scenarios due to the absence of the purchase of a gas separator. If this piece of equipment would be included in the investment, the NPV would drop an additional 10% for the DHC scenario and 20% for the CDY scenario.

44

4.2 Input sensitivity

To better illustrate the sensitivity of the other variables beyond the future gas prices, a sensitivity analysis is performed on the inputs of the reference scenario. For these analyses, the gas price scenario is either the high or the low case. Initially, each variable is sampled around its central value with a -20 and +20% change to illustrate the sensitivity of the model when a parameter is altered with an equal fraction. This is followed by a sensitivity analysis where the model's inputs are varied between realistic ranges to get a better understanding about the sensitivity of the individual parameters when ranged between possible values.
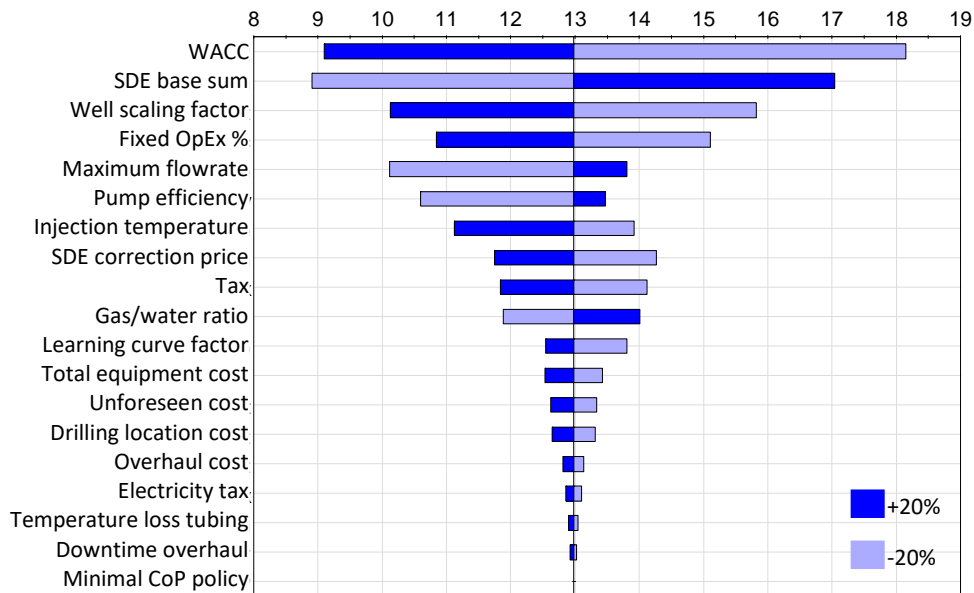
Figure 29:Sensitivity analysis at 50 years for the NPV index for the high gas price scenario with respect to the model's inputs in decreasing order of sensitivity. The NPV is calculated with a 20% change in respect to the central value in either direction.

It should be noted that not every variable of the model is part of the sensitivity analysis, since these variables are not continuous over time. Therefore, the overall interpretation of the analysis needs to be treated with caution. Additionally, in reality, certain variables like the WACC are very unlikely to change 20% from the central value in either direction.

What stands out from Figure 29 is the high sensitivity of the subsidy variables and the well scaling factor. This can be explained by the timing and volume of these cash flows. Both are paid for and received at early stages (first 20 years) of the project. These early cashflows are enhanced by the time value of money.
A 20% increase in maximum flow rate and pump efficiency have limited effect on the NPV compared to a 20% decrease. This difference is caused by the limited heat demand available in the reference scenario. A higher well capacity does not result in more revenues when there is no extra demand available.
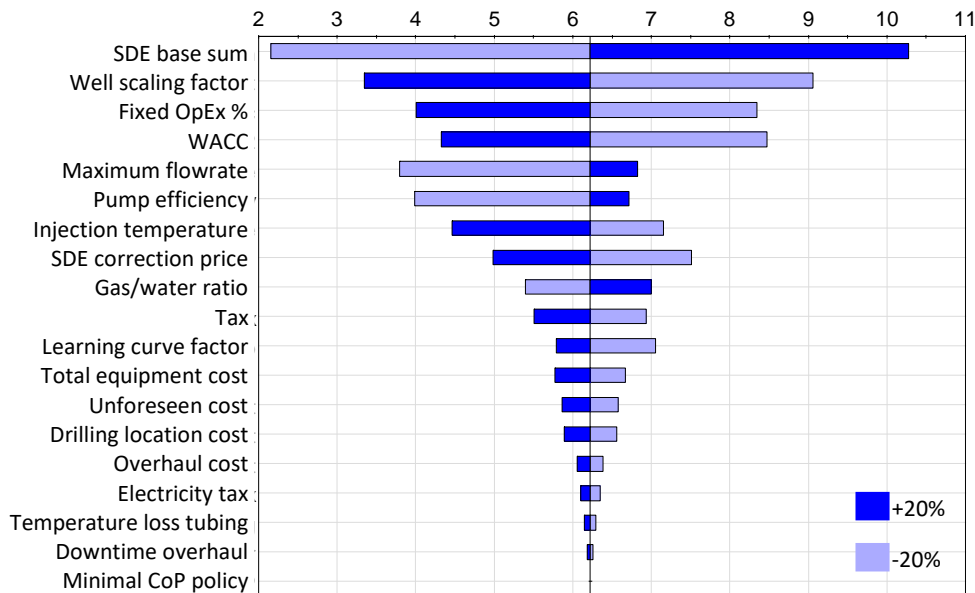
Figure 30: Sensitivity analysis at 50 years for the NPV index for the low gas price scenario with respect to the model's inputs in decreasing order of sensitivity. The NPV is calculated with a 20% change in respect to the central value in either direction.

Figure 30 shows the sensitivity results when the low gas price scenario is applied. At low gas prices, the sensitivity of some variables shifts compared to Figure 29. Low gas prices result in the minimum SDE correction price (base price) as central value for this analysis. This low heat price raises the sensitivity of the base sum over the other variables.

The fixed OpEx (Operational Expenses) rate scores high in terms of sensitivity for both Figures. This is an important result due to the uncertainty nature of this number. A central value of 5% of the construction + unforeseen cost is a very rough estimate for the fixed operational cost. It is certainly possible that this 5%
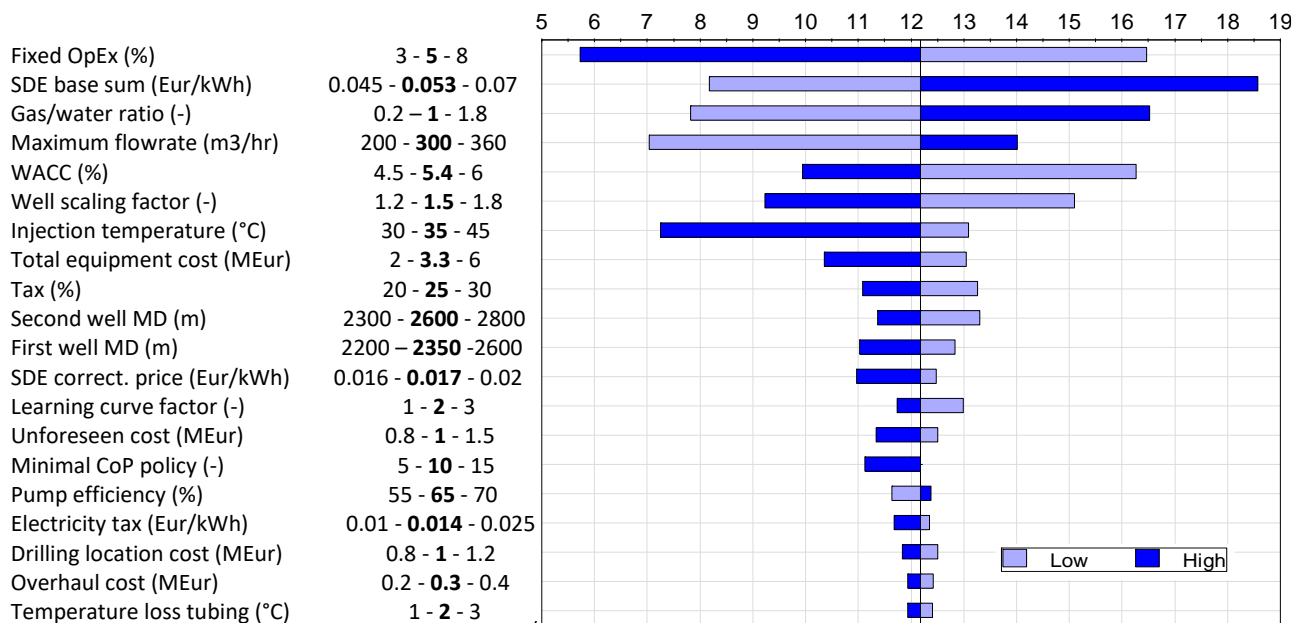
Figure 31: Sensitivity analysis at 50 years for the NPV index for the high gas price scenario with respect to the model's inputs in decreasing order of sensitivity. The NPV is calculated with a realistic change in respect to the central value in either direction. The input shown in this figure are a combination of literature values and default values from Table 2.

estimate can change with 20% in either direction.

For the realistic ranges shown in Figure 31, The fixed OpEx shows the highest sensitivity. The lowest maximum flow rate is 67% of the central value and will result in a nearly halved NPV. Here it is shown that if the WACC is sampled between possible ranges, the sensitivity decreases relative to the other variables. The learning curve

factor does not influence the NPV to a large extend. In a case study where more than one doublet would be drilled, the cost of drilling and learning curve factor, would score higher in sensitivity as they do now.

4.3   Individual results

In this chapter the individual scenario results are shown and discussed that further elaborate the differences in economic performance between the scenarios on a technical level. All additional results that the model can provide, that are not illustrated here are shown in Appendix B.

The legend with an NPV example of the reference scenario for the time history results is given in Figure 32. The colour changes for every scenario but an overall darker shade indicates a higher probability.
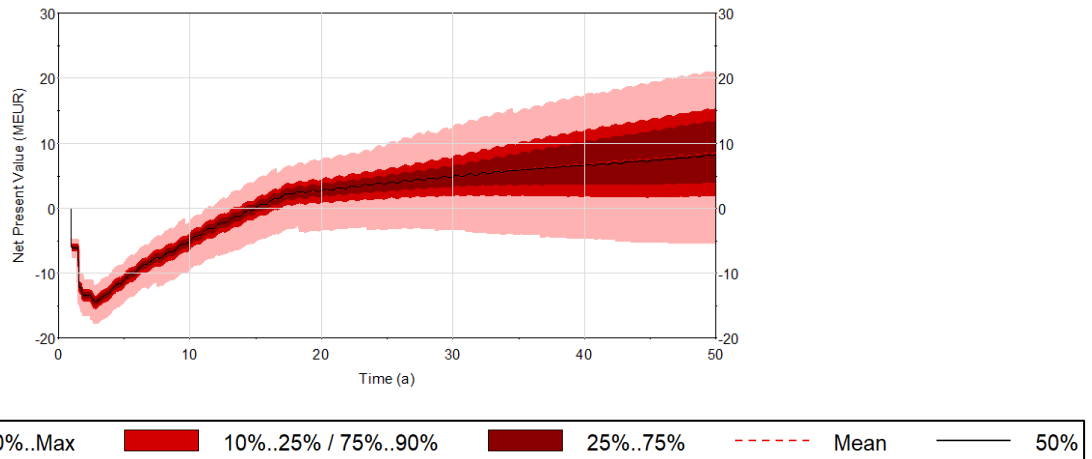
Figure 32: Time history distribution of the RF NPV results. The darkest shade indicates a probability between 25 and 75%. The middle shade from 10 to 25% and 75 to 90% probability. The lightest shade indicates the outliers from 1 to 10% and 90 to 99% probability.

4.3.1   Fixed Heat price scenario

The fixed heat price scenario (FHP) is characterized with a constant heat price of 7 Euro/GJ (0.252 Euro/kWh). The heat price from the reference scenario is set as 90% of the gas market price.
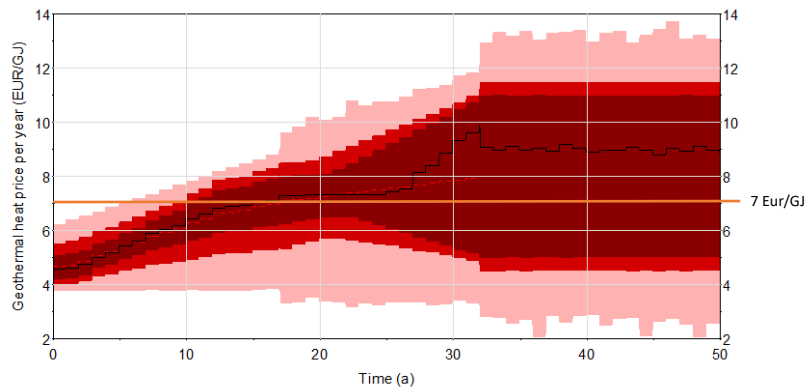
Figure 33: Geothermal heat price per year distribution in Euro/GJ (uninflated). The oragne line indicate the fixed heat price from this scenario.

In Figure 33, the heat prices for both scenarios are illustrated. Here it is visible that the fixed heat price is higher for the first 17 years compared to the average heat price of the reference scenario. This directly results in more heat revenues at the earlier stages of the project, as shown by Figure 34.
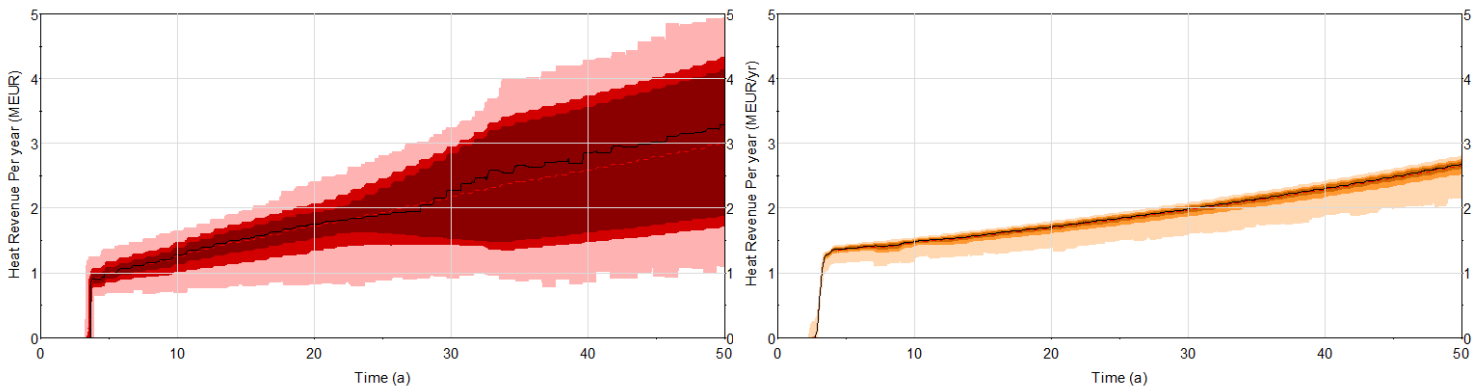
Figure 34: Heat revenue per year distribution in MEur (inflated). RF and FHP scenario on the left and right respectively. Due to the uncertain nature of the gas price, the RF scenario shows high variance in the amount of heat revenue earned per year.

After this period, the heat price from RF can either follow the low or high gas price scenario. High gas prices after this point directly result in a larger amount of heat revenues for the remaining production time. If the gas price would follow the low gas price scenario however, where the gas price declines, the fixed heat price will have a better outcome financially wise (Figure 34). Therefore, in terms of risk, a fixed heat price of 7 Euro/GJ would be more preferable over the reference scenario.

In terms of subsidy performance, higher initial heat revenues results in lower efficiencies of the subsidy as shown by the subsidy/heat revenue ratio in Figure 35. This means that the necessity of the subsidy decreases. However, a heat price of 7 Eur/GJ early on would decrease the competitiveness of this method of heating if compared to the heat price by burning natural gas.
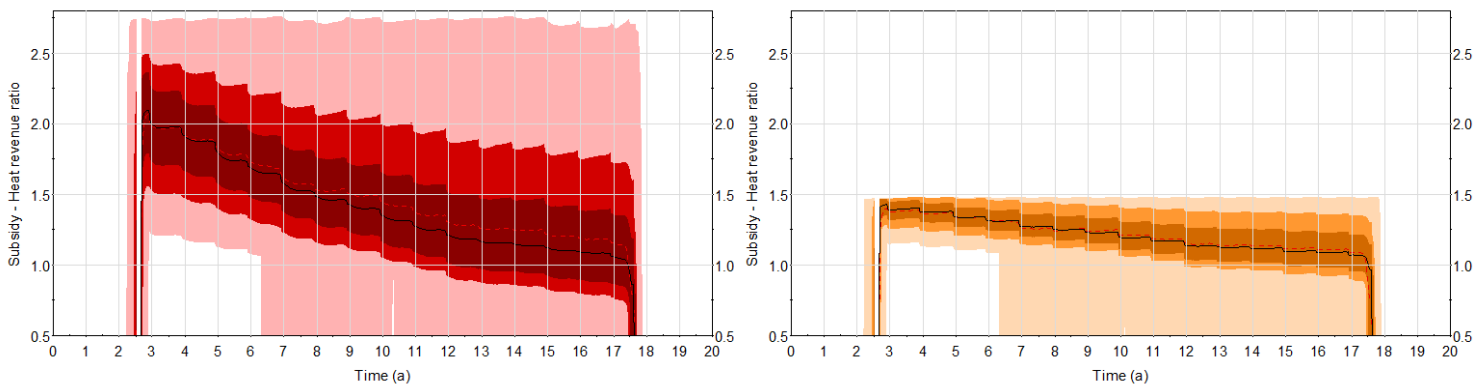
Figure 35: Subsidy/Heat revenue ratio distribution. RF and FHP on the left and right respectively. The amount of subsidy is the same for both scenarios, but the necessity of a subsidy decreases when a fixed heat price of 7 Euro/GJ is applied, compared to the heat price policies of today.

4.3.2   District heating concept subsidy SDE+ 2018

This scenario is based on a concept subsidy that is specifically designed for a project where the geothermal heat is utilized for district heating purposes. The base sum (cost of heat) for this subsidy, is set twice as high as the base sum for reference scenario. Obviously, with an unchanging correction price, this results in significantly higher subsidy revenues compared to the reference scenario as shown by Figure 36. High revenues early (first 20 years) in the project lifetime, result in the lowest payback time and highest profitability index of all scenarios considered here. This increases the attractiveness in terms of investing significantly.
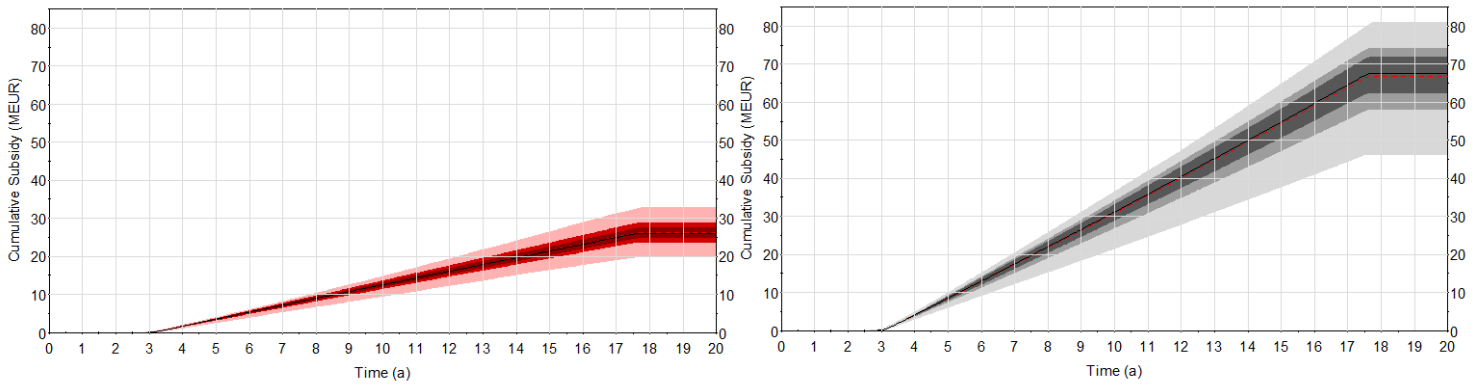
Figure 36: Cumulative subsidy distribution in MEuro (inflated). RF and DHC on the left and right respectively.

The second difference for this scenario is the total amount of full capacity hours of the subsidy. These are 3500 full capacity hours each year for this scenario (40% load factor), compared to the 6000 hours per year (68% load factor) for the subsidy of the RF scenario. This means that if a project would produce exactly at the full capacity hours described in both subsidies, the total amount of subsidies that are paid out for the district heating subsidy are always higher compared to the subsidy of the reference scenario. In Figure 37, the distribution for the full capacity hours of the model are illustrated, which are the same for this scenario as for the RF scenario:
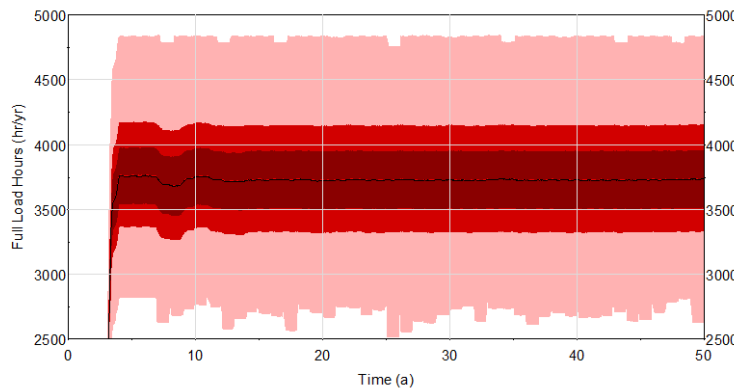
Figure 37: Full capacity hours distribution. The 25th to 75th percentile are close to the full capacity hours of this scenario's subsidy. This results in maximized subsidy income available.

Maximum subsidy efficiency is achieved when the full capacity hours of the project match the full capacity hours of the subsidy. Therefore, considering the full load hours shown in Figure 37, the district heating concept subsidy from this scenario is much more suitable for the case study as described in this thesis.

4.3.3   Increased injection temperature

For this scenario, the brine is reinjected into the reservoir at 10 °C higher compared to the reference scenario. The temperature that can be usefully extracted from the brine is therefore on average around 27% lower compared to the reference scenario as shown by Figure 38.
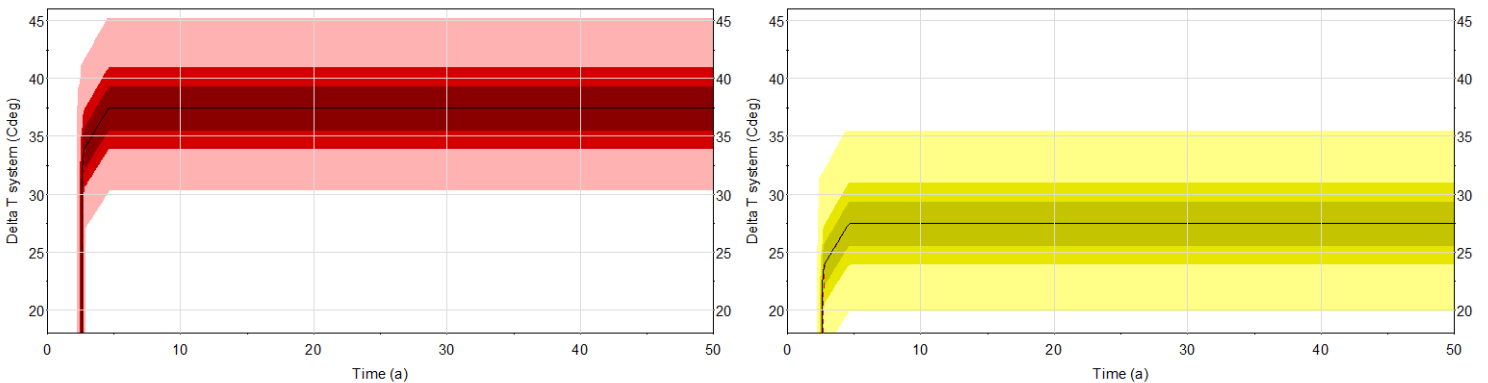
Figure 38: ΔT system in °C. The heat extracted from the brine by the heat exchangers is the aquifer temperature – system temperature losses – injection temperature. When aquifer temperatures are relatively low, high reinjection temperatures have significant influence on the usable temperatures overall

Less energy is extracted from the wells at similar flow rates and pump pressures. This means that the CoP of the system regularly drops below the lower limit value of 10 at maximum demand. When this limit is reached, a 13% correction is applied to the flow rate (Figure 39). This correction results in an additional decrease of the capacity of the wells and lowers the amount of heat and gas produced over time.
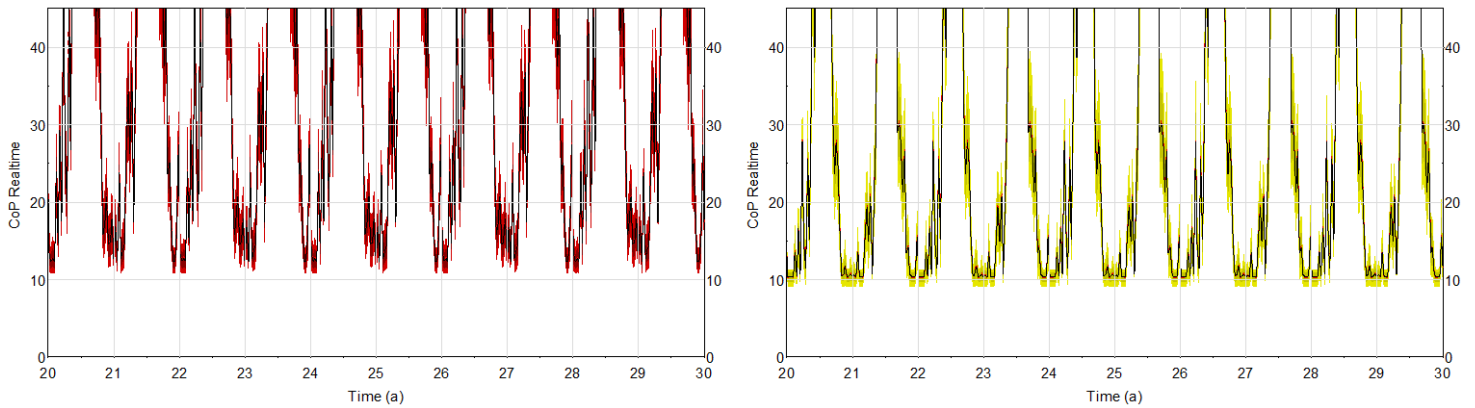
Figure 39: Real time CoP distribution during production. RF and IIT on the left and right respectively. ITT has a flatter pattern around the low COP values (~10). This is the result of the CoP adjuster that limits the minimum CoP around 10. For illustrating purposes, the min and max values are not shown.

With the capacity of the system being lowered by the higher injection temperature and CoP corrector, the yearly operational cost per kW capacity increases (Figure 40). The increased operational cost, combined with lower heat and gas revenues, results in the worst performing scenario overall.
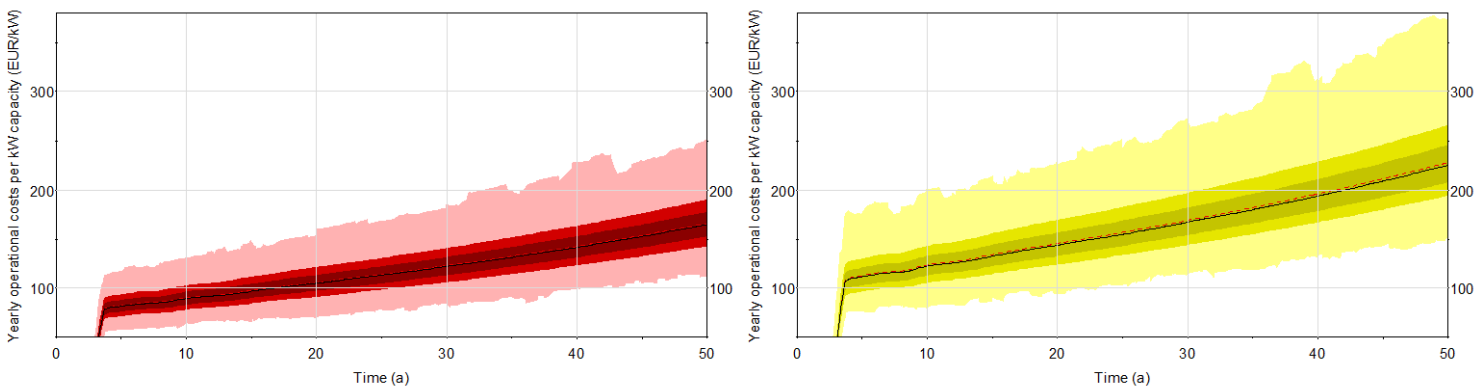
Figure 40: Yearly operational cost distribution in Euro/kW (inflated). RF and ITT on the left and right respectively.

With an increased return temperature, less energy is extracted with time from the reservoir. This results in a longer lifetime of the reservoir. If this return temperature is known before drilling the wells, the well spacing can be made shorter. Although this reduction in well spacing is not accounted for in the model, a shorter well spacing may reduce the cost of drilling by decreasing the depth along hole and can reduce the cost of operations by lowering the power required by the pumps. These two cost reductions can result in a higher NPV relative to this scenario, where the well spacing is equal for every scenario.

4.3.4 SDE+ realisation factor correction

For this scenario, the expected P50 capacity of the wells is decreased by a so-called power realization factor of 0.8. Historical data from 14 producing geothermal projects show a clear overestimation trend of the expected capacity of the doublet. When the projects were actually producing with a stable capacity, on average, 80% of the previously predicted P50 maximum capacity could be achieved [22].

For the reference scenario, the capacity of the wells is calculated by sampling a distribution for all the parameters of Equation 4, which are the maximum flow rate, temperature difference and the volumetric heat capacity of the brine. For this scenario, the capacity of the wells is a fixed value in the model instead of a distribution. The capacity is taken as the predicted P50 case for all elements of Equation 4. The capacity is then multiplied with the so-called Power realisation factor of 0.8.

Figure 41: Cumulative density function of the capacity of the wells and system for the RF on the left and RFC on the right. Hence the large distribution in probable capacity of the RF scenario overall. The high variance is the result of the large uncertainty of it inputs.

In terms of economic performance, this scenario is performing better than the ITT scenario, but is most similar compared to the other scenarios. Decreasing the P50 capacity with 80% has fewer negative consequences to the overall heat output and therefore heat revenues, compared to the scenario where the utilized temperature is lowered by 10 °C. The difference in heat output for these two scenarios is shown in Figure 42. Here, the effects are shown of the capacity distribution on the potential outcome in heat output. The realisation factor of 0.8 is based on the history of 14 geothermal projects in the Netherlands. In the future, when more projects are realized, the realization factor will have a better accuracy which can improve future doublet capacity estimates.
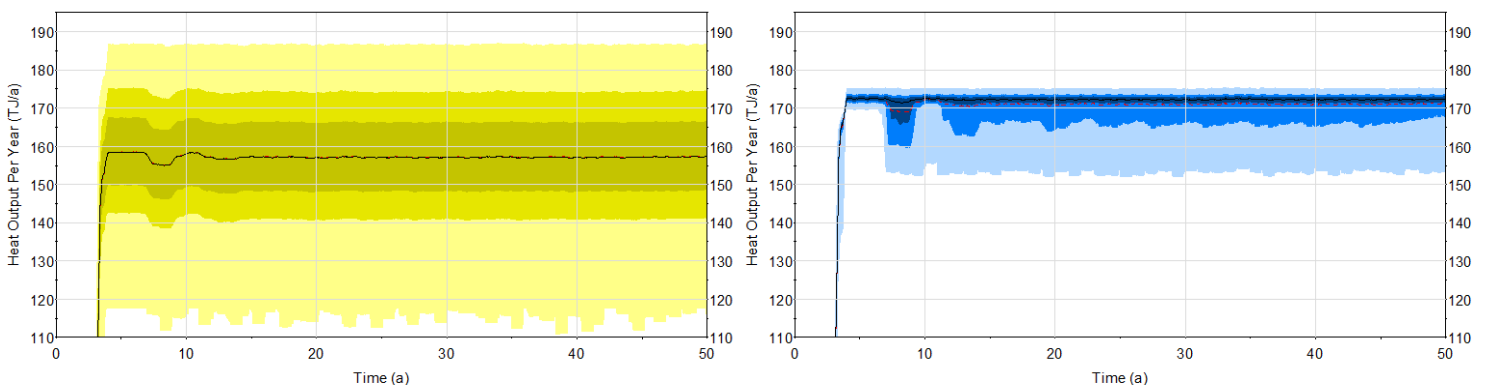
Figure 42: Heat output distribution in TJ/year for ITT and RFC on the left and right respectively. Here the difference in heat output variance is very well visible when the capacity of the wells is constant. An improved power realization factor improves the accuracy of future doublet capacity estimates.

When the capacity of the system is decreased relative to the RF scenario, fluctuations in the flowrate are lowered as they fit the TU Delft heat demand better, as shown by Figure 43. The wells for this scenario produce at a slightly higher and more stable rate. Although this is not simulated in the model, lower fluctuations in flow rate could increase the life expectancy of the pumps and general equipment overall which will lower the overall operational cost of a project.
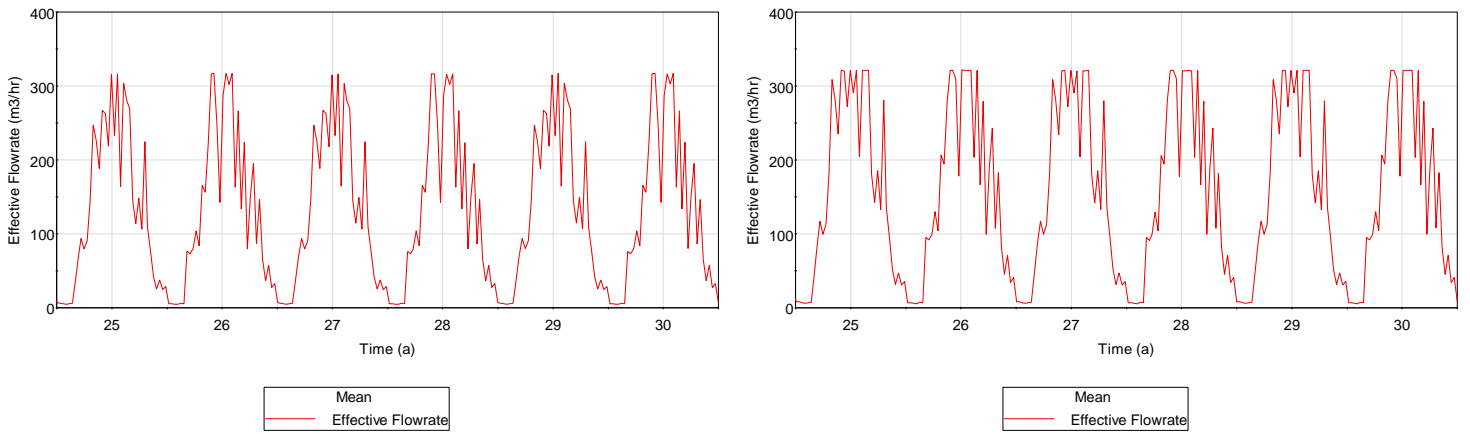
Figure 43: Real time average flowrate during production in m3/hr. RF and RFC on the left and right respectively. RFC produces less heat per year but has a more constant flowrate due to the absence of high capacity spikes. The CoP adjuster element in the model (section 3.4.4) is set to 0% for the RFC scenario due to the already existing limitation created by the power realisation factor.

4.3.5 Constant demand throughout the year

For this scenario, the heat demand is kept at a constant 80% of the maximum capacity of the wells, combined with an additional initial investment of 5 million Euro. This scenario has the highest Net Present Value at the 50 years mark but bears the largest uncertainty with it. The high profits are the result of a combination of high heat and gas production in general, combined with the maximum utilization of the subsidy revenues due to the full load hours at which this project produces (Figure 44).
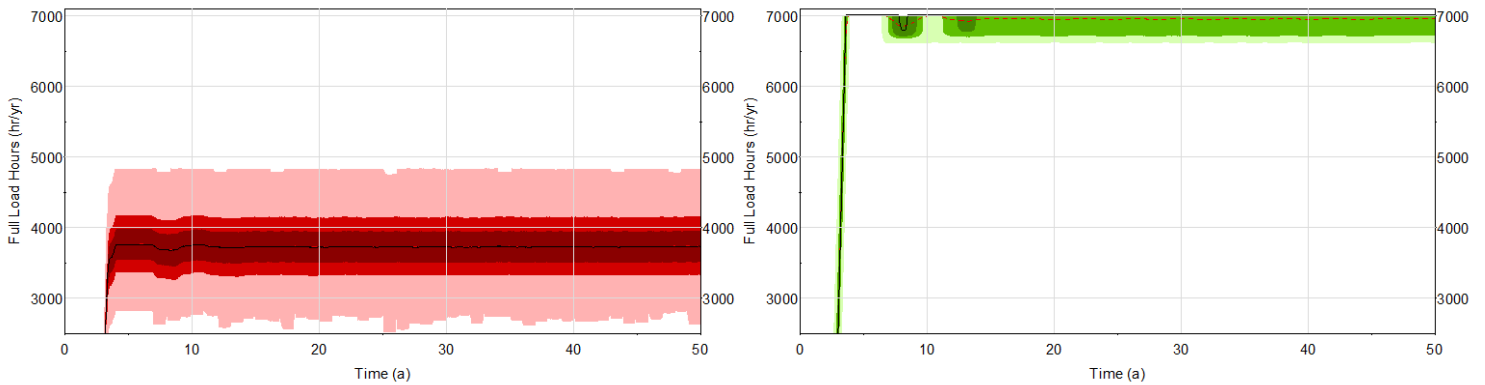
Figure 44: Full load hours distribution in hours/year. RF and CDY on the left and right respectively. 3700 and 7000 hours translates to a load factor of 42 and 80% respectively. Both have the same maximum capacity, but the CDY produces at 80% of this capacity whereas the RF scenario fluctuates according to the TU Delft Campus demand pattern.

The subsidy for both scenarios (RF and CDY) pays a maximum of 6000 full capacity hours per year. With 80% demand all year round, the full load hours exceed this number for the CDY scenario and therefore receives the maximum amount of subsidy available. This results in yearly subsidy pay-outs being around 1.5 times higher on average (Figure 45)
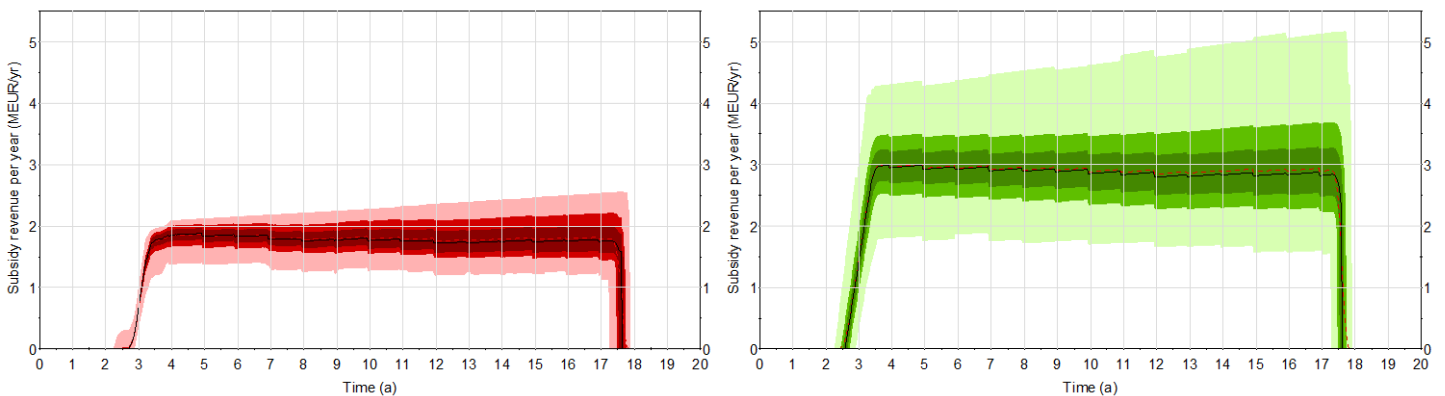
Figure 45: Subsidy revenue per year distribution in MEur/year. RF and CDY on the left and right respectively. High revenues in the subsidy term have a large influence on the NPV, IIR, PI and payback time.

The downside of this high, stable production scenario is the increased total operational cost of the project. This is caused by the increased electricity consumption of the pumps and the extra initial investment of 5 million. The fixed operational cost is calculated as 5% of the construction cost. If the construction cost increase, the operational cost increase as well. The overall operational cost per year for both scenarios are shown in Figure 46:
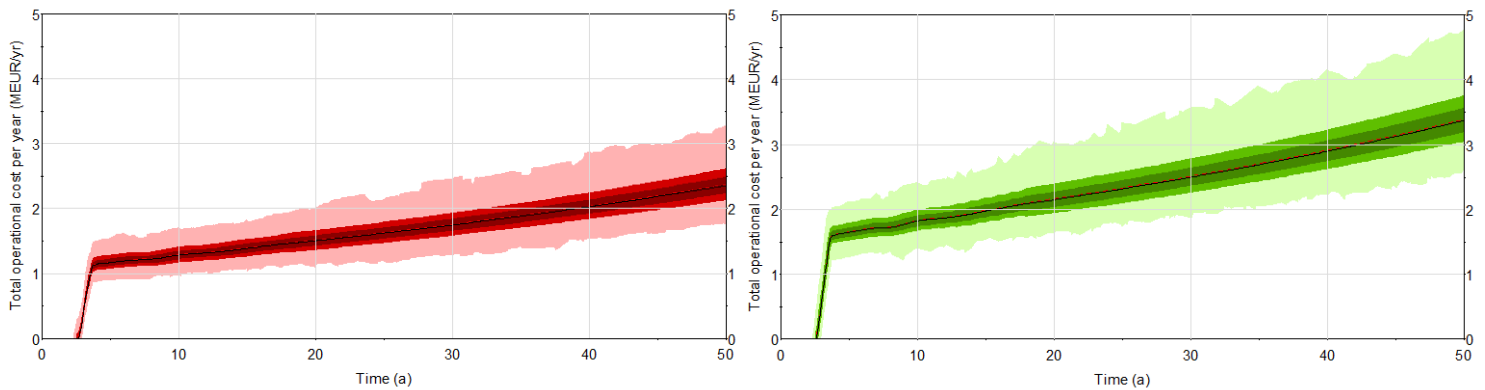
Figure 46: Total operational cost per year distribution (inflated) in MEur/year. RF and CDY on the left and right respectively.

With a mean CoP of 15.5 at 80% max capacity, high operational cost is not be a problem considering the high revenues received from the heat production. This also shows in the LCOH of this scenario, being to lowest overall. Nevertheless, a proper ESP design in regard to size, build and efficiency becomes more important with high, continues flow rates to keep operational cost down and increase overall profits.

The absence of peak loads on the pumps combined with a stable flowrate year-round (Figure 47) could be highly beneficial for the lifetime of the pumps and equipment if this would be considered in the model. Additionally, if a well is producing at lower capacity than it is designed for, extra margins are created for a scenario where the reservoir does not flow as easily as expected, which reduces the risk of a project overall.
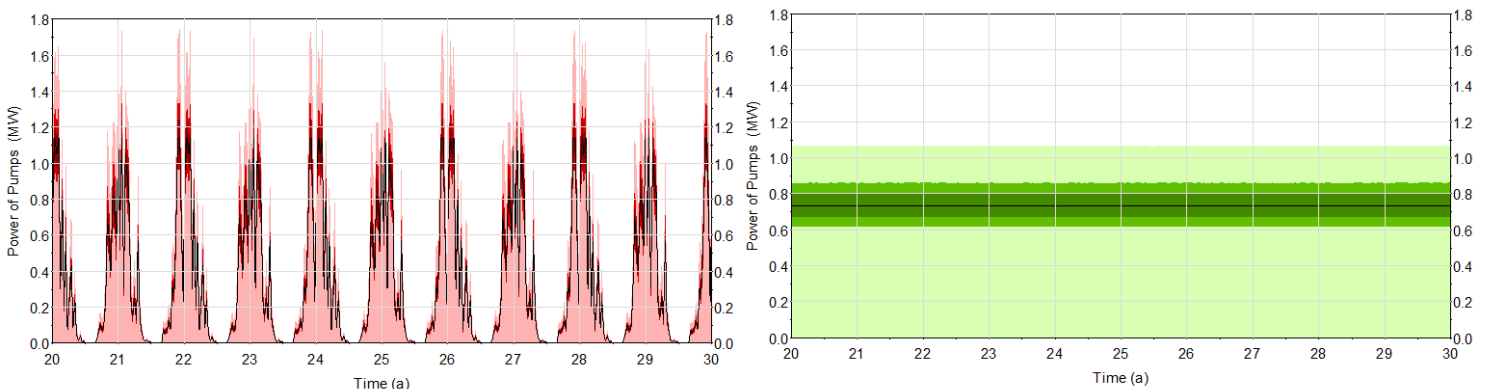
Figure 47: Real time pump power during production in MW. RF and CDY on the left and right respectively. The pumps are working much more efficient when a stable flowrate is applied that is under the maximum capacity of the wells. The P50 CoP of the CDY scenario is 15.4 compared to the lower CoP of the RF scenario as shown in Figure 39.

A potential negative result from producing at a constant high rate is the reduction of thermal breakthrough time. With a normal demand pattern, it is expected that the thermal breakthrough for the DAP well will be around 50 years with a possible small decline in production temperature. Nevertheless, when referring to the NPV, even if the temperature starts declining at 30 years of the project's life and production is stopped at this time, the CDY scenario still outperforms the NPV of most the scenarios at the 30 years mark.

4.3.6   Gas Utilized in gas generator

For this scenario, the produced gas is utilized in a gas generator. The purchase of this generator is added to the initial investment of the project. The economic performance of this scenario is very similar to the reference scenario in terms of NPV but has lower payback times and Levelized Cost of Heat. The latter is caused by the electricity produced by the generator that can be used for the pumps, combined with the additional heat

produced. The additional heat produced by the co-generator increases the production capacity with 1.3 MW on average, at maximum gas output (Figure 48).
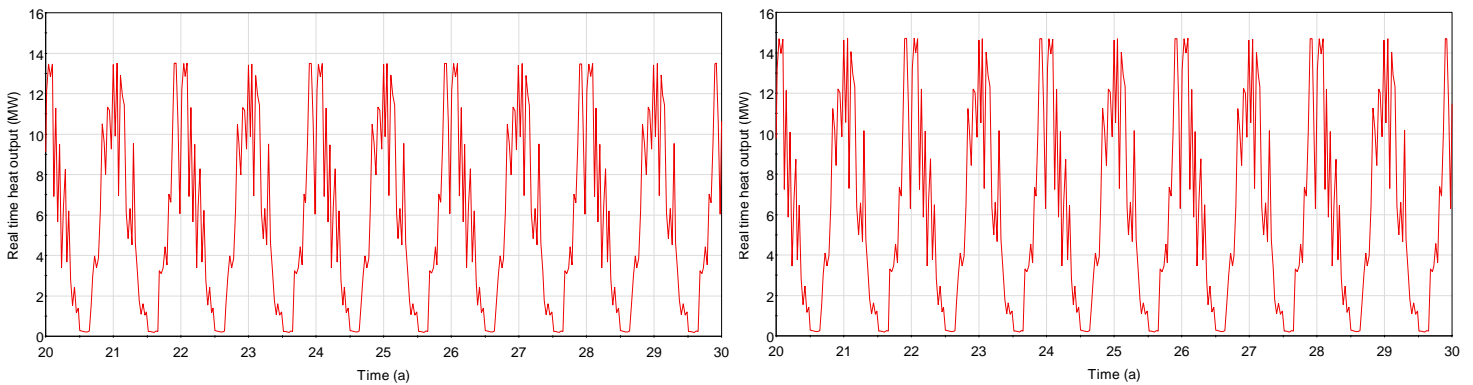
Figure 48: Average real time heat output of the system in MW. RF and GGG on the left and right respectively. Approximately 1.3 MW is added by the additional heat production at maximum gas input from the generator.

Surprisingly, this additional heat increases the heat revenues only slightly as shown in Figure 49. The difference in heat revenues between both scenarios could be significantly higher if additional demand were created at the lower levels of the demand curve.
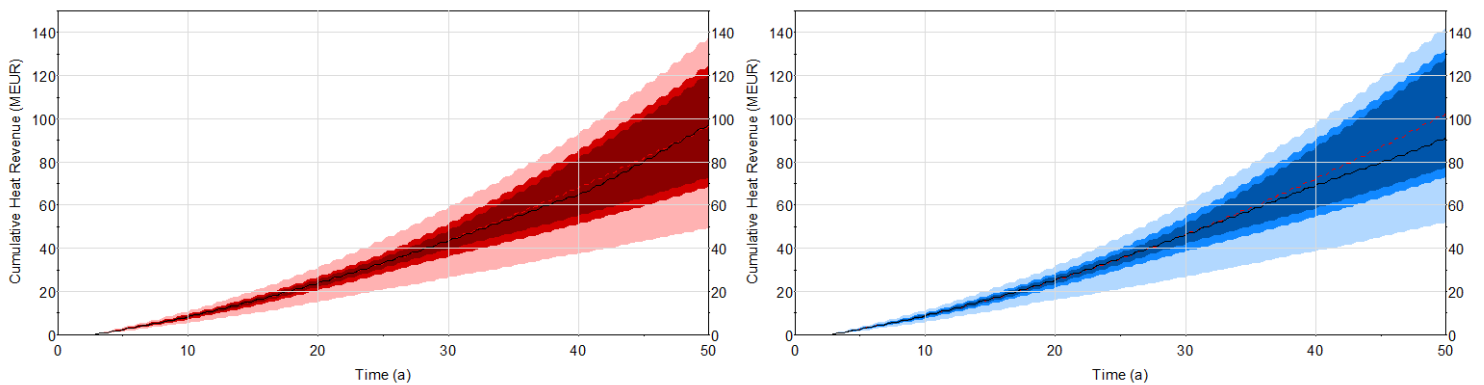
Figure 49: Cumulative heat revenue distribution in MEur. RF and GGG on the left and right respectively. Only minor extra revenues are generated by the additional heat production due to the limited demand of the case study.

Additional demand will increase the overall demand/max capacity ratio (Figure 50) and generate extra heat revenues which will make the purchase of a co-generator more attractive as a design option.
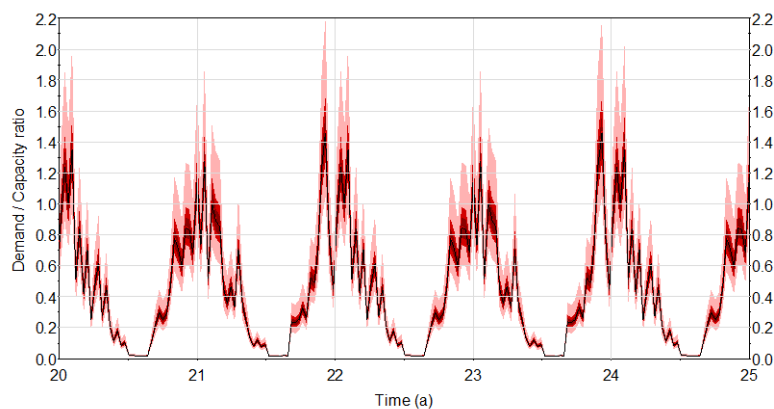
Figure 50: Demand/capacity ratio in real time for the reference scenario where only heat from the well is considered. A ratio above 1 is needed to generate extra revenues from the additional heat produced. These peaks above 1 need to be longer in duration to utilize the additional heat at its maximum.

When a co-generator is used, no or very little revenues are received from gas production. In return, energy costs of the pumps are saved, and any excess electricity can be sold back to the grid (Figure 51).
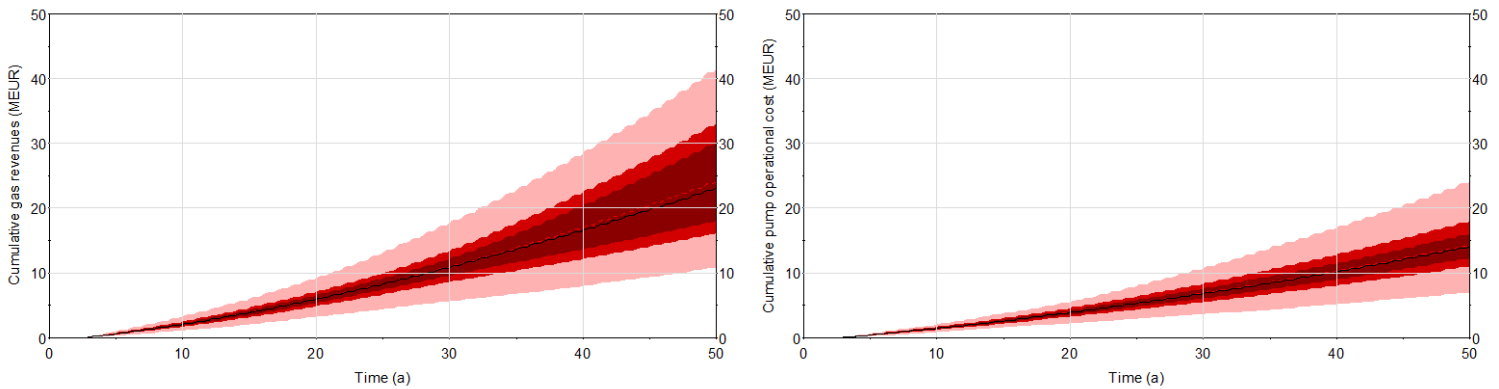
Figure 51: Cumulative gas revenues distribution compared to the saved cumulative pump cost when a generator is used. Gas revenues exceed the saved electricity cost from the pumps by a long stretch. Nevertheless, the combination of extra revenues from electricity and additional heat production does make this scenario competitive compared to the reference scenario.

The combination of receiving revenues from electricity (Figure 52) and additional heat combined with the saving on electricity cost of the pumps makes this scenario very competitive with the reference scenario. On the other hand, the investment risk for a co-generator is high, when a scenario is considered where the gas concentration is not stable but decreases rapidly after first production.
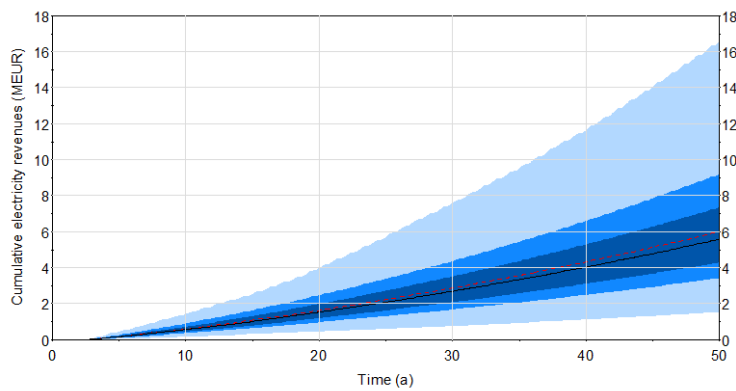
Figure 52: Cumulative electricity revenues distribution in MEuro for the GGG scenario.

4.3.7 Declining gas concentration during production period

In this scenario the gas/water ratio decreases at a certain time during the project's life. This decline initially starts from a P25-P75 value of 0.9-1.1 respectively, where the decline rate is sampled between a distribution of 5 to 15% per year (Figure 53).
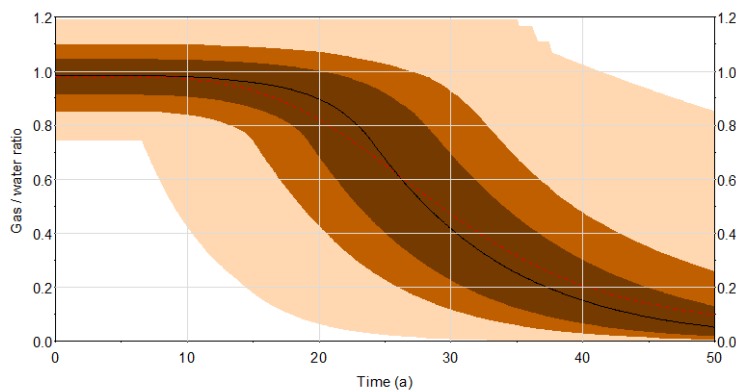
Figure 53: Gas/water ratio distribution curve for the DGC scenario

55

A declining gas/water ratio can have a high impact on the project revenues, especially when future gas prices are high. (Figure 54). Referring to P25 – P75 of both scenarios, a future value revenue of 9 to 15 million can be missed after 50 years of producing if the gas concentration declines early.
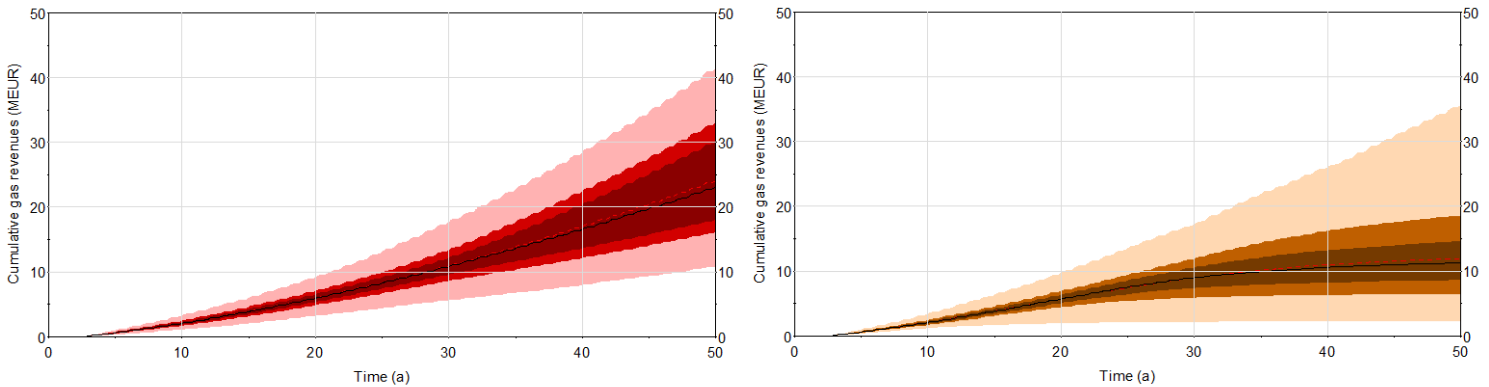
Figure 54: Cumulative gas revenues distribution in MEuro. RF and DGC on the left and right respectively. These revenues are shown as the future value and need to be discounted when compared to the Net Present Value.

Surprisingly, the median Net Present Value of this scenario is less than 2 million euro lower at the 50-year mark compared to the reference scenario. This can be explained with the time value of money. The financial losses associated with a decrease in gas production are worth less when they occur in later production stages of the project (Figure 55).
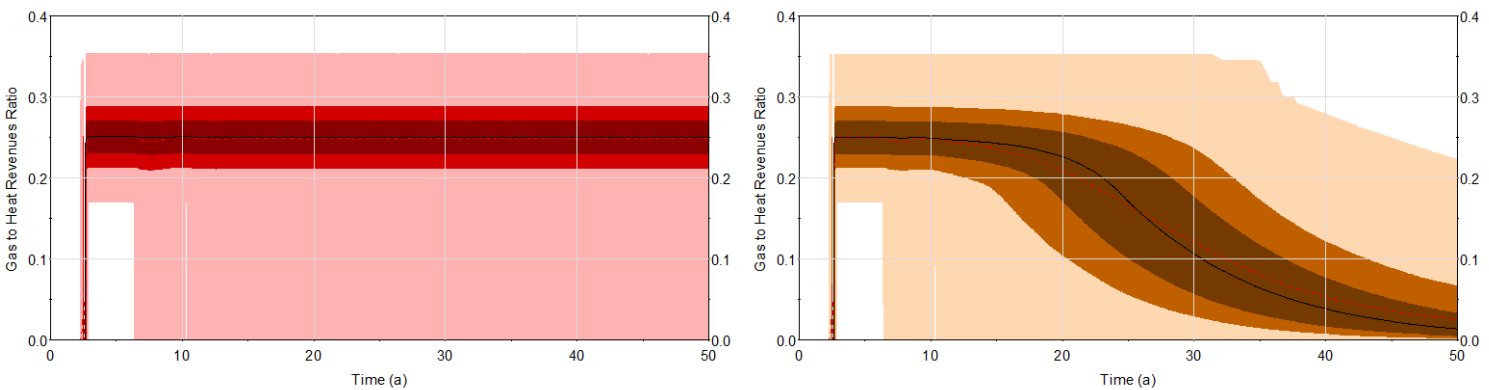
Figure 55: gas to heat revenues ratio distribution of the RF and DGC scenario on the left and right respectively. An initial decline in gas production at 15 years as shown in the right graph does not have a very large influence on the NPV compared to a scenario where no gas is produced at all. For the RF scenario, the minimum ratio is around 0.17 during the entire production period. The ratio drops to 0 on moments of maintenance when no heat or gas is produced.

4.3.8   No Gas Revenues

The absence of gas revenues results in the second worst economically performing scenario overall. Gas revenues account for 17 to 35% of the heat revenues for the reference scenario (Figure 55 left). If these revenues are not considered in a business case of a project like the DAP well, a large underestimation could be done of the potential project revenues if a constant, decent gas production can be realised for a longer period of time.
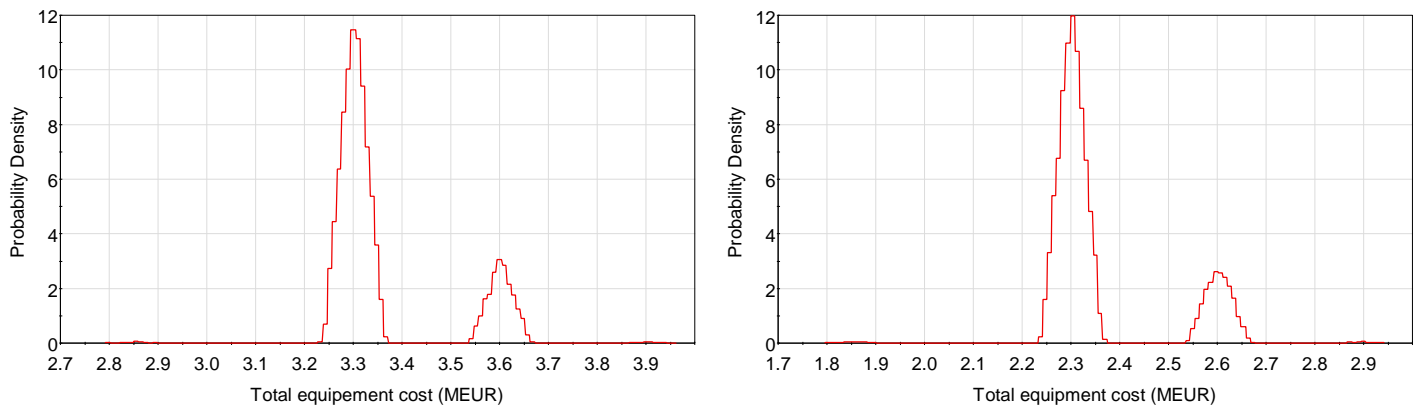
Figure 56: Probability density function of the total equipment cost of the RF and NGR scenario on the left and right respectively. The NGR scenario has a lower equipment cost due to the absence of the gas separator. The two peaks are explained by the shift in cost of the ESP after a certain ESP capacity is exceeded.

Gas production can also be a financial burden if the gas concentration starts high but decreases rapidly in the first few years of production. This is due to the necessity of the purchase of a gas separator. If this is piece of equipment is compared to the total equipment cost, the separator consists of a little less than 1/3 of the total equipment cost (Figure 56). This explains the lowered LCOH of this scenario where the separator is not included in the initial investment.

4.3.9 High initial subsidy

For this scenario, the base sum starts at 0.10 Eur/kWh with an annual decrease of 0.91^t, wherein t denotes the time in years. With this starting base sum and decline, an equal amount of subsidy is paid to the operator after the subsidy term of 15 years compared to the reference scenario (Figure 57).
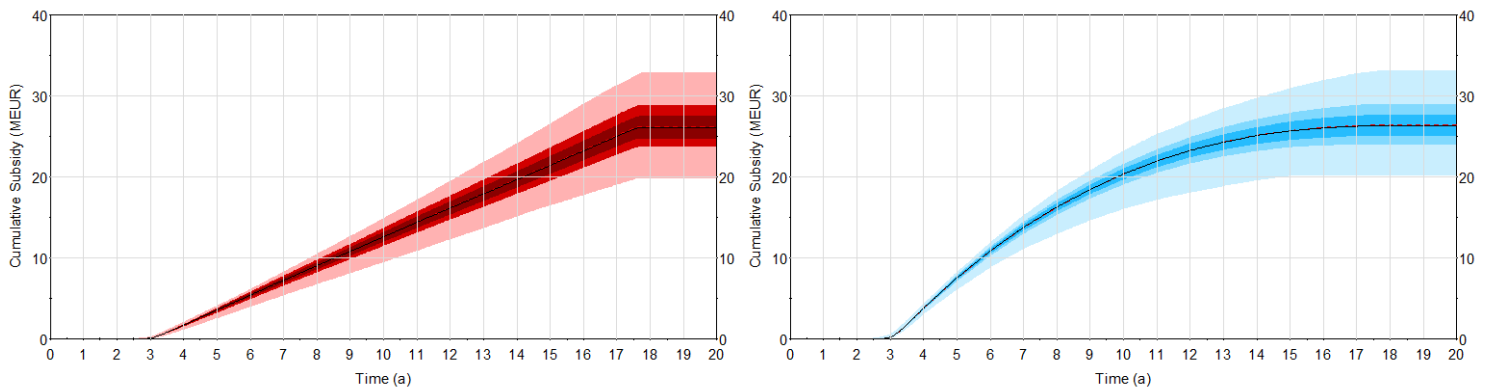
Figure 57: Cumulative subsidy in million Euro for the RF and HIS scenario on the left and right respectively.

The early high subsidy payments do not change the cumulative cash flow compared to the reference scenario but do improve the P50 NPV significantly with an 40% and 22% increase at the 30 and 50 years mark respectively due to the time value of money. The starting amount of subsidy revenue is double compared to the reference scenario and decreases to zero after roughly 15 years. (Figure 58)
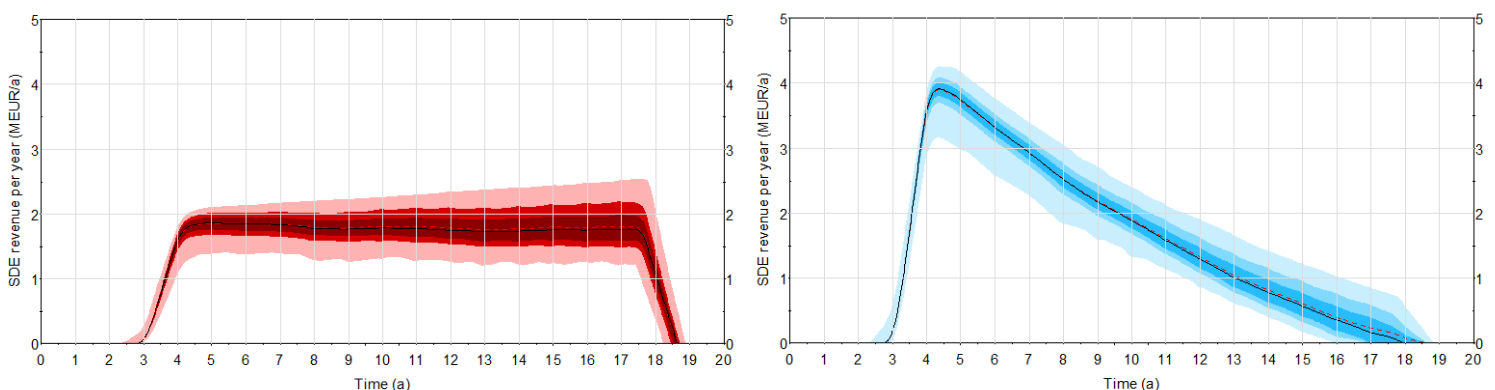
Figure 58: Subsidy revenue in million Euro per year for the RF and HIS scenario on the left and right respectively.

57

This method of subsidizing results in a P50 payback time of 7.7 years. This is the second-best payback time of all scenarios without adjusting the total amount of heat produced or subsidy received. The amount of available heat networks sufficient for geothermal district heating purposes is considered a limited factor today in terms of available demand and will grow slowly in the future. A higher subsidy at the start of production can help a project stay profitable with limited initial demand and be more independently profitable when networks, and therefore demand is improved with time. Nevertheless, this method of subsidizing does also have its limitations. For one, high subsidy-based profits in the first years of production can lead to decreased incentive to continue producing when most of the subsidy revenues are received. Additionally, when a project starts producing, they can often experience startup problems in terms of well performance, that limits the amount of heat produced in the first 1 to 2 years. This can become very costly in terms of missed subsidies if desired production rates are achieved on a later stage than expected.

4.4   Answering the research sub questions
This section will provide the answers to the sub questions that are obtained with the models results.

How does the current Dutch subsidy scheme perform on an individual project level of today? How could it be made more efficient?
At this moment the necessity for a subsidy is undoubted for individual geothermal projects. The high initial investment combined with the moderate cash flows associated with direct heat utilization makes it next to impossible for a project to be financially viable without subsidy support. Only a scenario where the project is upscaled to multiple doublets, where the heat production is significantly higher and costs per doublet are decreased can potentially be independent from subsidy income, if sufficient demand is available. As of today, a subsidy scheme is provided that has been designed especially for the needs of greenhouse heating. The case study in this thesis is developed for district heating purposes and therefore does not benefit from the subsidy to its maximum potential. With limited demand and lower well capacity due to potentially higher return temperatures, the cost per kWh increases compared to greenhouse heating projects. The district heating concept subsidy is adjusted in terms of base sum and full capacity hours to supplement the increased production cost. When this concept subsidy is applied to the case study, a far better economic performance is delivered from the project if a return temperature of 35°C can be realized. Even if gas revenues are not considered, the concept subsidy provides a sufficient economical buffer when essential variables like injection temperature, well flow performance and operational cost are estimated too optimistic (Figure 28) and therefore decrease the risk of investment.

Geothermal district heating has recently been introduced in the Netherlands, combined with many challenges. The biggest challenge today is the amount of demand available. More demand is created by the installation or adjustments of existing heat networks, but this is a slow process. A district heating project realized in the near future will meet with expanding demand during the first years of production but starts off with a lower number of full capacity hours because of this. The initial low demand can result in a limitation of subsidies received that in turn increase the production cost per kWh. The function of a geothermal subsidy is to supplement the insufficient heat revenues of a project. These heat revenues are generally the lowest in the first few years of production as a result of limited demand occasionally combined with unstable well performance. Therefore it is advised to adjust the base sum from a constant sum, to a subsidy where the base sum decreases with time, similar to the HIS scenario. The starting base amount and declining rate need to be designed in such a way that the subsidy creates a positive revenue during and after the subsidy period without decreasing the incentive to continue producing after the subsidy term has ended. This can only be achieved when subsidies are created on a more individual basis instead of a one base sum fits all principle.

What is the effect of decoupling the geothermal heat price from fossil fuel prices?
In today's policies, the heat price is equivalent to the energy price of gas. This makes the level of heat revenues and subsidy contributions dependent on future gas price developments. If the heat price is decoupled to a fixed price as shown by the FHP scenario, the distribution in potential economic outcomes are reduced significantly. A fixed heat price of 7 Euro/GJ results in a positive NPV with high certainty (min 90%), but the overall profits are moderate compared to the reference scenario in a case of high gas prices. In a realistic sense, a constant heat price would not be possible for 50 years in a row. Contracts are signed for about 10 years, partly based on the prices of alternative energies available. So in a way, the heat price, even when decoupled, would stay partly

dependent on the prices of alternative energies. Nevertheless, a fixed heat price will be preferable over a gas dependent price in terms of risk. The price of heat as it is set in the subsidy of today is highly fluctuant. If the price of gas suddenly declines, a geothermal project with contract-based heat prices will be better off financially, if the contracts are long term.

What is the sensitivity of the financial performance to the various technical and economic uncertainties of geothermal projects/systems?

Many variables, each with their own uncertainty, are combined to generate the results of the financial outcome of a project. The model's variables from Table 1 are collected from intensive literature research such as journal publications, manuals, websites, reports and personal communication. The overall availability of such data is limited, due to their commercial value, specific design and changing nature. Many of the data from Table 1 were gathered from historical data, based on only a small number of geothermal projects in the Netherlands. With time, more data will become available from newly realized projects, which decreases the uncertainty of these inputs. The data from Table 2 were requested from the operator. The uncertainty of the parameters they provide are highly dependent on the quality of the geological research they performed. Estimates about the flow rate and associated pump pressures, expected demand, well design and return temperatures are often estimated too optimistically, which can result in a lower performance of the wells at initial production. By modelling the different scenarios, where parameters variations like the ones mentioned are inserted, a general overview is established of the potential outcomes of such scenarios. Additionally, the sensitivity analysis provides an overview of the variable's independent sensitivity.

In terms of economic performance of the model, the most sensitive variables in decreasing order of importance are subject to the heat price, heat demand, subsidy amount, operational cost, well capacity and drilling cost. The highest potential earnings are produced from the CDY scenario where a constant, high heat demand is simulated. With the high heat and subsidy revenues and an additional investment of 5 million euro, the NPV can reach up to 3 times the NPV of the reference scenario. Additionally, LCOH for this scenario are the lowest compared to the other scenarios. The large distribution from this scenario is mainly caused by a combination of the uncertainty of the heat price, capacity of the wells and the revenues from gas production and subsidy income. The other highly performing scenario is the DHC scenario where the subsidy is altered to lower full capacity hours combined with a double base sum for the purpose of district heating. This subsidy scenario fits the characteristics of the case study better in terms of full capacity hours and results in the best payback time as a result of high, early cash flows which are enhanced in the NPV analysis as a result of the time value of money.

5 Conclusions

For this project, a probabilistic techno-economic model is developed for deep, direct use geothermal projects in the Netherlands. The model is a revised and expanded version of the model described in [24]. As a case study, the data from the future DAP well is inserted wherein multiple scenarios are researched that model variations in well capacity, energy prices, project design, government policies, brine gas content and heat demand. For the case study, the model considers a technical and economic uncertainty over a period of 50 years using 15000 Monte Carlo simulations. By modeling these scenarios, an overview is developed of the economic feasibility of a deep geothermal district heating project including an evaluation of the effectiveness of the Dutch subsidy scheme and the main financial obstacles associated with geothermal exploitation. The aim of this research is summarized in the following research questions:

What is the current status regarding the economic feasibility of deep, direct use geothermal projects in the Netherlands and how can this be improved for future projects?

The current economic status is answered by modelling the geological data of the case study combined with data from literature that is generally based on historical data from the 17 greenhouse heating projects that are currently producing in the Netherlands.

The economic and individual technical results show large variations and uncertainty in the potential economic outcome of a geothermal project. The data is subjected to high variance, especially for variables such as heat price, heat demand, subsidy amount, operational cost, well capacity and drilling cost. Single number analysis as seen in several business case examples are therefore unsuited for an economic performance analysis.

Highest NPV sensitivity is found in the operational cost as a percentage of the construction cost. This method of fixed operational cost is used in multiple geothermal performance analyses and should therefore be further researched.

The subsidy base sum is considered a constant in the SDE subsidy of today. An alteration of this number results in the second highest sensitivity parameter of the data followed by the gas/water ratio, maximum flow rate, discount rate and well drilling and completion costs. Normally the maximum flowrate would be higher in the ranks of sensitivity but is bounded by the low demand of the reference scenario in a case where higher flow rates can be achieved. The cost of well drilling and completion for the case study is comparable to historical cost based on 14 geothermal wells in the Netherlands. Large investments can be saved on well drilling when more wells are drilled per contract as a result of the potential drilling learning effect and logistical advantages.

The economic performance evaluation tools used in this research are dependent on the time value of money. Therefore, the timing of the cashflows is important in terms of project design and geothermal exploitation. The period of exploration and construction need to be planned and payed for in a stepwise manner. Expenses postponed to later stages of a project can improve the NPV and lower the overall risk of a project whereas profits should be earned as soon as possible in the project's lifetime.

The reference scenario of the DAP well, where gas revenues are considered, results in a positive NPV at the 30 and 50 years mark for at least 90% of the data with a median NPV resulting in 4.9 and 8.2 million euro at both time periods respectively. Without gas revenues, at least 75% of the data results in a positive NPV where the median NPV is 2 and 4 million Euro lower at the 30 and 50 year mark respectively.

Assuming a gas/water ratio of around 1, a decline in gas concentration at later stages of a project (>15 years) does not influence the NPV to a large extend. When this decline initiates at an earlier moment however, the purchase of a gas separator and co-generator decreases the NPV of a project even further. When a generator is purchased, slight improvements in terms of NPV can be seen for both time periods relative to the reference scenario, if a constant gas concentration can be realized. The relatively low heat demand of the case study does not utilize the additional heat produced from the generator to its fullest potential. Therefore the gas concentration and heat demand throughout the project's lifetime are two very important aspects when a co generator is considered for purchase in terms of project profitability.

There are two scenarios modelled where the capacity of the wells is lower as expected. One as a result of higher return temperatures and for the second scenario a 20% overall reduction in capacity is simulated. An increase in return temperature of 10 °C results in the worst performing scenario overall with a 25% chance on a negative NPV at both time periods.

The price of heat is dependent on the price of gas. To decouple this dependency, a scenario is simulated where a constant heat price is modelled. A constant heat price does not perform better in terms of NPV, compared to the reference scenario but decreases the risk of potential losses and improves the payback time.

A scenario is modelled where an alternative subsidy payment is considered without adjusting the total sum of subsidy received. Higher initial subsidies can supplement the starting period of production, often characterized with low initial demand for district heating and unstable well performance.

The highest potential earnings are produced from the Constant Demand throughout the Year (CDY) scenario where a constant, high heat demand is simulated. High heat and subsidy revenues combined with an additional investment of 5 million, result in an NPV that can reach up to 3 times the NPV of the reference scenario combined with the lowest LCOH compared to the other scenarios. The second high performing scenario is the District Heating Concept subsidy SDE+ 2018 (DHC) scenario where the subsidy is altered to lower full capacity hours combined with a double base sum for the purpose of district heating. This scenario results in the shortest payback time and the highest NPV at the 30 year mark for the 90th percentile. Even when no gas revenues are considered, sufficient economic buffer is created when the well capacity is lower than expected.

In district heating, high capacity doublets that are characterized with high investment cost, are only profitable when sufficient demand is available. A combination of a subsidy that supplements the low initial demand combined with a higher, stable heat demand later on result in an economically viable project even when gas revenues are not considered. Therefore, to realise the growth stated by the masterplan in terms of district

heating projects, focus should be aimed at the realisation of sufficient heat network deployment, heat storage options and more project specific subsidies.

6   Recommendations

As a result of this thesis, additional research is recommended on various parameters of the model. As shown by the sensitivity analysis, operational cost as a fixed percentage of the construction cost show high sensitivity to the economic outcome of a project. Therefore it is advised to collect and compare investment and operational cost data from the geothermal projects producing at the time, to improve the accuracy of the average operational cost as a percentage of the investment. The other variable is the gas/water ratio. For most of the scenarios, the gas/water ratio is constant. In reality, this ratio usually decreases at a certain point during production, but there are also cases known where this number actually increases after a certain production time. Considering that this ratio is the third most sensitive variable of the model for the reference scenario, more understanding needs to be collected about the behaviour of dissolved gas concentration in low enthalpy reservoirs.

To really show the positive economic effects of project upscaling, additional case studies such as a project with multiple doublets or an ultra-deep project should be considered in the model as well. Case study like these can improve the visualization of the benefits of the drilling learning effect and could provide a better understanding of the sensitivity of variations in geological parameters involved.

The high variation and uncertainty of the future energy prices resulted in an overall dominant effect in economic performance uncertainty. Therefore it is advised for further scenario analysis to separate the low and high gas price scenarios from the other variables. In other words, one future energy price scenario should be considered when running a simulation, to get an improved visualisation of the uncertainty of all other variables involved in the analysis.

The last recommendation is subjected to the reservoir temperature during production. If the model would be improved in the future, the addition of a breakthrough element will improve the model's scenarios overall. In a scenario where the injection temperature is increased for example, a well spacing reduction could make this scenario profitable if breakthrough time is considered.

7 Appendixes

Appendix A: Simulation accuracy
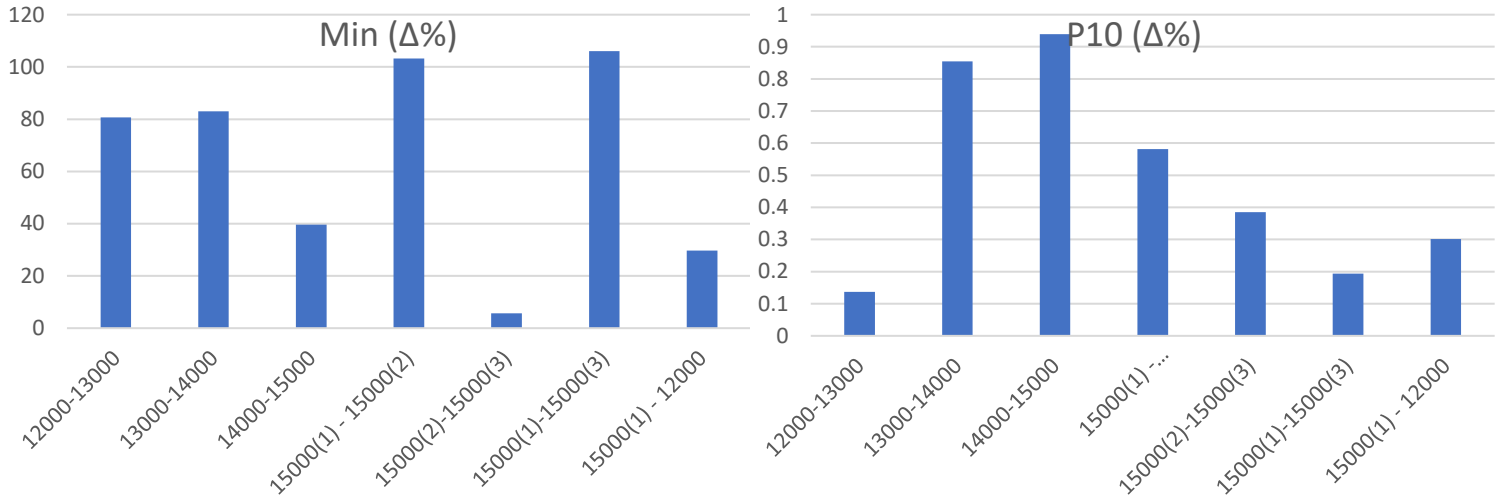
Figure 59: P0 and P10 average result difference from 4 time periods (20, 30, 40 and 50 years) between different number of iterations. The legend shows the number of iterations ran.
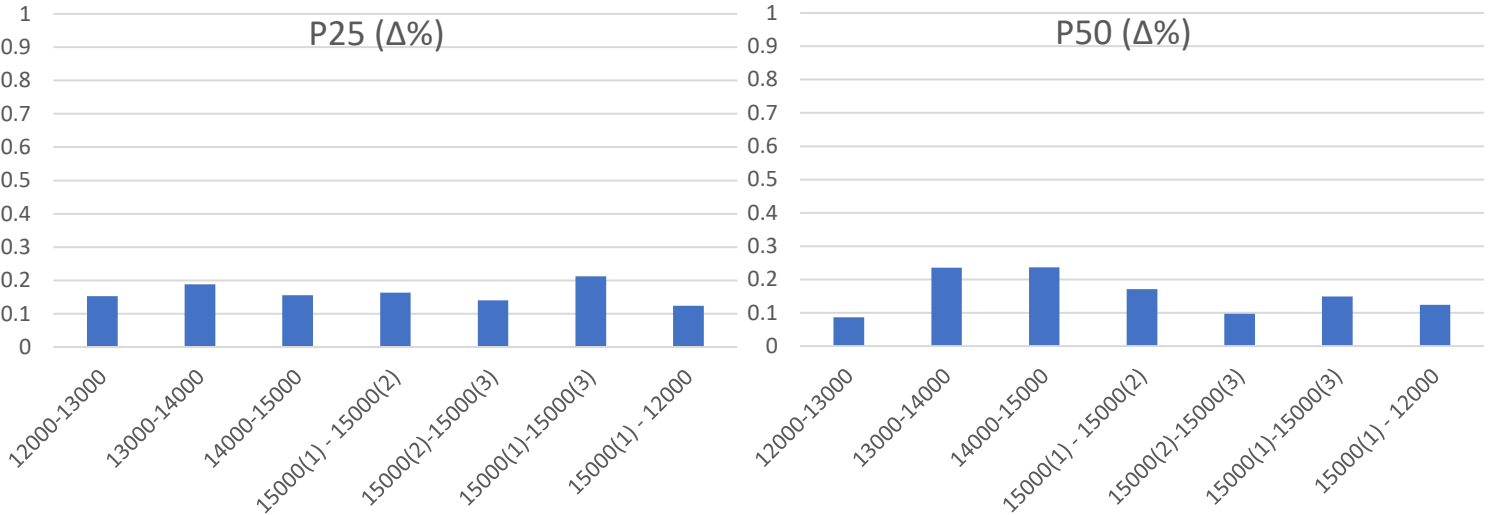
Figure 60: P25 and P50 average result difference from 4 time periods (20, 30, 40 and 50 years) between different number of iterations. The legend shows the number of iterations ran.
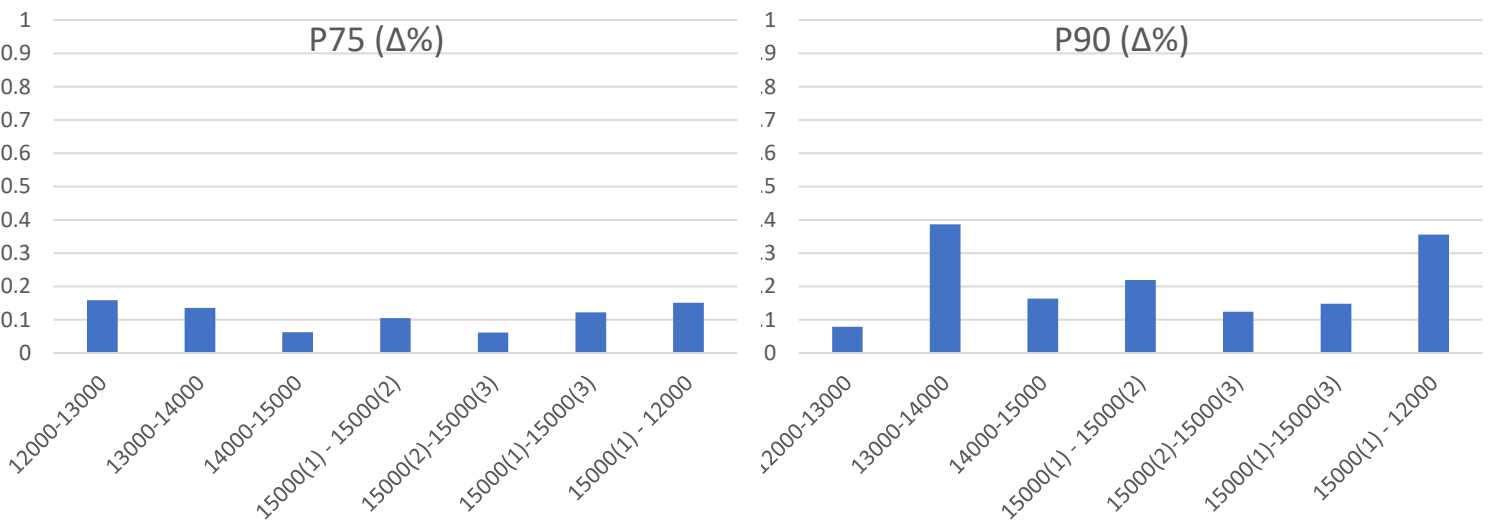
Figure 61: P75 and P90 average result difference from 4 time periods (20, 30, 40 and 50 years) between different number of iterations. The legend shows the number of iterations ran.
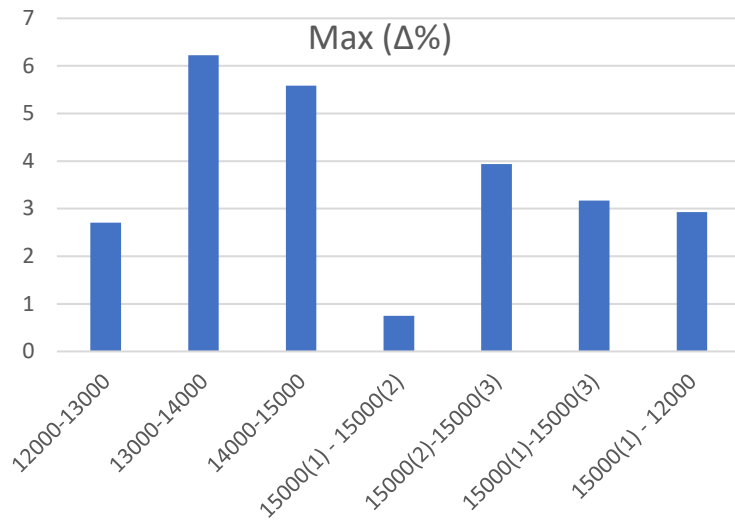
Figure 62: P100 average result difference from 4 time periods (20, 30, 40 and 50 years) between different number of iterations. The legend shows the number of iterations ran.

Appendix B: Additional model results RF scenario.

B.1 Development and investments
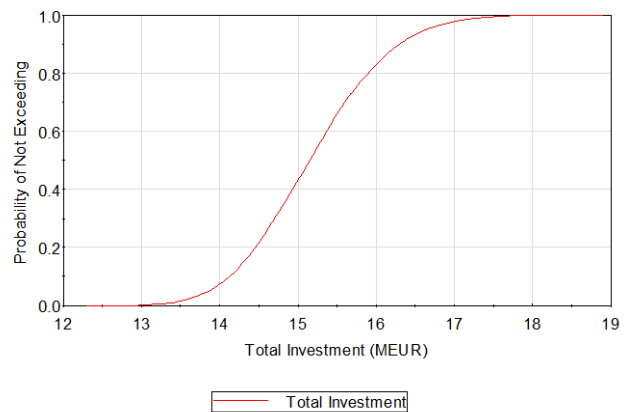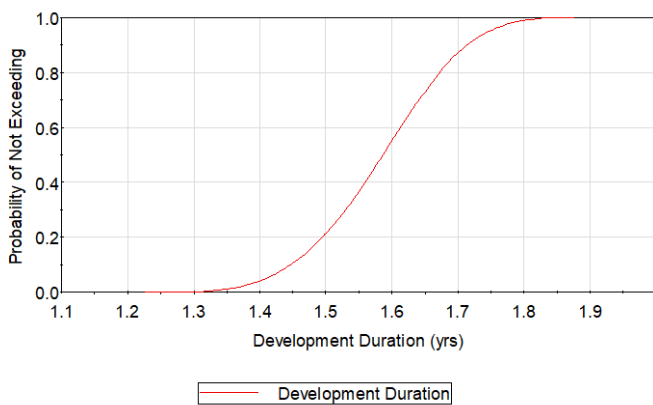
Figure 63: Development duration and total investment Cumulative Density Function (CDF) on the left and right respectively

B.2 Well capacity elements
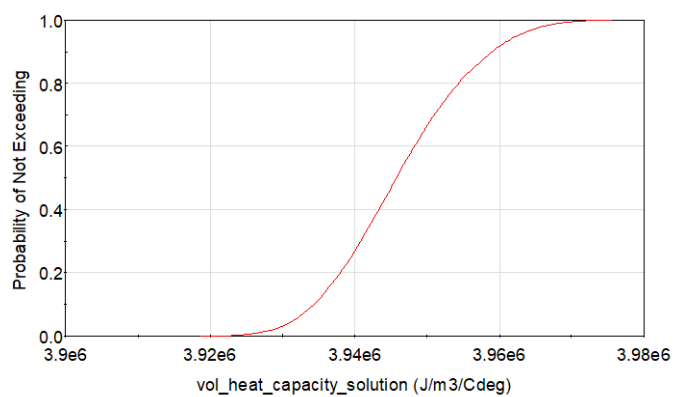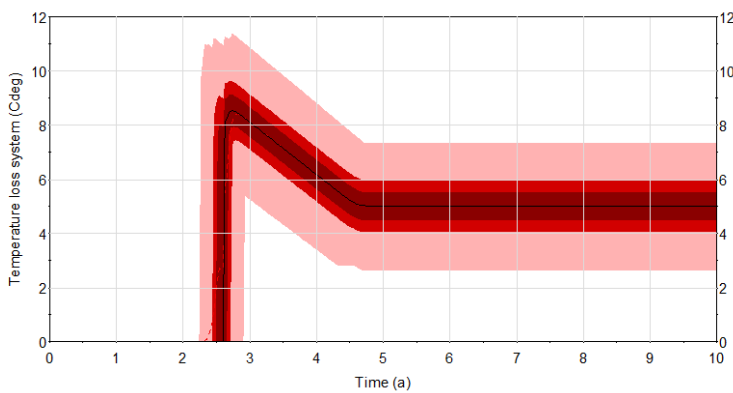
Figure 64:Temperature loss system distribution and volumetric heat capacity CDF on the left and right respectively

B.3 Pump parameters
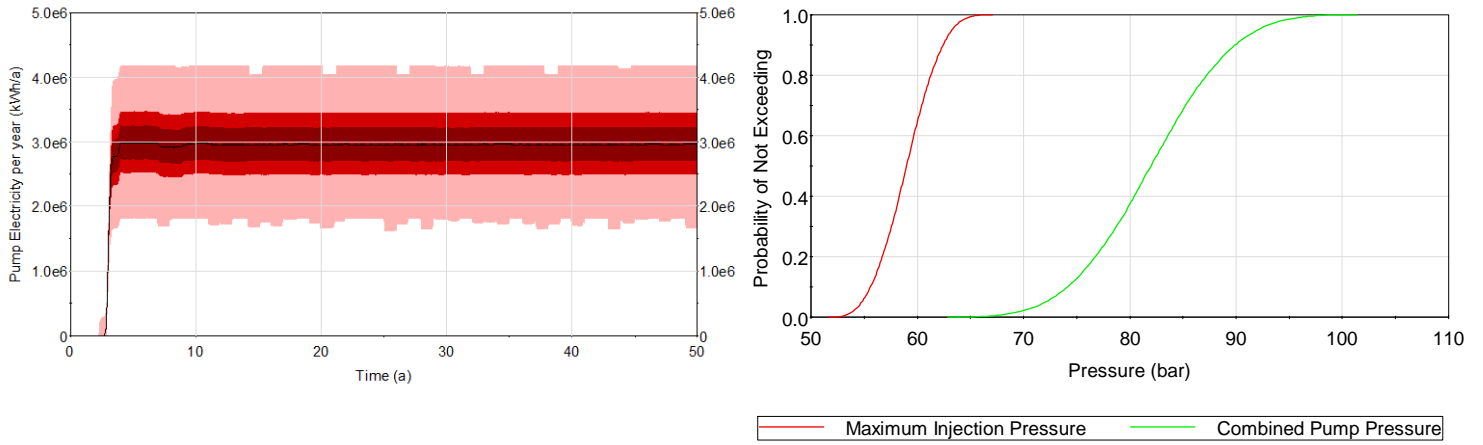
Figure 65: Pump electricity required per year distribution and pump pressure CDF on the left and right respectively

B.4 Gas production volumes
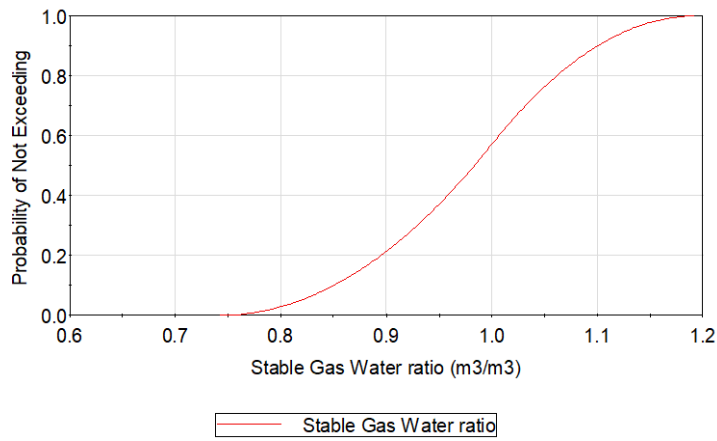
Figure 66: CDF of the Gas/Water ratio
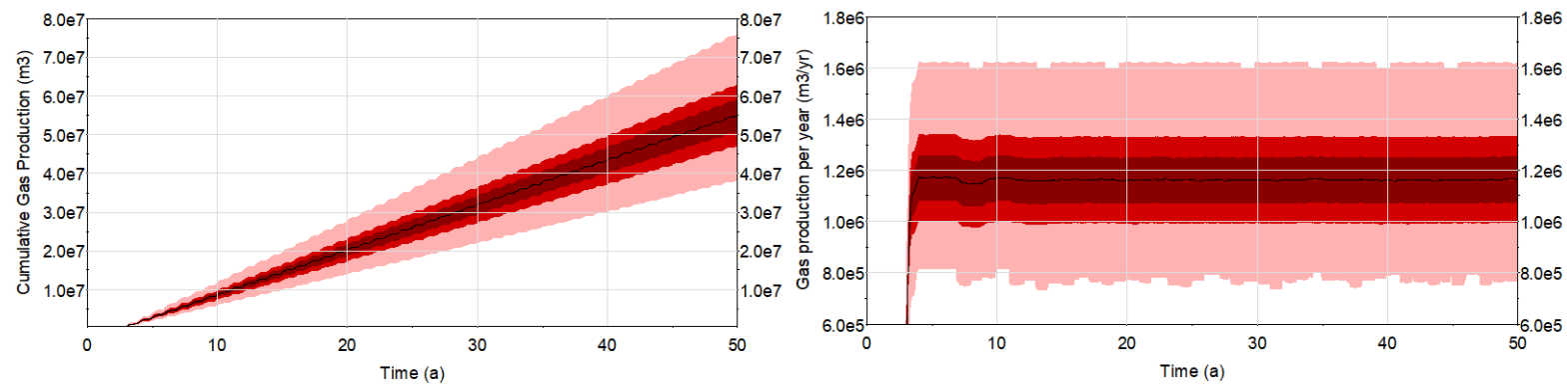
Figure 67: Gas production volumes cumulative and per year on the right and left respectively

B.5 Financial parameters
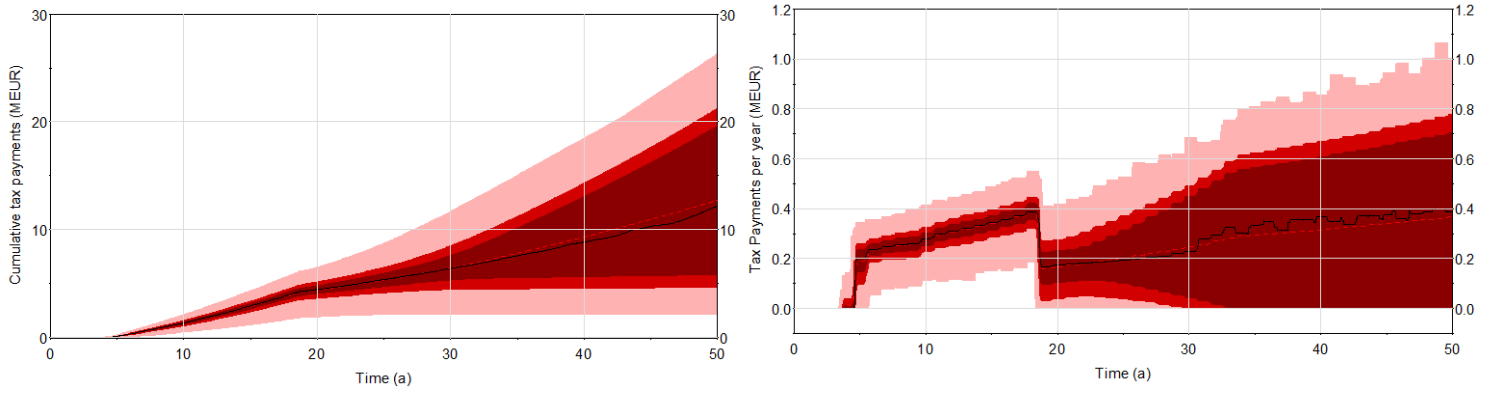
Figure 68: Cumulative and Yearly tax payments distribution on the left and right respectively
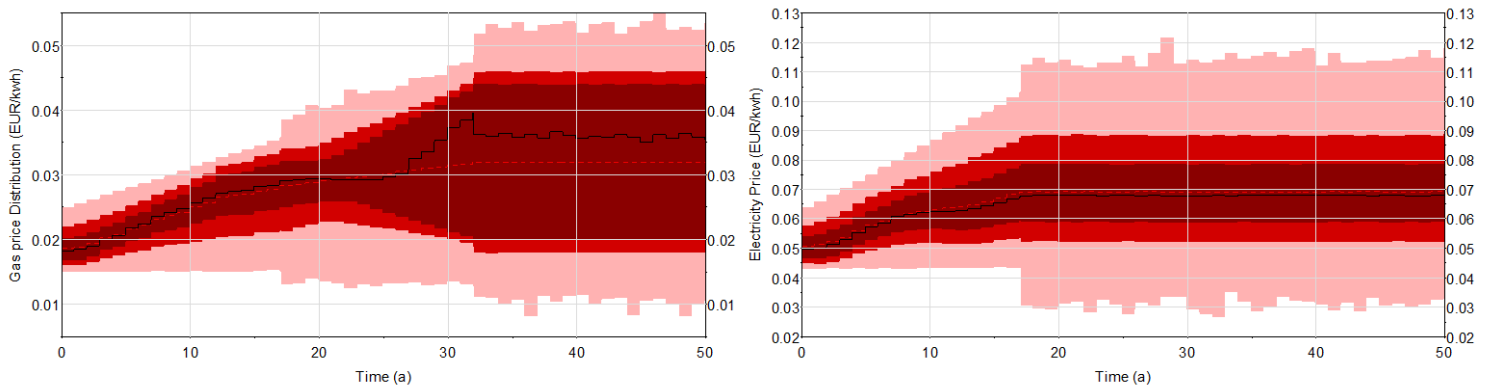
Figure 69: Gas and electricity price distribution on the left and right respectively
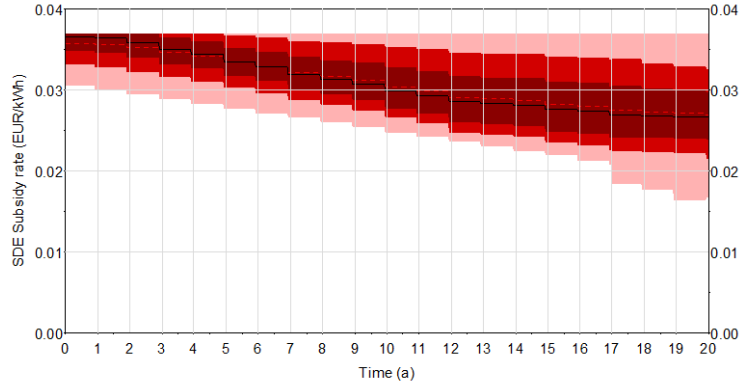
Figure 70: SDE subsidy rate distribution

B.6: Operational cost
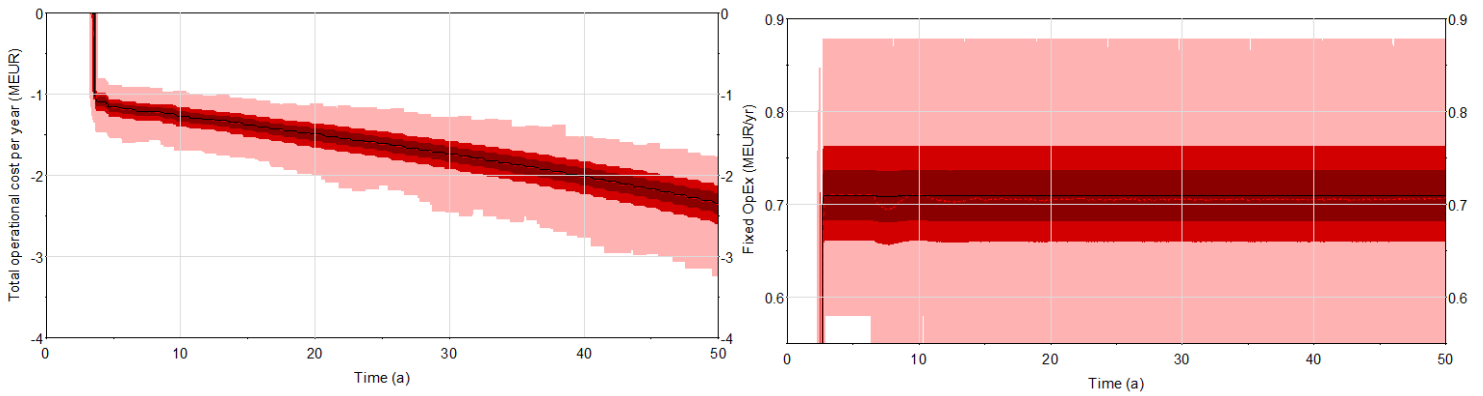
Figure 71: Total operational cost per year and fixed operational cost per year distribution on the left and right respectively

B7 Financial evaluation elements
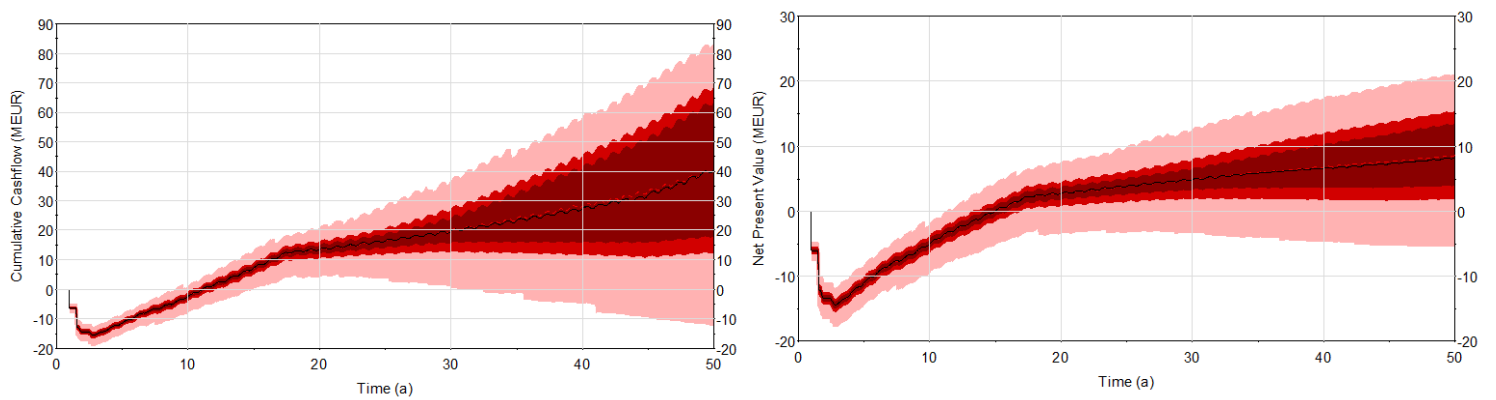
Figure 72: CCF and NPV distribution on the left and right respectively
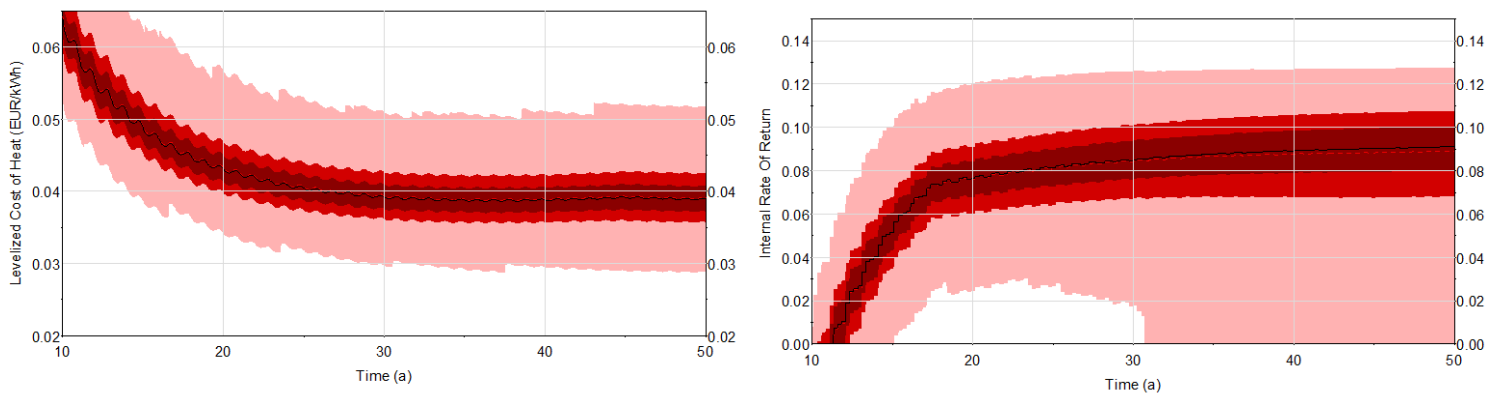
Figure 73: LCOH and IRR distribution on the left and right respectively
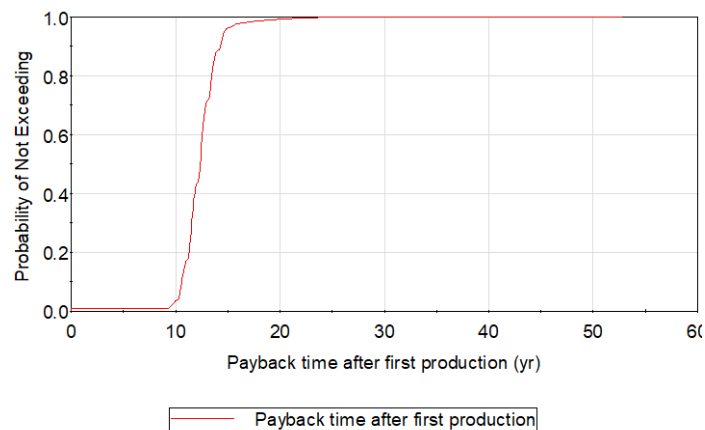
Figure74: Payback time

8 References

[1]   M. H. Dickson and M. Fanelli, *Geothermal Energy: Utilization and Technology*. 2006.

[2]   J. W. B. J. A. Tester, "The Future of Geothermal Energy: Impact of Enhanced Geothermal Systems (EGS) on the United States in the 21st Century," *Technology*, vol. Im, no. November, p. 372, 2006.

[3]   R. Bertani, *Deep Geothermal Energy for Heating and Cooling*. Elsevier Ltd, 2015.

[4]   U.S. Energy Information Administration, "International Energy Outlook 2017," *Int. Energy Outlook*, vol. IEO2017, no. 2017, p. 143, 2017.

[5]   E. Barbier, "Geothermal energy technology and current status: an overview," *Renew. Sustain. Energy Rev.*, vol. 6, no. 1–2, pp. 3–65, Jan. 2002.

[6]   I. B. Fridleifsson, "Geothermal energy for the benefit of the people," *Renew. Sustain. Energy Rev.*, vol. 5, no. 3, pp. 299–312, 2001.

[7]   J. TGE Research, GEA, IGA, "Global geothermal capacity reaches 14,369 MW – Top 10 Geothermal Countries, Oct 2018." [Online]. Available: http://www.thinkgeoenergy.com/global-geothermal-capacity-reaches-14369-mw-top-10-geothermal-countries-oct-2018/.

[8]   M. Antics, R. Bertani, and B. Sanner, "Summary of EGC 2016 Country Update Reports on Geothermal Energy in Europe," *Eur. Geotherm. Congr. 2013*, vol. 1998, p. 18, 2016.

[9]   I. Dincer and B. Sanner, "Shallow Geothermal Energy," *GHC Bull.*, vol. June, no. 2, pp. 19–25, 2001.

[10]   G. Bakema and F. Schoof, "Geothermal Energy Use, Country Update for The Netherlands," *Eur. Geotherm. Congr.*, pp. 19–24, 2016.

[11]   A. Daniilidis, "Stochastic modelling and economic evaluation of geothermal systems AESM1306SET/AESM1470," 2018.

[12]   General Secretariat of the Council, "European Council (23 and 24 October 2014) Conclusions," 2014.

[13]   Ministry of Economic Affairs, "Energy Agenda," 2016.

[14]   H. H. Thorsteinsson and J. W. Tester, "Barriers and enablers to geothermal district heating system development in the United States," *Energy Policy*, vol. 38, no. 2, pp. 803–813, 2010.

[15]   K. F. Beckers, M. Z. Lukawski, B. J. Anderson, M. C. Moore, and J. W. Tester, "Levelized costs of electricity and direct-use heat from Enhanced Geothermal Systems," *J. Renew. Sustain. Energy*, vol. 6, no. 1, 2014.

[16]   S. A. Kyriakis and P. L. Younger, "Towards the increased utilisation of geothermal energy in a district heating network through the use of a heat storage," *Appl. Therm. Eng.*, vol. 94, pp. 99–110, 2016.

[17]   G. Willemsen, "Geothermie kan goedkoper door schaalvergroting," *IF*, 2018. [Online]. Available: https://www.iftechnology.nl/geothermie-kan-goedkoper-door-schaalvergroting.

[18]   Platform geothermie, EBN, DAGO, and WN, "Masterplan Aardwarmte in Nederland," 2018.

[19]   L. Gonzalez, "Research sustainability Geothermal Wells in the Netherlands," *Platf. Geotherm.*, p. 32, 2017.

[20]   S. de Boer, E. Bourdon, G. Butterman, and N. de Fijter, "Evaluatie Algemeen instrumentarium geothermie," *IF*, 2016.

[21]   E. C. & R. van E. Magda Smink, Jos van den Broek, Tamara Metze, "Samen kennis aanboren," 2017.

[22]   B. in't Groen, C. De Vries, H. Mijnlieff, and S. Koen, "Conceptadvies SDE+ 2019 Geothermie," *PBL*, 2018.

[23]   R. van den Boschh, B. Flipse, and R. Vorage, "Stappenplan Winning Aardwarmte voor Glastuinbouw," *Kas*

als Energiebron, no. December, 2013.

[24]   A. Daniilidis, B. Alpsoy, and R. Herber, "Impact of technical and economic uncertainties on the economic performance of a deep geothermal heat system," *Renew. Energy*, vol. 114, pp. 805–816, 2017.

[25]   M. Z. Lukawski *et al.*, "Cost analysis of oil, gas, and geothermal well drilling," *J. Pet. Sci. Eng.*, vol. 118, pp. 1–14, 2014.

[26]   "Stichting DAP," 2018. [Online]. Available: http://www.delftaardwmteproject.nl/.

[27]   M. E. Donselaar, D. Gilding, and R. Groenenberg, "Reservoir Geology and Geothermal Potential of the Delft Sandstone Member in the West Netherlands Basin," no. April, 2015.

[28]   C. J. L. Willems, H. M. Nick, T. Goense, and D. F. Bruhn, "The impact of reduction of doublet well spacing on the Net Present Value and the life time of fluvial Hot Sedimentary Aquifer doublets," *Geothermics*, vol. 68, pp. 54–66, 2017.

[29]   R. A. Crooijmans, C. J. L. Willems, H. M. Nick, and D. F. Bruhn, "The influence of facies heterogeneity on the doublet performance in low-enthalpy geothermal sedimentary reservoirs," *Geothermics*, vol. 64, pp. 209–219, 2016.

[30]   C. Hellinga, "Introduction of a geothermal well at the TU Delft campus." 2018.

[31]   GoldSim Technology Group, "GoldSim User Guide," p. 79, 2017.

[32]   M. van Soerland, *Personal Communication (Trias Westland)*. .

[33]   P. Ungemach, "Definition of Electrosubmersible pump (ESP) design and selection workflow," no. June, 2016.

[34]   Ministry of Economic Affairs, "Notitie bijvangst koolwaterstoffen bij aardwarmte," pp. 1–5, 2012.

[35]   A. van Adrichem, *Personal communication (Duijvestijn Tomaten)*. .

[36]   A. van Adrichem *et al.*, "Handboek Geothermie 2014," 2014.

[37]   Jan Willem Rösingh, *Financial business case and personal communication*. 2018.

[38]   S. Lensink, "Voorlopige correctiebedragen 2017 (SDE+)," 2016.

[39]   "Jenbacher Co-Generator," 2018. [Online]. Available: https://www.ge.com/power/gas/reciprocating-engines.

[40]   M. P. D. P. en J. G. V. H.F. Mijnlieff, A.N.M. Obdam, A. Kronimus, J.D.A.M. van Wees, P. van Hooff, "DoubletCalc 1.4 handleiding," *TNO Rep.*, 2012.

[41]   J. Van Wees *et al.*, "Geothermal aquifer performance assessment for direct heat production–Methodology and application to Rotliegend aquifers," *Netherlands J. Geosci.*, vol. 91, no. 4, pp. 651–666, 2012.

[42]   S. M. Lensink and H. Cleijne, "Notitie Financiering SDE + 2018 Introductie op proces Financiële kaders," 2017.

[43]   "Wat u betaalt aan energiebelasting," 2018. [Online]. Available: https://www.minder.nl/faq/energiebelasting-en-ode.

[44]   Ministry of Economic Affairs, "SDE+ voorjaar 2018," 2018.

[45]   ECN, "Eindadvies basisbedragen SDE + 2018," no. november 2017, 2017.

[46]   Rijksdienst voor ondernemend Nederland, "Energieinvesterings aftrek (EIA)," 2018.

[47]   Rijksdienst voor ondernemend Nederland, "Risco's dekken voor Aardwarmte," 2017.

[48]   Minister van Economische Zaken en Klimaat, "Staatscourant," 2017. [Online]. Available:

https://zoek.officielebekendmakingen.nl/stcrt-2017-69690.html.

[49]   Nederlandse vereniging van banken, "Financiering en financierbaarheid van geothermie projecten," 2015.

[50]   M. Z. Lukawski, R. L. Silverman, and J. W. Tester, "Uncertainty analysis of geothermal well drilling and completion costs," *Geothermics*, vol. 64, pp. 382–391, 2016.

[51]   J. D. A. M. va. Wees, L.Kramers, R.A.Kronimus, M. P. D. Pluymaekers, H. F. MijnLieff, and G.J.Vis, "ThermoGISTM V1.0 Part II : Methodology," *TNO Rep.*, 2010.

[52]   P. Heidinger, "Integral modeling and financial impact of the geothermal situation and power plant at Soultz-sous-Foreˆt," *Comptes rendus - Geosci.*, vol. 342, no. 7–8, pp. 626–635, 2010.

[53]   M. Batzle and Z. Wang, "Seismic properties of pore fluids," *Geophysics*, vol. 57, no. 11, pp. 1396–1408, 1992.

[54]   A. Ramalingam and S. Arumugam, "Experimental study on specific heat of hot brine for salt gradient solar pond application," *Int. J. ChemTech Res.*, vol. 4, no. 3, pp. 956–961, 2012.

[55]   A. Lokhorst, "Aardwarmte in Nederland Verslag van het Onderzoekprogramma " Instandhouding Kennis Aardwarmte Exploratie en Exploitatie in Nederland (1997-2000)"," *TNO Rep.*, p. 81, 2000.

[56]   J. D. A. M. Van Wees, G. Degens, M. Zijp, J. De boer, A. Obdam, and F. J. Eyvazi, "TNO BIA Geothermal Report : The Causes and Solutions to Poor Well Performance in Dutch Geothermal Projects," pp. 1–48, 2012.

[57]   A. Lokhorst, "Aardwarmte in Nederland," 2000.

[58]   SODM and TNO, "protocol injectiedrukken bij aardwarmte," no. november, pp. 2–3, 2013.

[59]   Netherlands Enterprise Agency [RVO], "SDE+ najaar 2017," pp. 3–26, 2017.

[60]   K. Schoots, M. Hekkenberg, and P. Hammingh, "Nationale Energieverkenning 2017," *Energieonderzoek Cent. Ned.*, pp. 1–238, 2017.

[61]   J. Matthijsen, R. Aalbers, and R. van den Wijngaart, "Cahier Klimaat en energie," 2015.

[62]   A. Van Der Welle and S. Lensink, "Notitie Samenvatting Langetermijnenergieprijs," 2017.

[63]   Investopedia, "Weighted Average Cost of Capital (WACC)." [Online]. Available: https://www.investopedia.com/terms/w/wacc.asp.

[64]   J. R. Birge and V. Linetsky, "Financial Engineering," p. 1027, 2008.

[65]   "Perpetuum Energy Partners." [Online]. Available: www.pnrgp.com.

[66]   Nlog, "Production figures PNA-GT-01," 2018. [Online]. Available: https://www.nlog.nl/nlog/requestData/nlogp/allBor/metaData.jsp?table=BorLocation&id=596144601.

[67]   J. Limberger *et al.*, "Geothermal energy in deep aquifers: A global assessment of the resource base for direct heat utilization," *Renew. Sustain. Energy Rev.*, vol. 82, no. August 2017, pp. 961–975, 2018.

[68]   D. of Energy, "Transparent Cost Database," 2018. [Online]. Available: https://openei.org/apps/TCDB/.

9 Acknowledgements

First of all I like to thank Alexandros Daniilidis (Alex) for his continues and patient guidance throughout my thesis period. We had many coffees together to discuss all the difficulties that were endured while adjusting and improving the model and writing the thesis. His positive and informal attitude in these meetings gave me new energy to continue improving the work. I wish him all the best in his academic career at TU Delft

The second person I'd like to thank is professor David Bruhn. Before I started my thesis, his expressed enthusiasm and passion for the geothermal sector at the DAP symposium really triggered my interest in geothermal exploitation. Our meetings where always fruitful, containing new ideas, suggestions and discussions about the challenges in geothermal exploitation and overall thesis progression. His kind appearance and expertise about the subject is really a great addition to the academic staff of TU Delft.

The third person I like to thank is Jan Willem Rösingh from Perpetuum Energy Partners BV. He provided me the DAP well data and took the time and effort to come to TU Delft for a meeting to discuss this data and clear up any confusion I had about the sector.

Lastly, I would like to thank all my friends and family who supported me during my studies and thesis period. Without them I would not have made it this far. The whole process was not always easy but having uplifting friends and family really kept me going.